AD-A158 648 EVALUATION OF NEW RESIN SYSTEMS(U) ROCKWELL 1/2
INTERNATIONAL THOUSAND OAKS CA SCIENCE CENTER
P J DYNES MAY 85 SC5338.85FR AFWAL-TR-85-4053
UNCLASSIFIED F33615-82-C-5064 F/G 11/4 NL

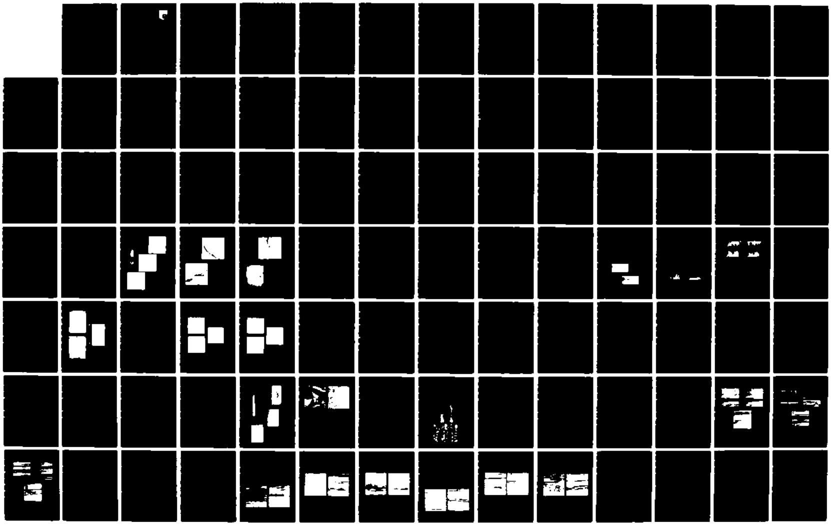

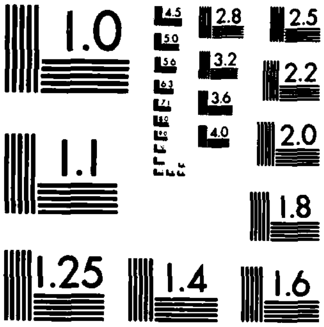

MICROCOPY RESOLUTION TEST CHART
NATIONAL BUREAU OF STANDARDS-1963-A

3

AFWAL-TR-85-4053

AD-A158 648

EVALUATION OF NEW RESIN SYSTEMS

Paul J. Dynes

Rockwell International Science Center
1049 Camino Dos Rios
Thousand Oaks, CA 91360

May 1985

Final Report for Period 20 September 1982 - 20 January 1985

MATERIALS LABORATORY
AIR FORCE WRIGHT AERONAUTICAL LABORATORIES
AIR FORCE SYSTEMS COMMAND
WRIGHT-PATTERSON AIR FORCE BASE, OHIO 45433

NOTICE

This technical report has been reviewed and is approved for publication.

Frederick L Hedberg
FREDERICK L. HEDBERG, Research Chemist
Structural Materials Branch
Nonmetallic Materials Division

Charles E. Brow
CHARLES E. BROWNING, Act. Chief
Structural Materials Branch
Nonmetallic Materials Division

FOR THE COMMANDER

GEORGE E HUSMAN, Chief
Nonmetallic Materials Divsion

UNCLASSIFIED
SECURITY CLASSIFICATION OF THIS PAGE

AD - A158 648

REPORT DOCUMENTATION PAGE

1a. REPORT SECURITY CLASSIFICATION
Unclassified

1b. RESTRICTIVE MARKINGS

2a. SECURITY CLASSIFICATION AUTHORITY

2b. DECLASSIFICATION/DOWNGRADING SCHEDULE

3. DISTRIBUTION/AVAILABILITY OF REPORT
Approved for public release;
distribution unlimited

4. PERFORMING ORGANIZATION REPORT NUMBER(S)
SC5338.85FR

5. MONITORING ORGANIZATION REPORT NUMBER(S)
AFWAL-TR-85-4053

6a. NAME OF PERFORMING ORGANIZATION
Rockwell International
Science Center

6b. OFFICE SYMBOL *(If applicable)*

7a. NAME OF MONITORING ORGANIZATION
Materials Lab
AFWAL/MLBC

6c. ADDRESS *(City, State and ZIP Code)*
1049 Camino Dos Rios
Thousand Oaks, CA 91360

7b. ADDRESS *(City, State and ZIP Code)*
Wright-Patterson AFB
Ohio 45433

8a. NAME OF FUNDING/SPONSORING ORGANIZATION
Air Force Wright
Aeronautical Laboratories

8b. OFFICE SYMBOL *(If applicable)*
AFWAL/MLBC

9. PROCUREMENT INSTRUMENT IDENTIFICATION NUMBER
Contract No. F33615-82-C-5064

8c. ADDRESS *(City, State and ZIP Code)*
AFWAL/MLBC
Wright-Patterson AFB
Ohio 45433

10. SOURCE OF FUNDING NOS.

PROGRAM ELEMENT NO.	PROJECT NO.	TASK NO.	WORK UNIT NO.
62102F	2419	03	31

11. TITLE *(Include Security Classification)*
EVALUATION OF NEW RESIN SYSTEMS (U)

12. PERSONAL AUTHOR(S)
Dynes, Paul J.

13a. TYPE OF REPORT
Final Report

13b. TIME COVERED
FROM 09/20/82 TO 01/20/85

14. DATE OF REPORT *(Yr., Mo., Day)*
MAY 1985

15. PAGE COUNT
146

16. SUPPLEMENTARY NOTATION

17. COSATI CODES

FIELD	GROUP	SUB. GR.
11	04	
11	04	

18. SUBJECT TERMS *(Continue on reverse if necessary and identify by block number)*
HR600P Resin
m-ATS Resin
Composite Materials
Resin Characterization
BATQ-H (ATP) Resin
Fracture Toughness
Microtensile Specimens
ATB Resin
Hot-melt impregnation
Composite Testing

19. ABSTRACT *(Continue on reverse if necessary and identify by block number)*

Four new acetylene terminated resins were evaluated as matrix materials for advanced aerospace composites. They were Hughes HR600P and three Air Force developed resins including BATQ-H(ATP), ATB and m-ATS. Given one pound of each of the materials, neat resin tensile properties were first studied to determine the optimum cure cycle and service temperature capability. Graphite prepreg was prepared using a single tow hot--melt prepregger. Small unidirectional laminates were then fabricated and baseline mechanical properties generated for varying temperature conditions for both dry and moisture conditioned states. The following tasks were accomplished:

- Differential scanning calorimetry, thermograviometric analysis and Rheometrics cure rheological analysis were performed on the four candidate resins.
- Neat resin microtensile specimens of HR600P, BATQ-H(ATP) and ATB were prepared and tested to determine the optimum postcure cycle for these materials.
- AS4/BATQ-H(ATP), AS4/ATB and AS4/m-ATS prepreg were prepared with a laboratory hot-melt prepregger.

20. DISTRIBUTION/AVAILABILITY OF ABSTRACT
UNCLASSIFIED/UNLIMITED ☒ SAME AS RPT. ☐ DTIC USERS ☐

21. ABSTRACT SECURITY CLASSIFICATION
Unclassified

22a. NAME OF RESPONSIBLE INDIVIDUAL
F.L. Hedberg

22b. TELEPHONE NUMBER *(Include Area Code)*
(513) 255-2201

22c. OFFICE SYMBOL
AFWAL/MLBC

DD FORM 1473, 83 APR

EDITION OF 1 JAN 73 IS OBSOLETE.

UNCLASSIFIED
SECURITY CLASSIFICATION OF THIS PAGE

(Continued from Block 19)

G subscript 1C

- High quality laminates of AS4/ATB and AS4/m-ATS were prepared with the "no bag" autoclave technique.
- Void free laminates of AS4/BATQ-H(ATP) were prepared by press molding.
- Interlaminar shear, flexure, transverse flexure and G_{1c} composite mechanical tests were performed.
- Physical property evaluations included prepreg resin content, cured laminate resin content, void evaluation and Tg (Rheometrics).
- Interlaminar shear and G_{1c} delamination failure surfaces were analyzed by SEM.

FOREWORD

This final report covers the work performed under Contract F33615-82-C-5064, "Evaluation of New Resin Systems," during the period September 20, 1982 to January 1, 1985. This program was conducted under the technical direction of Dr. F.L. Hedberg, Air Force Wright Aeronautical Laboratories, Wright-Patterson AFB, OH 45433.

The subject program was carried out at the Science Center Division of Rockwell International Corporation, Thousand Oaks, CA. Mr. P.J. Dynes was Program Manager and Principal Investigator. Mr. J.S. Jones and Mr. E.J. Derbyshire of Space Transportation System Division of Rockwell International Corporation, Downey, CA, served as Project Engineers for autoclave processing support.

Acknowledgements are given to Mr. C.D. Mauthe for experimental support and to Dr. C.L. Hamermesh for polymer chemistry consultation.

TABLE OF CONTENTS

TABLE OF CONTENTS

Page

TABLE OF CONTENTS

Page

LIST OF FIGURES

LIST OF FIGURES

LIST OF FIGURES

LIST OF FIGURES

LIST OF FIGURES

LIST OF FIGURES

LIST OF FIGURES

LIST OF TABLES

LIST OF TABLES

LIST OF TABLES

LIST OF TABLES

1.0 INTRODUCTION AND APPROACH

The present generation of advanced composites is based primarily on Ciba-Geigy MY720 epoxy resin and an aromatic amine. This combination cures at 177°C (350°F) to yield coherent nonporous laminates.

This system, however, suffers from two shortcomings as a matrix resin. The first is its brittle nature, making its composites susceptible to damage by impact. A second drawback is absorption of water resulting in a reduced glass transition temperature. This, in turn, causes an unacceptable drop in mechanical properties at 177°C (350°F).

Many new resin systems are being synthesized which are designed for improved fracture toughness and/or moisture sensitivity. It is imperative that such systems be evaluated thoroughly, yet cost effectively, as composite matrices.

The objective of the current program was to provide a link between early neat resin data obtained with ~ 50 g of material and expensive large-scale synthesis efforts involving pilot plant quantities. At present, prediction of the translation of neat resin behavior into composite performance is not sufficiently accurate to base the acceptance of a matrix resin on neat resin properties alone. It has therefore been necessary to design an evaluation scheme which, given an intermediate of resin (1 lb), is capable of determining to a high degree of confidence the potential of new matrix resins.

The program consisted of five tasks. A summary of each task is given below.

Task I. Materials Validation

This task was designed to establish that the 1 lb sample was essentially the same material as was characterized in prior 50 g evaluation studies by the Air Force Materials Laboratory. This validation consisted primarily of calorimetric and rheological cure characterization.

Task II. Neat Resin Cure Cycle Development

In Task II, the curing behavior of the neat resins were examined in regard to optimization of properties, the practicality of the cure cycle, and the ability to employ the cure cycle in the autoclave curing of composite made from the resin. The first step in the optimization involved the evaluation of a number of cure cycles selected on the basis of what service temperature was anticipated for the material. Thermomechanical analysis (TMA) for glass transition temperature, residual cure exotherm by differential scanning calorimetry (DSC), and thermal stability by thermogravimetric analysis (TGA) were used to select at least three cure cycles for further evaluation. The final selection of the cure cycle was based on the results of neat resin microtensile data as characterized by the "failure envelope" concept. Using the cure cycle which resulted in the best set of resin mechanical properties, microtensile specimens were prepared and tested at ambient and two elevated temperatures. Tests were performed with both dry and moisture equilibrated (71°C, 160°F, 95% RH) specimens.

Task III. Composite Cure Cycle Development

Graphite-based prepreg and composite were prepared in Task III. Initially, the resin was assessed with regard to prepregging by a hot-melt or solvent technique. The hot-melt technique was optimized with respect to resin viscosity, resin content, fiber areal weight, and fiber collimation. If hot-melt impregnation could not be used, a solvent-based technique was developed based on factors such as solubility, boiling point, complexing tendency and toxicity.

The second objective of Task III was to develop autoclave procedures for fabricating small laminates. Parameters affecting layup and bagging procedures such as temperature, pressure or vacuum were evaluated as to their effect on quality of the composite produced. Based on these results, the procedure and parameter controls which led to the highest quality composite were employed to produce unidirectional laminates (~ 7 " x 7" x 0.080") to characterize the capability of the resin as a matrix for graphite composite.

Task IV. Composite Testing and Evaluation

Task IV consisted of composite mechanical testing. Shear testing was made using four-point geometry which ensures true interlaminar failure. Short-beam shear tests were carried out for comparative purposes. Standard ASTM 0° flexural tests were made. Transverse 90° flexural tests were made to determine strain-to-failure and modulus. Fracture toughness was evaluated by the Mode I delamination technique. Scanning electron microscopy was used to characterize the failure surfaces.

2.0 SUMMARY

Hughes HR600P and three Air Force developed acetylene-terminated resins, including ATB, BATQ-H (ATP) and m-ATS, were evaluated as matrix materials for advanced composite. From a one-pound sample, neat resin characterization and tensile testing, as well as basic composite properties, were obtained.

Neat resin characterization included differential scanning calorimetry, thermogravimetric and Rheometrics cure rheological analysis. Neat resin microtensile specimens were prepared and the "failure envelope" approach used to determine the optimum cure cycles.

Prepreg was prepared from unsized Hercules AS4, 12K graphite fiber using a laboratory single tow hot-melt prepregger. Areal fiber weight, resin content and fiber collimation of the prepreg were evaluated.

Small preliminary laminates about 3 in. x 3 in. were prepared in developing a processing method. The "no bag" autoclave technique was found to produce high quality void-free laminates for ATB and m-ATS resins. A press molding technique was used to fabricate AS4/BATQ-H (ATP) composite. HR600P composite was processed by standard vacuum bag autoclaving.

Laminates were tested for resin content, voids and T_g by Rheometrics dynamic mechanical analysis. Mechanical tests included four-point interlaminar shear, three-point 0° and four-point 90° flexure and G_{1c} delamination fracture toughness. Short beam shear tests were made for comparative information. Testing was carried out at room temperature and two elevated temperatures. Four-point shear and 0° three-point flexural tests were made on specimens moisture conditioned to equilibrium at 71°C (160°F) and 95% RH.

A successful processing technique could not be found to fabricate high quality Celion/HR600P laminates. Several autoclave procedures, as well as press molding, failed to solve a persistent porosity problem. Later studies by Hughes Aircraft and National Starch Corporation established that amic acid forms of the prepolymer, present in early lots of HR600P, were responsible for the porosity problem. Newer lots of resin, now called IP600 by National Starch Corporation, are reported not to suffer from this problem.

A solvent impregnation technique and press molding procedure were developed which permitted good quality void-free laminates of AS4/BATQ-H (ATP) to be prepared. The outstanding tensile strength and strain-to-failure properties determined for BATQ-H (ATP) neat resin were not clearly translated to composite mechanical performance. Interlaminar shear strength was poor, and in elevated temperature flexure tests at 177°C (350°F) and 232°C (450°F) the material underwent severe creep. At room temperature, good transverse flexure strength and strain-to-failure were observed. G_{1c} tests of composite revealed a multiple crack front failure resulting in inflated delamination fracture toughness values.

High quality AS4/ATB laminates were prepared by the "no bag" autoclave processing technique. The unique moisture resistance of the material was confirmed, but the interlaminar shear and 0° flexure properties were inferior to state-of-the-art 177°C (350°F) service graphite/epoxy composites. Transverse flexure strength and strain-to-failure were similr to graphite/epoxy material. The G_{1c} test, as in the case of AS4/BATQ-H (ATP), showed a failure which appeared to occur in more than a single ply. Even so, the G_{1c} value for AS4/ATB was about the same as for Hercules AS1/3501-5A composite.

The "no bag" autoclave process was also used to prepare void-free high qualty AS4/m-ATS laminates. The interlaminar shear and 0° flexure properties were equivalent to AS4/ATB. The matrix toughness, as determined by the 90° flexure and G_{1c} tests, was significantly poorer than obtained for AS4/ATB. Generally, the composite mechanical properties are similar to those reported for the earlier ATS resin from Gulf Research and Development Corporation. The poor mechanical properties for AS4/ATB and AS4/m-ATS also indicate that the extended hold at 140°C (285°F) during the cure cycle is not effective for improving resin toughness.

3.0 TECHNICAL DISCUSSION

3.1 Hughes HR600P Resin

Hughes HR600P is an acetylene-terminated polyimide resin developed by Hughes Aircraft Company. It is a modification of the earlier Thermid 600 resin system which was licensed by Hughes to Gulf Oil and Chemicals Company. The chemical structure of HR600P resin is shown in Fig. 1. The isoimide oligomer is much more soluble and exhibits better flow characteristics than the imidized prepolymer used in Thermid 600. Isomerization of the isoimide takes place during processing to yield the imide structure, while crosslinking occurs through reaction of the acetylene end groups. HR600P and related resins are currently licensed by Hughes Aircraft to National Starch Corporation and are identified as the IP600 resin series. The HR600P resin studied in the current program was part of a lot of material (Lot No. M1126-39D) delivered by Hughes to the Air Force Materials Laboratory.

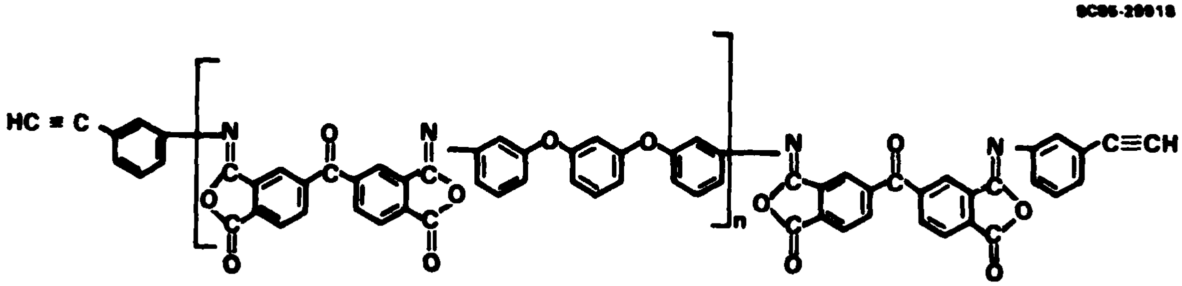

Fig. 1 Molecular structure of Hughes HR600P resin.

3.1.1 Materials Validation

3.1.1.1 Differential Scanning Calorimetry

The cure behavior of HR600P resin is shown in the DSC thermograms in Fig. 2. At scanning rates of 10 and 20°C/min, a single, nearly symmetric exotherm peak is found. At heating rates below 10°C/min, however, a second small

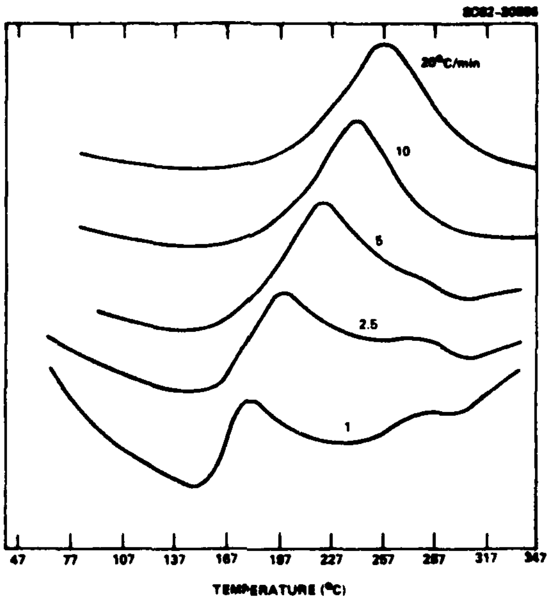

Fig. 2 DSC thermograms of HR600P resin.

exothermic peak becomes apparent at ~ 275°C. The effect of heating rate ϕ on the exotherm peak temperature, T_{max}, is plotted in Fig. 3 according to a modified Arrhenius expression developed by Duswalt,[1] where the slope defines an activation energy as

$$E_a = \frac{-R \, d\ell n\phi}{1.052 \, d(1/T_{max})} \quad . \qquad (1)$$

The activation energy for polymerization of the uncured resin is 17.0 kcal/mole, a typical value for thermoset matrix resins. A summary of the thermal characteristics of HR600P is given in Table 1.

A similar DSC analysis was carried out on HR600P resin which had undergone a series of heating steps involved with its molding, which will be described in Section 3.1.2.1. After the molding cycle, the reactions which are involved in the major exotherm centered at 244°C (471°F) are almost over.

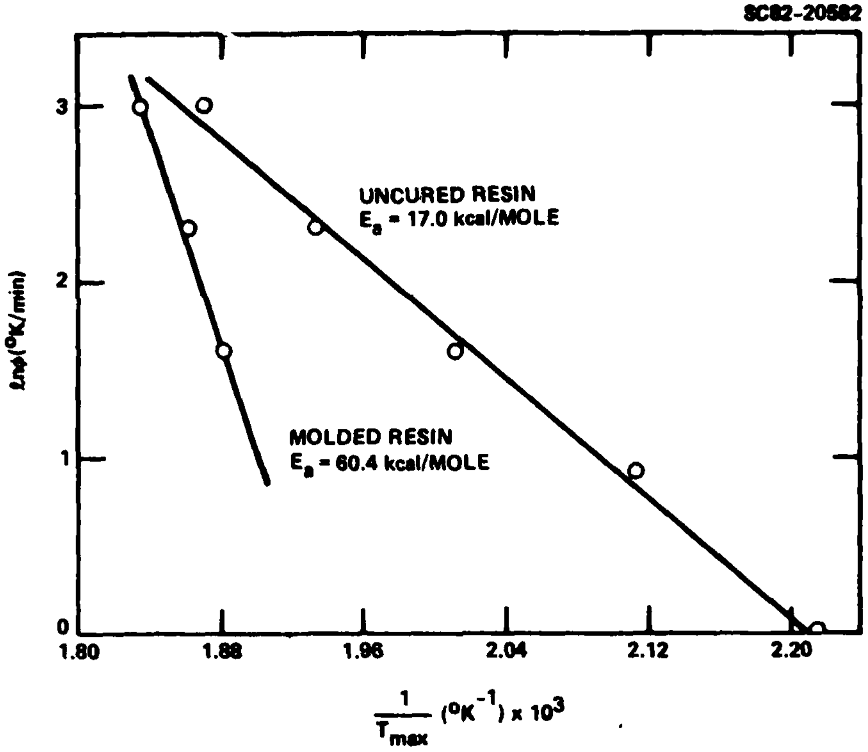

Fig. 3 Dependence of DSC exotherm peak temperature with heating rate for HR600P resin.

Table 1

DSC Analysis of Hughes HR600P Neat Resin

Uncured melt temperature		~ 120°C (243°F)
Exotherm onset temperature	(ϕ = 10°C/min)	156°C (311°F)
Exotherm peak temperature	(ϕ = 10°C/min)	244°C (471°F)
Exotherm completion temperature	(ϕ = 10°C/min)	305°C (581°F)
Heat of polymerization		92 cal/g
Activation energy for polymerization		17.0 kcal/mole

The rest of the cure is mostly due to reactions which make up the second small, high temperature peak, noted above. If the same kinetic analysis is applied to this molded material, a much higher activation energy of ~ 60 kcal/mole is found, as shown in Fig. 3. This process, which may be the isoimide-imide conversion, will be discussed in Section 3.1.2.2.

3.1.1.2 Cure Rheology

The rheological properties of HR600P resin were studied for various linear heating rates and are plotted in Fig. 4. The resin begins to soften near 120°C (248°F) and by ~ 160°C (320°), its dynamic viscosity is within range of the parallel-plate technique. Relative to state-of-the-art epoxy matrix resins, HR600P shows very little flow. It is much better, however, than its predecessor, Thermid 600. That resin's dynamic viscosity during a 2°C/min heat ramp is above the limit (~ 10^7 Poise) of the parallel-plate technique. As will be shown later, however, this poor flow behavior does not appear to be an impediment to molding or autoclave processing of the resin. The isothermal cure rheology of HR600P resin is shown in Fig. 5.

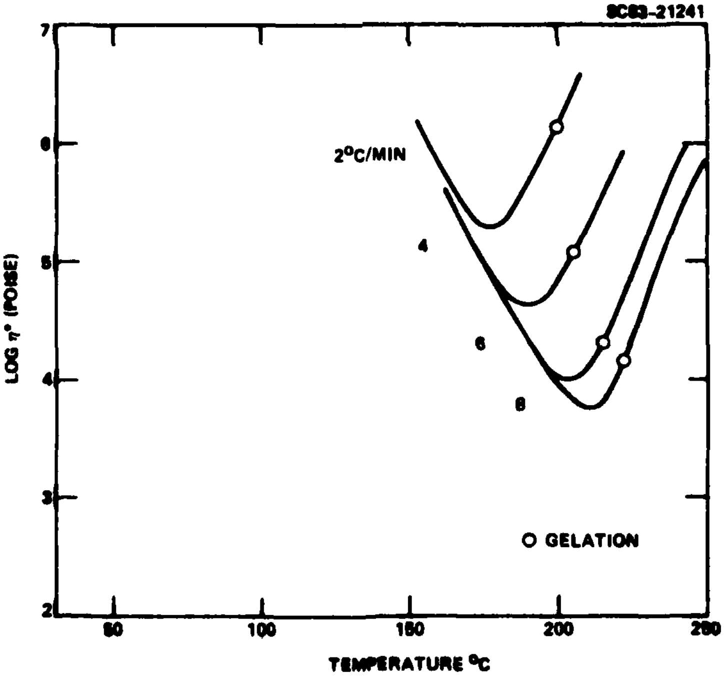

Fig. 4 Dynamic viscosity during cure of HR600P resin at different heating rates.

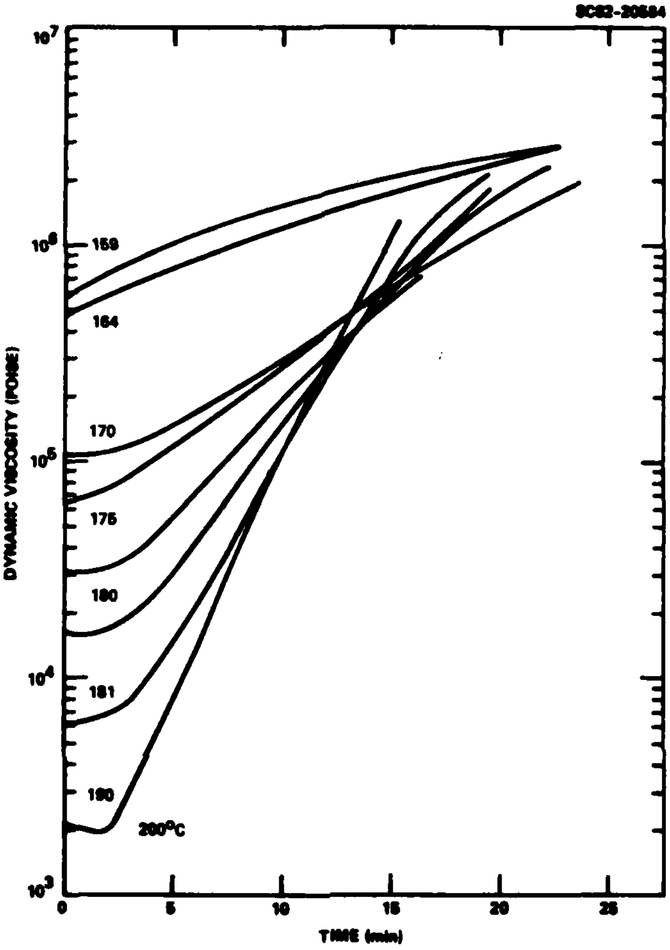

Fig. 5 Dynamic viscosity during cure of HR600P resin at different temperatures.

A summary of the data derived from these experiments is given in Table 2. The initial or minimum dynamic viscosity (η* min) data are helpful in choosing a temperature for molding neat resin specimens. The time to reach gelation, as defined by the point at which the dynamic shear storage modulus G' and the dynamic shear loss modulus G" become equal during cure,[2] varies a relatively small amount from 14.6 min at 200°C to 22 min at 169°C. These gel times are plotted in Fig. 6 according to the standard Arrhenius relationship.

Table 2
Dynamic Viscoelastic Analysis of Gelation in HR600P Resin

Cure Temp (°C)	T (°F)	$t_{G' = G''}$ (min)	η^* min (Poise)
159	318	17.7	6.0×10^5
164	327	16.4	4.8×10^5
169	336	22.0	1.1×10^5
175	347	19.5	6.5×10^4
180	356	18.5	3.0×10^4
181	358	18.6	2.8×10^4
190	374	16.3	6.0×10^3
200	392	14.6	2.0×10^3

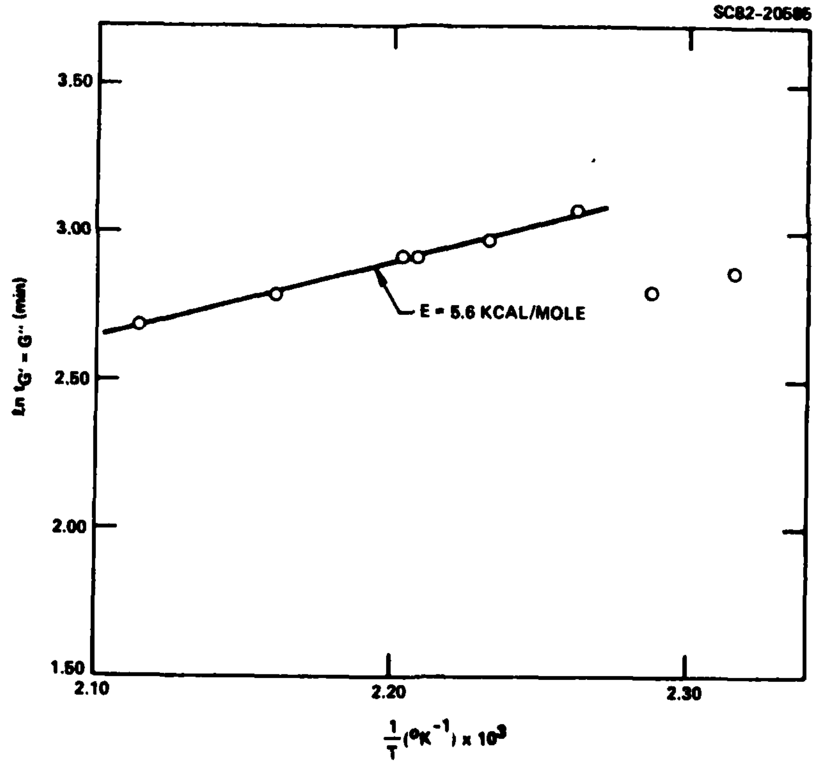

Fig. 6 Dependence of dynamic moduli crossover time with cure temperature for HR600P resin.

The small variation in gel time with temperature results in an unusually low activation energy to gelation of 5.6 kcal/mole. Values of 20-30 kcal/mole are typical for thermoset resins. The poor correlation of the two lowest temperature experiments may be due to vitrification effects as the cure temperature approaches T_{gg}, the glass transition of the resin at the gel point. Previous studies have shown that the dynamic modulus crossover relationship for gelation is valid only at cure temperature > 30°C above T_{gg}.

3.1.2 Neat Resin Cure Cycle Development

3.1.2.1 Microtensile Specimen Preparation

The first step in the development of a neat resin cure cycle for HR600P was to prepare void-free microtensile specimens by compression molding. The most critical factor to control was the viscosity of the resin. Isothermal rheology tests indicated that an appropriate level of viscosity (~ 10^4-10^5 Poise) occurs at temperature ranging from 170-180°C (338-356°F).

Production of void-free specimens of HR600P was also affected by residual solvent present in the neat resin. It was found that a temperature held above the softening point of the resin (~ 120-130°C) was required to completely remove the solvent. A time of 1 h at 150°C was found adequate for solvent removal without causing excessive staging of the resin. The resin was degassed in a matched metal mold under vacuum for the 1 h at 150°C (302°F). The mold was then transferred to a press set at 177°C (350°F) and a pressure of 500 psi applied. The rheological changes which occur during this molding cycle are shown in Fig. 7. The approximate viscosity at the point where pressure is applied is ~ 10^5-10^6 Poise, which is the desired range. Molding can be done at temperatures greater than 177°C; however, more extensive staging would be required to maintain an initial viscosity of > 10^5 Poise. Good consolidation was achieved with this processing cycle, but the specimens were very brittle and difficult to remove from the mold without breaking. This problem was overcome by adding a 1 h 232°C (450°F) hold to the processing

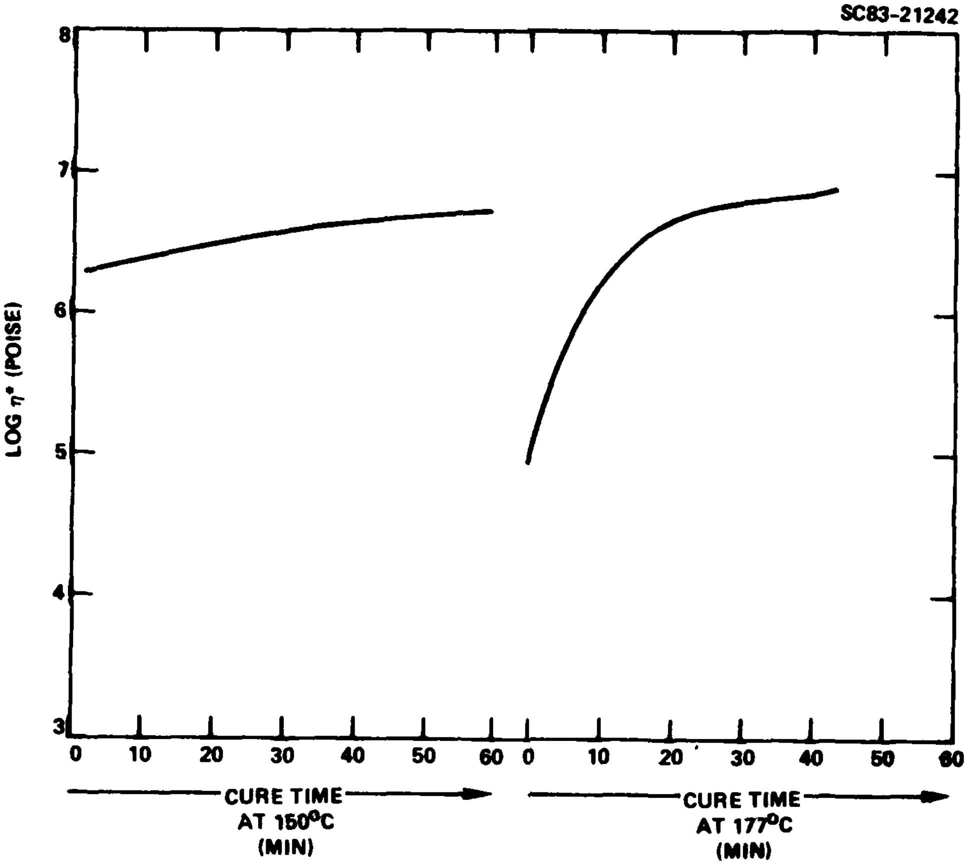

Fig. 7 Dynamic viscosity changes in HR600P resin during neat resin compression molding process.

cycle. A summary of the molding procedure is given in Table 3. Specimens were 40-50 mils thick and of the design used by the Air Force Materials Laboratory. They were void-free and had a tensile strength at room temperature of 11.2 ksi (77.2 MPa) with a strain-to-failure of 1.85%.

3.1.2.2 Thermomechanical Analysis

The second step in the development of a cure cycle for HR600P neat resin was to determine the optimum postcure conditions. The primary composite application for HR600P was expected to be as a high temperature (316°C (600°F)) service material. It was therefore necessary that the cured T_g be somewhat greater than 316°C (600°F). A 316°C (600°F) postcure of 15 h gave a TMA T_g of 283°C (541°F) and reached only 293°C (559°F) after 30 h. Only by going to a 371°C (700°F) postcure was it possible to achieve a greater than

Table 3

Compression Molding Procedure for Hughes HR600P Neat Resin Microtensile Specimens

1. Charge mold at room temperature and wrap with shrink tape.
2. Degas 1 h at 150°C (302°F) under vacuum in oven.
3. Place in preheated 177°C (350°F) press and apply 500 psi and hold 1 h.
4. Ramp temperature to 232°C (450°F) and hold 1 h.
5. Remove specimen from mold while hot.

316°C (600°F) T_g. This narrowed the search for the optimum neat resin cure cycle to the postcure time required at 371°C (700°F); times of 4, 8 and 15 h were investigated. A summary of the T_g data is shown in Table 4. Little difference was found in T_g for these three cure cycles with values ranging from 320-340°C (608-644°F). The difficulty in raising T_g may involve the isoimide-imide conversion or reaction which is responsible for the high DSC activation energy described in Section 3.1.1.1.

Table 4

The Effect of Postcure Conditions on the Glass Transition Temperature of Hughes HR600P Resin

Postcure	T_g (°C)	T_g (°F)
None, molded only	226	438
4.0 h 371°C (700°F)	334	633
8.0 h 371°C (700°F)	316	601
15 h 371°C (700°F)	329	625

3.1.2.3 Thermogravimetric Analysis

The thermogravimetric analysis (TGA) of HR600P resin in nitrogen is shown in Fig. 8 for the material at three stages of processing. All TGA data were obtained at a heating rate of 5°C/min (9°F/min). The onset temperature

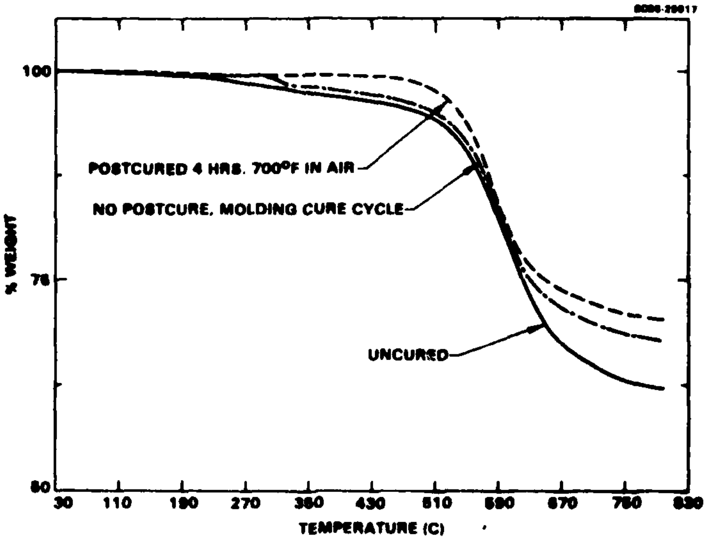

Fig. 8 Thermogravimetric behavior of HR600P resin in nitrogen.

for weight loss of postcured resin occurs at ~ 413°C (775°F) with the "knee" or temperature inflection point for major degradation at ~ 530°C (986°F). Prior to the 413°C (775°F) onset temperature, uncured resin loses ~ 3% weight and molded resin ~ 2%. Weight loss during postcuring of neat resin microtensile specimens at 371°C (700°F) ranged from 3-4%. The Air Force Materials Laboratory reported a total weight loss of 4% to 350°C (662°F) for HR600P, and identified the volatiles as isopropyl alcohol, tetrahydrofuran, water, propene and hydrogen fluoride. A char yield of 70% to 800°C was observed for the resin in nitrogen.

A comparison of the thermogravimetric behavior of postcured HR600P resin in air and nitrogen is shown in Fig. 9. Thermal stability in air and nitrogen are similar up to a temperature just above the "knee" point at ~ 530°C (986°F). Beyond this temperature, the resin undergoes rapid degradation in air.

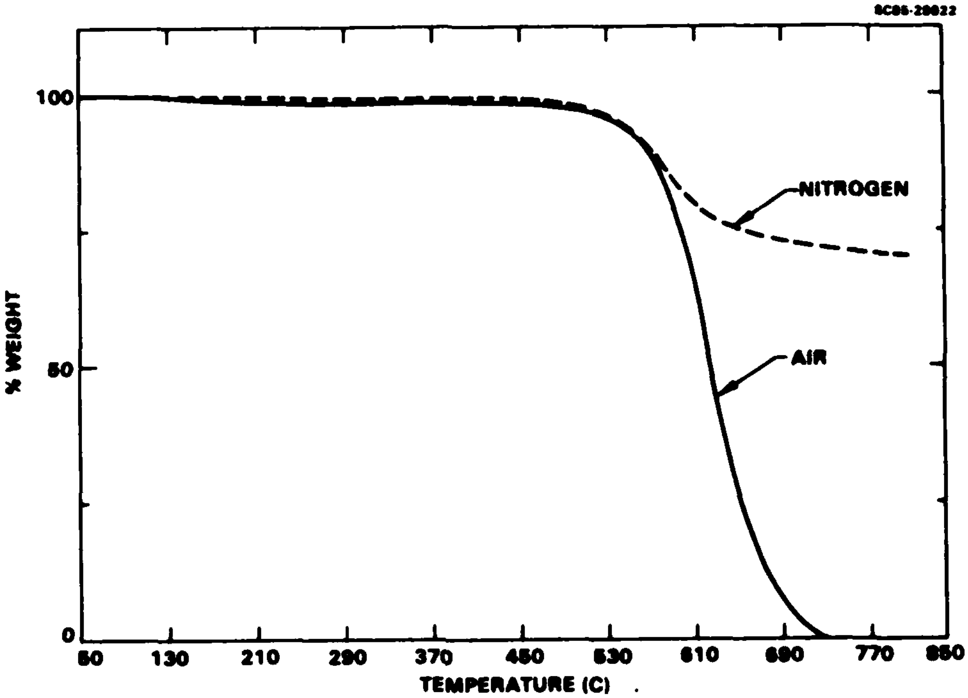

Fig. 9 The effect of environment on the thermogravimetric behavior of HR600P resin postcured 4 h at 371°C (700°F) in air.

Early in the program, the question of an air vs inert environment for postcuring arose. A comparison of the thermal stability in air for resin cured 15 h in air and nitrogen is shown in Fig. 10. The specimen cured in nitrogen shows a slightly slower degradation in air than resin postcured in air.

The effect of postcure time in air on the thermal stability of HR600P resin is shown in Fig. 11. The 4 h postcure at 371°C (700°F) appears to provide the best thermal stability. The same result was obtained when the effect of postcure time in nitrogen was measured, as shown in Fig. 12. Finally, the comparison of resin cured for the optimum time of 4 h in air vs nitrogen is shown in Fig. 13. A result similar to that in Fig. 10 is indicated, with the nitrogen postcured resin showing better thermal stability than air postcured material when tested in air.

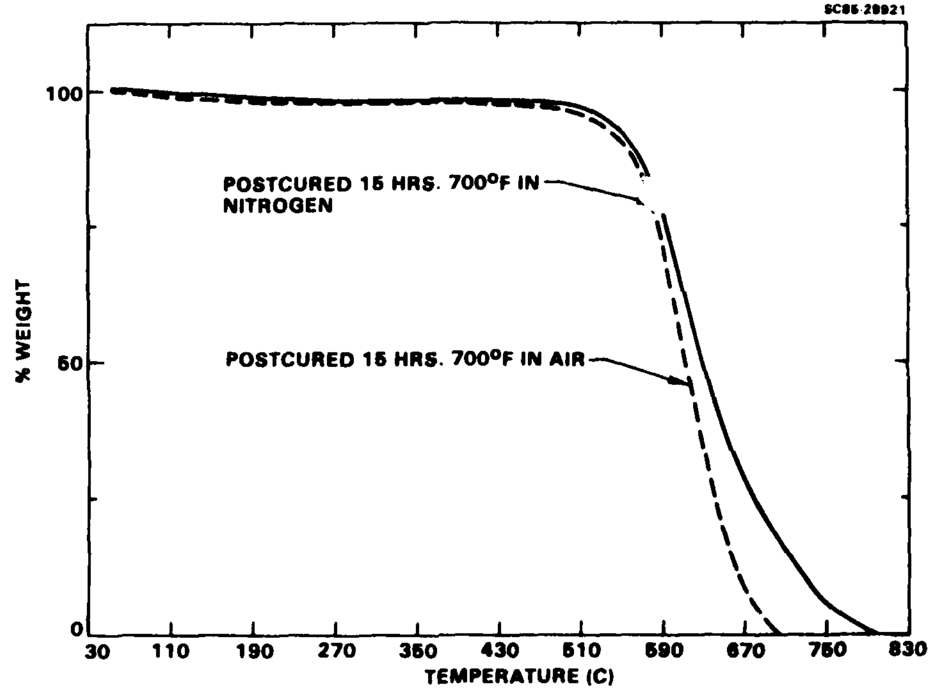

Fig. 10 The effect of postcure environment on the thermogravimetric behavior of HR600P resin in air.

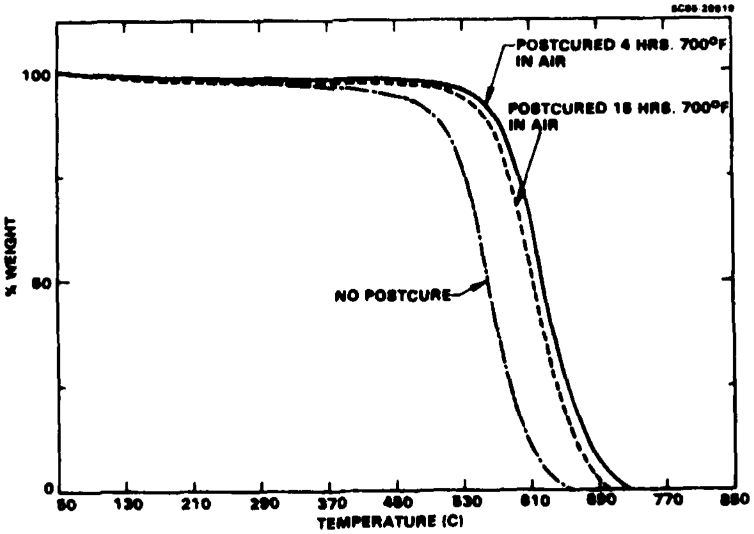

Fig. 11 The effect of postcure time at 371°C (700°F) in air on the thermogravimetric behavior of HR600P resin in air.

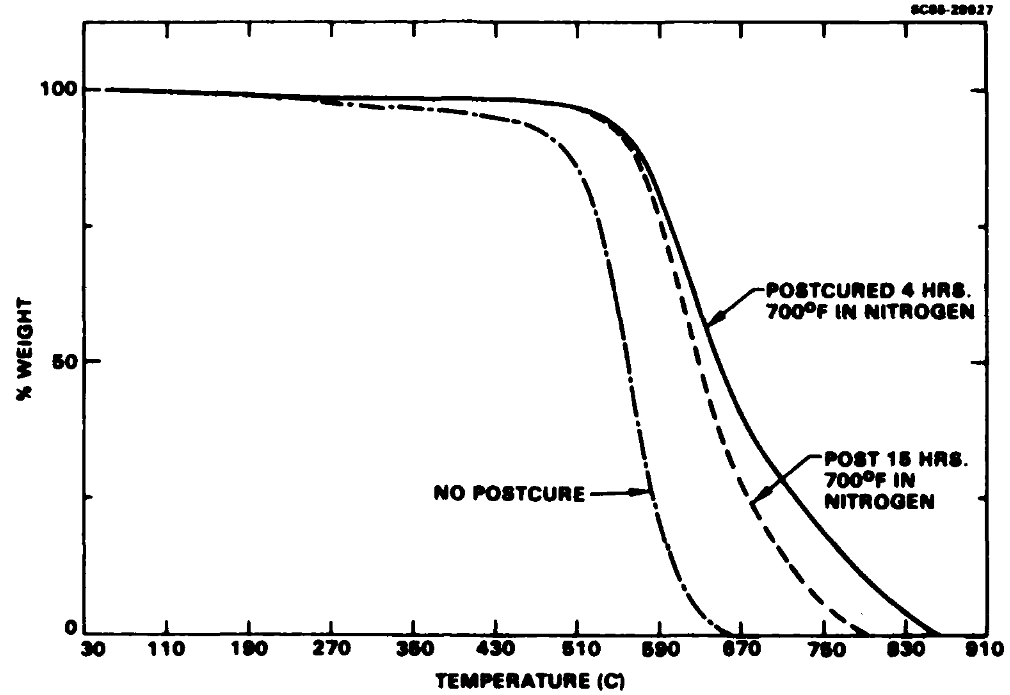

Fig. 12 The effect of postcure time at 371°C (700°F) in nitrogen on the thermogravimetric behavior of HR600P resin in air.

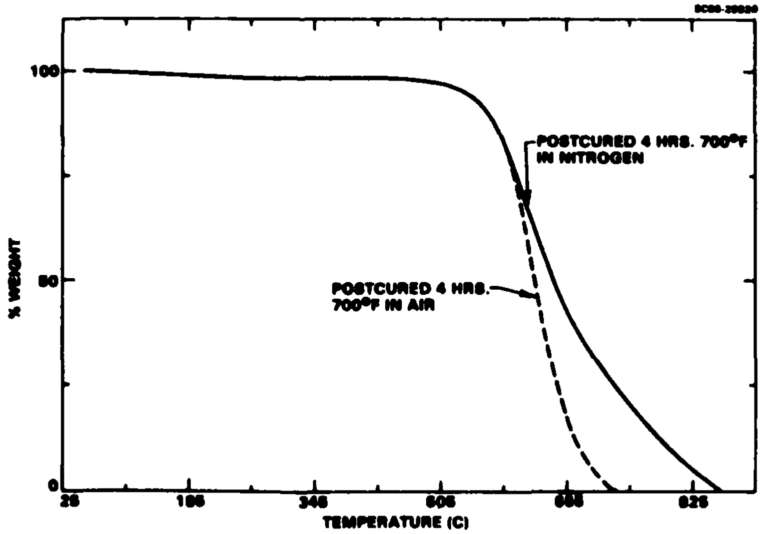

Fig. 13 The effect of postcure environment on the thermogravimetric behavior of HR600P resin in air.

The thermal scanning TGA data indicate that a nitrogen postcure environment results in a more thermally stable resin. Experiments such as isothermal weight loss of postcured material and neat resin microtensile properties, however, would be needed to show conclusively the superiority of nitrogen postcuring.

3.1.2.4 Mechanical Properties

The mechanical behavior of molded neat resin microtensile specimens was the most important factor in selecting the optimum postcure cycle for HR600P resin. The room temperature, 260°C (500°F) and 316°C (600°F) neat resin mechanical properties are given in Tables 5, 6 and 7, respectively. These ultimate stress and strain data are plotted by the failure envelope method in Fig. 14. The 15 h 371°C (700°F) postcure appears to result in a degradation of tensile strength and elongation-to-failure. The 4 and 8 h 371°C (700°F) differ at 316°C (600°F) in elongation, but are similar otherwise. Considering the mechanical property data, together with the thermogravimetric results and the T_g values, the 4 h 371°C (700°F) postcure seemed to provide the best overall properties for HR600P neat resin.

The mechanical properties of HR600P neat resin microtensile specimens are given in Table 8. These specimens were postcured for the optimum cycle of 4 h at 371°C (700°F) in air. At a temperature of 177°C (130°F), the resin retains about 75% of its room temperature tensile strength. This value drops to 40% at 260°C (500°F) and further to 20% at 316°C (600°F). Moisture conditioning was carried out by exposing microtensile specimens to 71°C (160°F) and 95% RH until equilibrium occurred. The elevated temperature "wet" data given in Table 9 are similar to the dry values. With the microtensile experimental setup used, the test could not be made quickly enough to prevent most of the moisture from diffusing out of the specimen before testing.

Table 5

23°C (73°F) Mechanical Properties of Hughes HR600P Molded Neat Resin Microtensile Specimens

Postcure (In Air)	Tensile Strength MPa (ksi)	Tensile Modulus GPa (ksi)	Elongation To Break (%)
None (molded only)	77.4 (11.2) ± 8.5 (1.2)	4.26 (617) ± 0.13 (19)	1.85 ± 0.17
4 h at 371°C (700°F)	75.8 (11.0) ± 5.9 (0.8)	3.77 (548) ± 0.19 (28)	2.21 ± 0.35
8 h at 371°C (700°F)	74.8 (10.9) ± 2.1 (0.3)	3.31 (479) ± 0.28 (40)	2.54 ± 0.22
15 h at 371°C (700°F)	53.9 (7.82) ± 3.5 (0.51)	3.47 (503) ± 0.23 (33)	1.54 ± 0.11

Table 6

260°C (500°F) Mechanical Properties of Hughes HR600P Molded Neat Resin Microtensile Specimens

Postcure (In Air)	Tensile Strength MPa (ksi)	Tensile Modulus GPa (ksi)	Elongation To Break (%)
4 h at 371°C (700°F)	30.4 (4.41)	1.28 (186)	2.3
8 h at 371°C (700°F)	30.7 (4.45)	1.89 (274)	2.1
15 h at 371°C (700°F)	23.2 (3.36)	2.25 (327)	1.0

Table 7

316°C (600°F) Mechanical Properties of Hughes HR600P Molded Neat Resin Microtensile Specimens

Postcure (In Air)	Tensile Strength MPa (ksi)	Tensile Modulus GPa (ksi)	Elongation To Break (%)
4 h at 317°C (700°F)	15.6 (2.26) ± 0.8 (0.11)	0.020 (29.0)	8.0
8 h at 371°C (700°F)	12.9 (1.87) ± 1.2 (0.18)	0.031 (45.0)	3.6
15 h at 371°C (700°F)	12.9 (1.87) ± 2.0 (0.29)	0.090 (130)	1.1

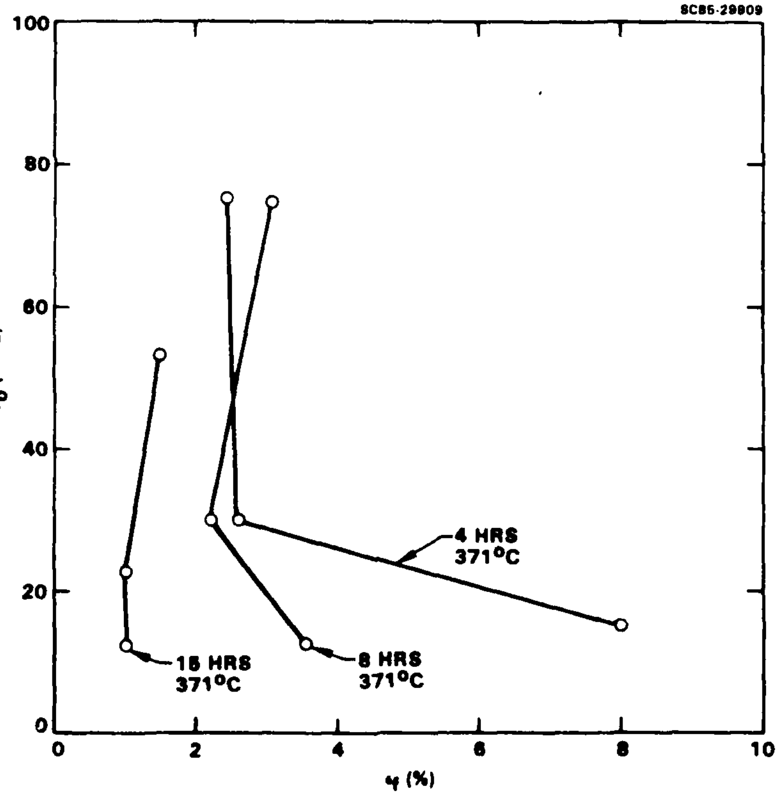

Fig. 14 The effect of postcure on the tensile failure envelopes of HR600P resin.

Table 8

Mechanical Properties of Hughes HR600P Molded Neat Resin Microtensile Specimens Cured 4 h at 371°C (700°F) in Air

Test Condition	Tensile Strength MPa (ksi)	Test Modulus GPa (ksi)	Elongation to Break (%)
24°C (75°F) dry	75.8 (11.0) ± 5.9 (0.8)	3.77 (548) ± 0.19 (28)	2.21 ± 0.36
177°C (350°F) dry	55.9 (8.11) ± 4.3 (0.62)	2.59 (376) ± 0.06 (9)	2.50 ± 0.30
260°C (500°F) dry	30.4 (4.41)	1.28 (186)	2.3
316°C (600°F) dry	15.6 (2.26)	0.020 (29)	8.0

Table 9

Mechanical Properties of Hughes HR600P Molded Neat Resin Microtensile Specimens Moisture Conditioned 4 h at 371°C (700°F) in Air

Test Condition	Tensile Strength MPa (ksi)	Tensile Modulus GPa (ksi)	Elongation To Break (%)
24°C (75°F) wet	75.5 (10.9) ± 9.3 (1.3)	4.56 (661) ± 0.40 (57)	1.80 ± 0.50
177°C (350°F) wet	53.9 (7.82) ± 4.1 (0.60)	2.58 (374) ± 0.12 (18)	2.30 ± 0.30
260°C (500°F) wet	33.9 (4.92) ± 4.1 (0.60)	--	--
316°C (600°F) wet	14.6 (2.12) ± 1.3 (0.19)	--	--

3.1.2.5 Tensile Fracture Surface Analysis

The fracture surfaces of HR600P microtensile specimens were examined by SEM. The fracture surface of a typical room temperature tested specimen is shown in Figs. 15-17. Fracture characteristics of a brittle material are found. Smooth cleavage planes are observed with the "thumbnail" origin zone of fracture well defined.

3.1.3 Composite Cure Cycle Development

3.1.3.1 Prepreg Preparation

Two-thirds of the 1 lb sample of HR600P resin, Lot M1126-39D, was prepregged on Celanese Celion 6000 graphite fiber with PI03 polyimide finish by U.S. Polymeric, Santa Ana, CA. The prepreg was made by the hot-melt method, using a concentrated solution of resin solids in a 4:1 methylethylketone/toluene solvent. Inadvertently, this 0.67 lb of resin was mixed with 2 lb of HR600P, Lot 01-2018P1, and the entire 2.67 lbs of resin prepregged. Lot 01-2018P1 was part of a 110 lb batch of HR600P prepared more recently by Hughes. According to Hughes, this material was very similar to that of Lot No. M1126-39D, except for a narrower molecular weight distribution. Lot M1126-39D of HR600P was part of an earlier lot of resin delivered to the Materials Laboratory by Hughes. Several characterization tests were made to determine the equivalence of the two materials.

A clear distinction between the two resins is shown by the size exclusion liquid chromatographic separations of the two HR600P resin lots in Fig. 18. Lot 01-2018P1 shows a distribution which is shifted to earlier eluted, higher molecular weight oligomers compared to Lot M1126-390. This result was expected, as a more efficient removal of lower molecular weight oligomers was reported by Hughes in the larger scale synthesis.

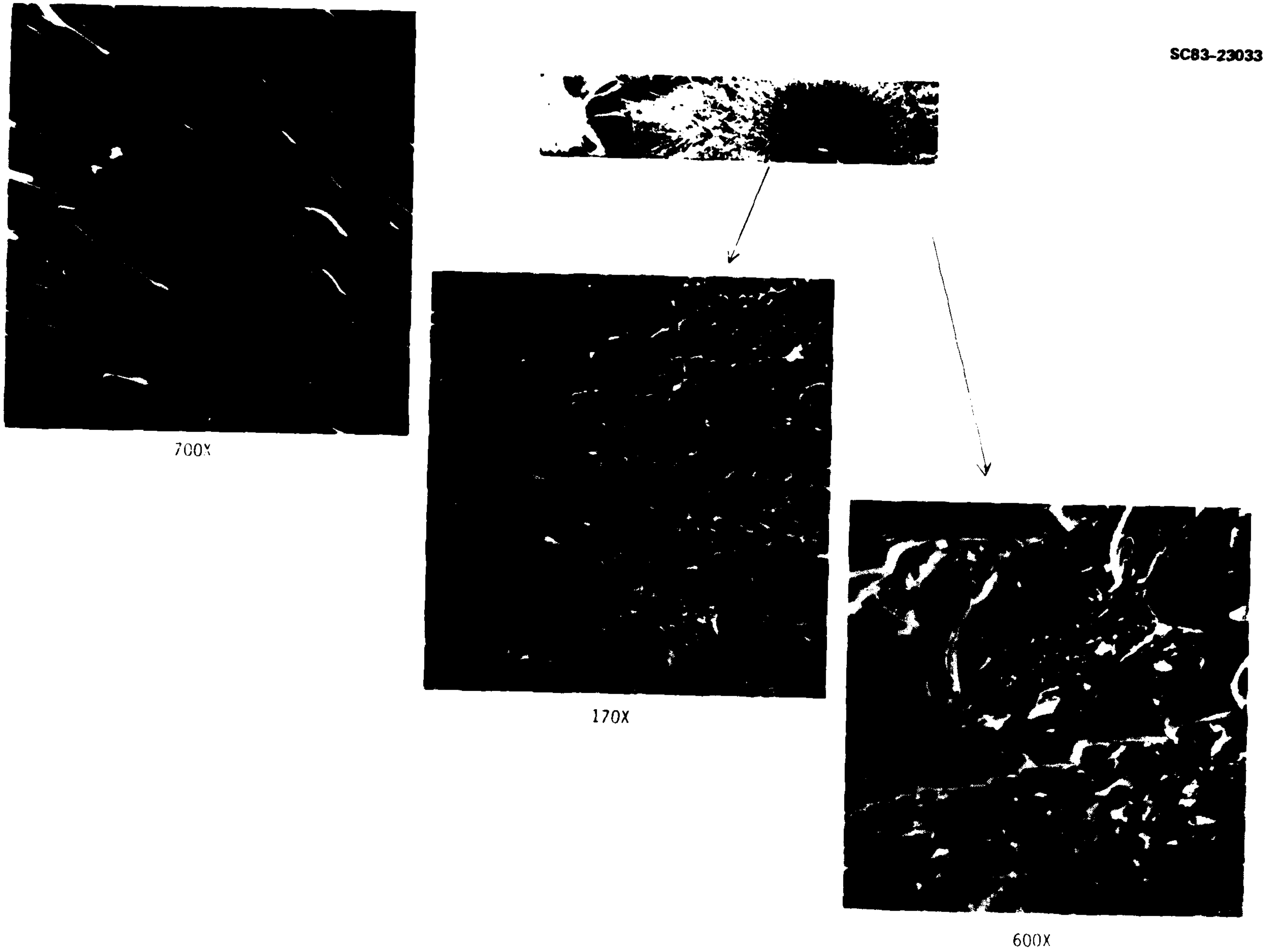

Fig. 15 SEM micrographs of HR600P neat resin tensile fracture surface.

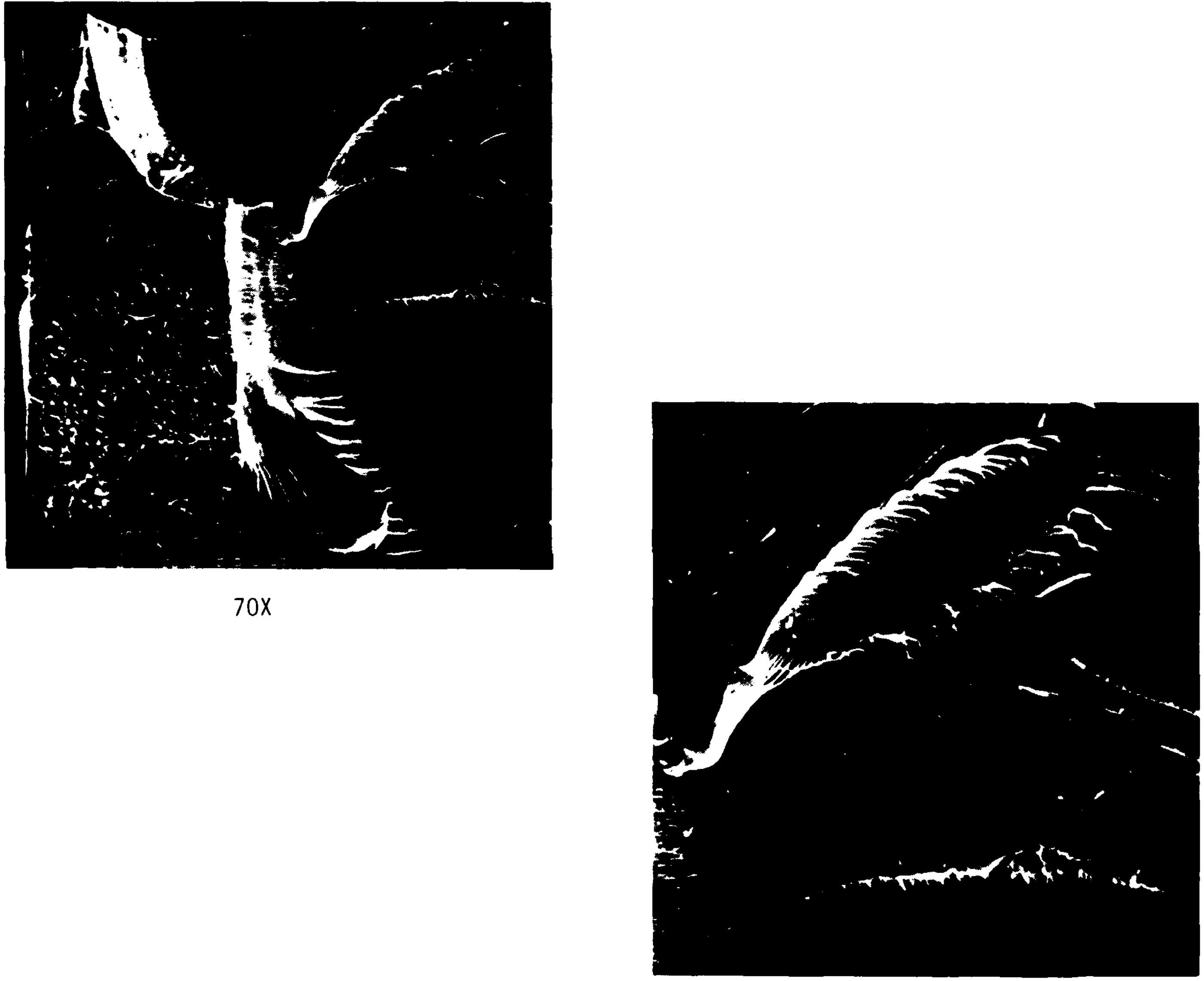

70X

140X

Fig. 16 SEM micrographs of HR600P neat resin tensile fracture surface.

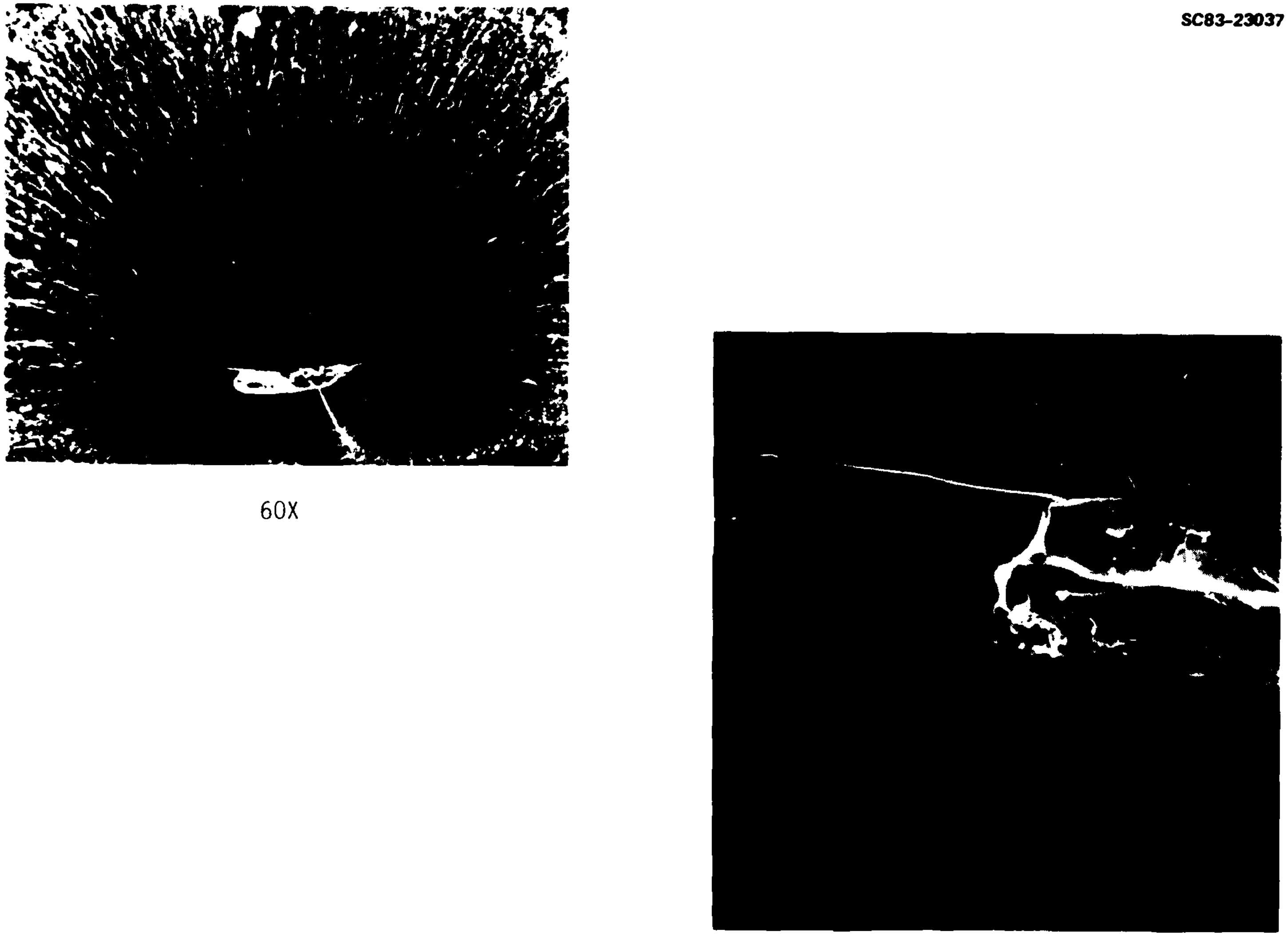

60X

500X

Fig. 17 SEM micrographs of HR600P neat resin tensile fracture surface.

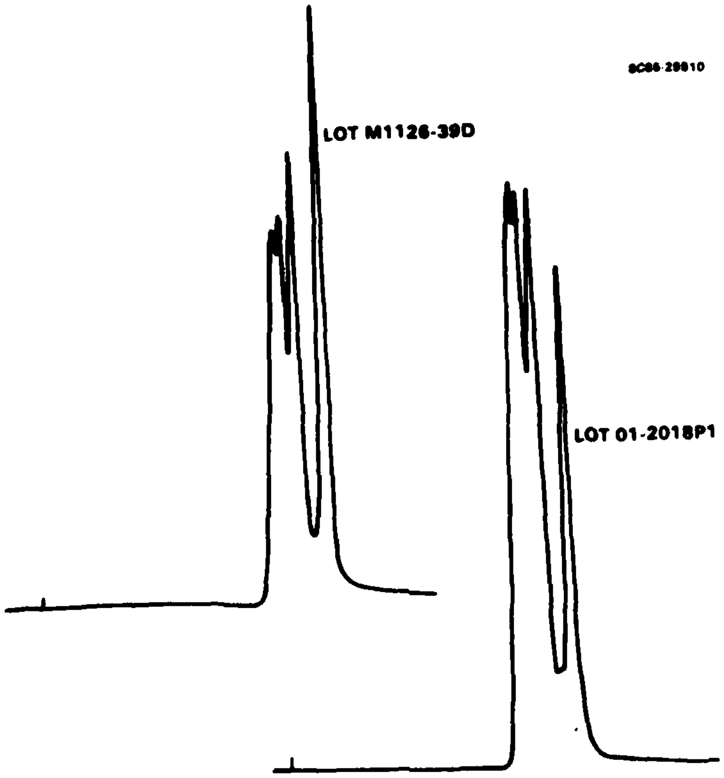

Fig. 18 Size exclusion liquid chromatographic analysis of HR600P resin materials.

A comparison of the dynamic viscosity of the two resins during a 2°C/min (3.6°F/min) heating ramp is shown in Fig. 19. The flow behavior of the two resins is similar. Gelation also occurs at about the same temperature for the two materials.

The physical characteristics of the two Celion 6K/HR600P prepreg lots prepared by U.S. Polymeric are given in Table 10. These include the material prepared from the mixing of the two resin lots and that prepared exclusively from resin Lot 01-2018P1. The total volatiles measured for a 204°C (400°F) exposure were close to 5% with an additional loss of about 1% on subsequent exposure to 371°C (700°F). The prepreg was fragile and had no tack or drape as received. The overall cosmetic quality was good; however, the surface of the prepregs had a powdery layer of resin which was easily removed in handling.

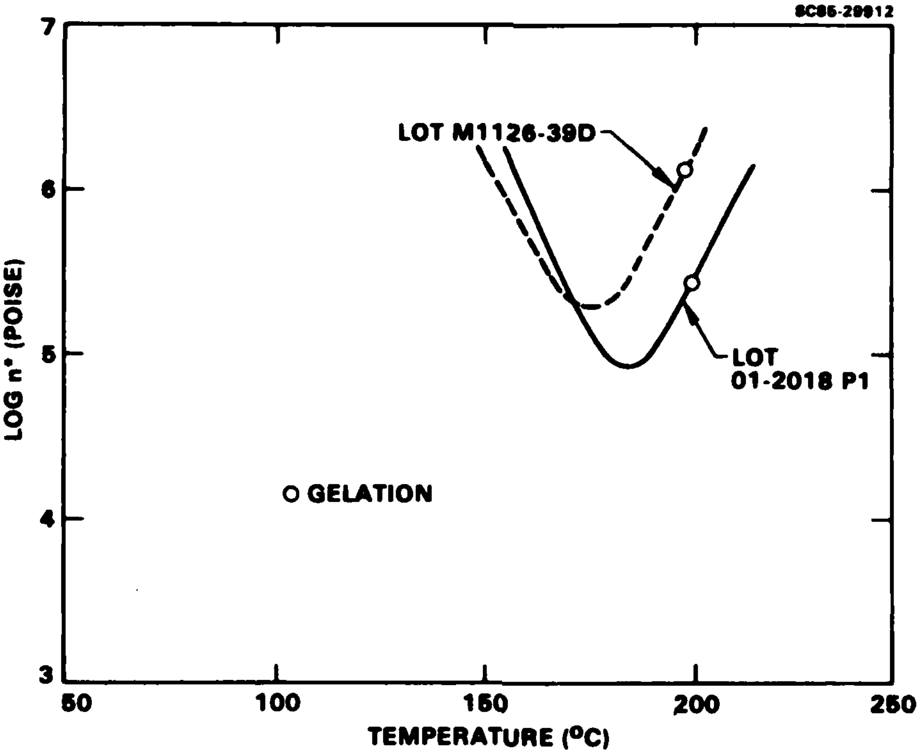

Fig. 19 Dynamic viscosity during cure of HR600P resins at 2°C/min (3.6°F/min).

Table 10

Physical Properties of Hughes Celion 6K/HR600P Prepreg Tape

Property	Prepreg Lot 3W 2498 "Mixed"	Prepreg Lot 3W 2497 "Pure"
Resin Content	34%	37%
Total volatiles to 400°F	4.96%	5.32%
Total volatiles to 700°F	6.08%	6.69%
Tack	None	None
Drape	None	None

3.1.3.2 Laminate Fabrication

Preliminary studies of HR600P processing were made as part of an IR&D program at Rockwell's Shuttle Orbiter Division in Downey, CA. The prepreg used in those experiments was prepared from HR600P resin from the 110 lb lot

(Lot 01-2018P1) with 7781 E-glass fabric. The prepreg was prepared by the solvent impregnation technique using a 4:1 methylethylketone/toluene solvent by U.S. Polymeric, Santa Ana, CA. The glass fabric was sized with a polyimide based resin identified as CS721. The volatiles for the individually prepared prepreg sheets averaged 3-4% to 204°C (400°F) and the resin solids 37-39%. Early experiments indicated that a process consisting of a 30 min dwell at 157°C (315°F) with 2 in. Hg vacuum, followed by application of 150 psi with full vacuum and heating to 204°C (400°F), and holding for 2 h gave a laminate of proper per ply thickness and appearance. Ultrasonic C-scan measurements were made on these 9 ply ~ 5 in. x 5 in. panels before and after a 4 h postcure at 371°C (700°F). The results of the C-scan experiments are shown in Figs. 20-24. Most of the laminates showed some porosity prior to postcure, but all blistered with postcure to give blank C-scans. Photomicrographs with an example of the porosity are shown in Fig. 25.

A series of graphite panels were prepared using the optimum 30 min 157°C (315°F) dwell condition. A summary of the cure conditions are given in Table 11. C-scans for six of the seven panels before and after postcure are shown in Figs. 26-31. In all cases, the C-scans indicate the presence of porosity before postcure. Subsequent postcure again resulted in blistering and further deterioration in C-scan data. An example of the voids present in these graphite laminates is shown in the photomicrographs of Fig. 32.

Compression molding of HR600P prepreg was investigated as an alternative to autoclave processing. Four-point shear specimens of dimensions 3.5 in. x 0.5 in. x 0.14 in. (27 plies) were fabricated in steel molds. Prepreg from the mixed lot was used. The first specimens were molded as close as possible to the preliminary autoclave cure cycle consisting of a 30 min hold in vacuum at 157°C (315°F), after which 150 psi was applied and the temperature increased to 204°C (400°F) and held 2 h. These specimens also showed significant porosity as shown in photomicrographs of cross sections. The four-point shear strength of these was ~ 53 MPa (7.7 ksi).

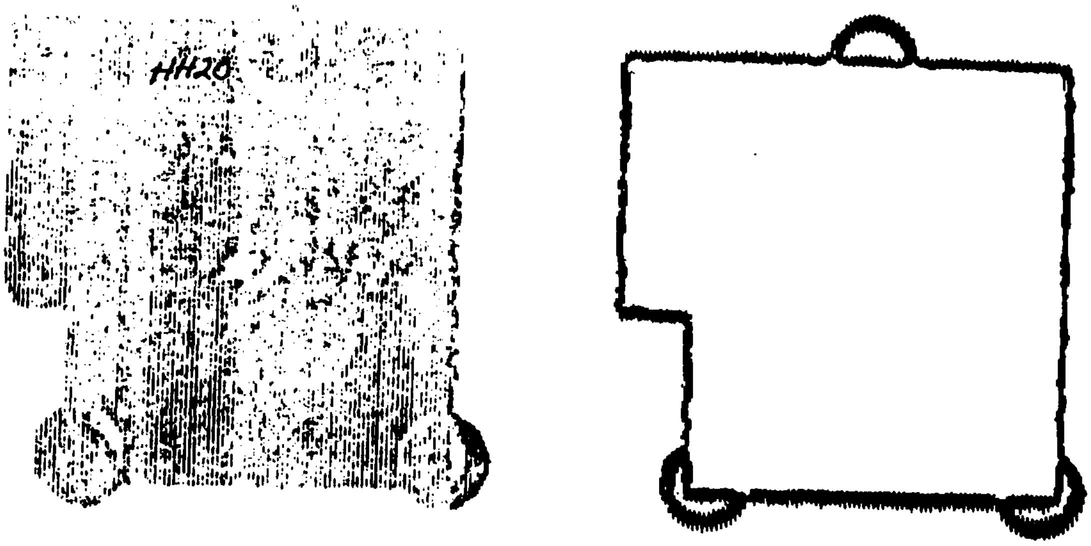

BEFORE POSTCURE

AFTER POSTCURE

Fig. 20 Ultrasonic C-scan of 7781E/HR600P laminate.

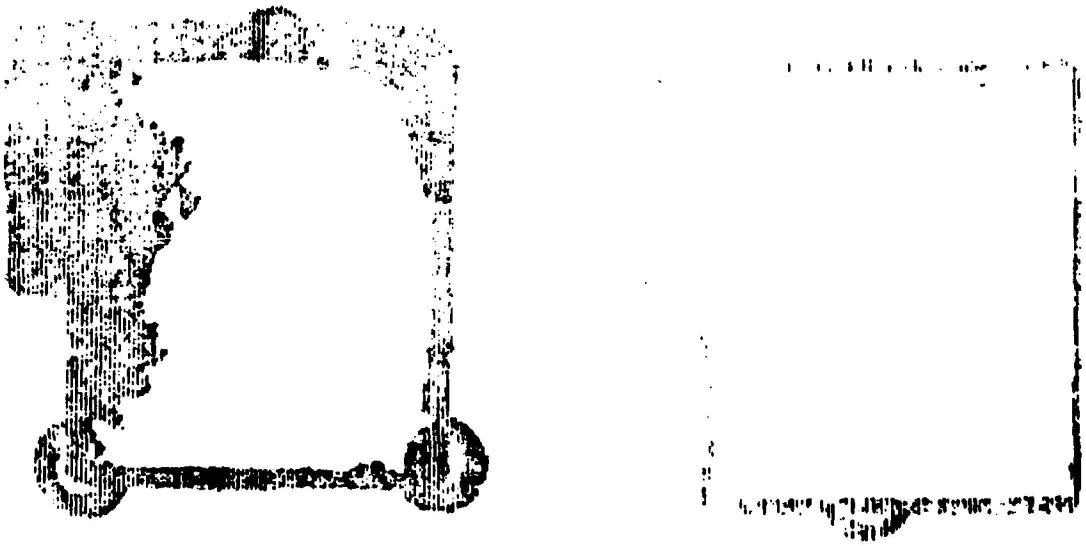

BEFORE POSTCURE

AFTER POSTCURE

Fig. 21 Ultrasonic C-scan of 7781E/HR600P laminate.

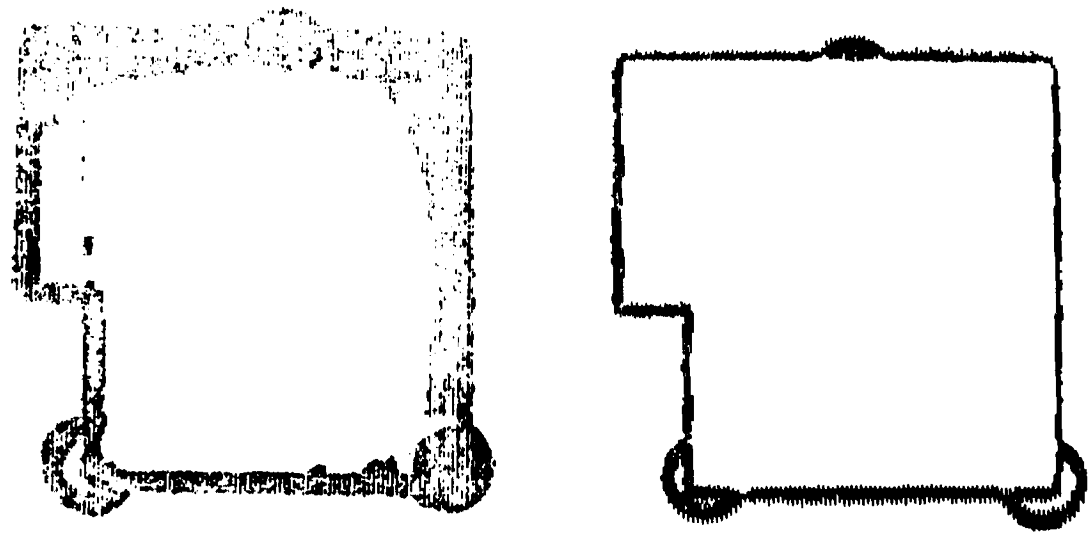

BEFORE POSTCURE

AFTER POSTCURE

Fig. 22 Ultrasonic C-scan of 7781E/HR600P laminate.

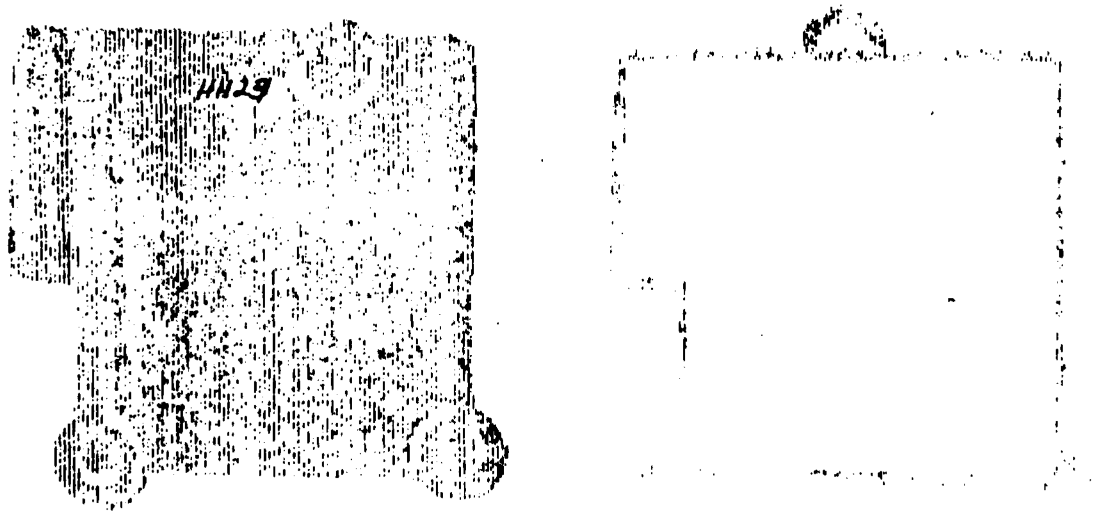

BEFORE POSTCURE

AFTER POSTCURE

Fig. 23 Ultrasonic C-scan of 7781E/HR600P laminate.

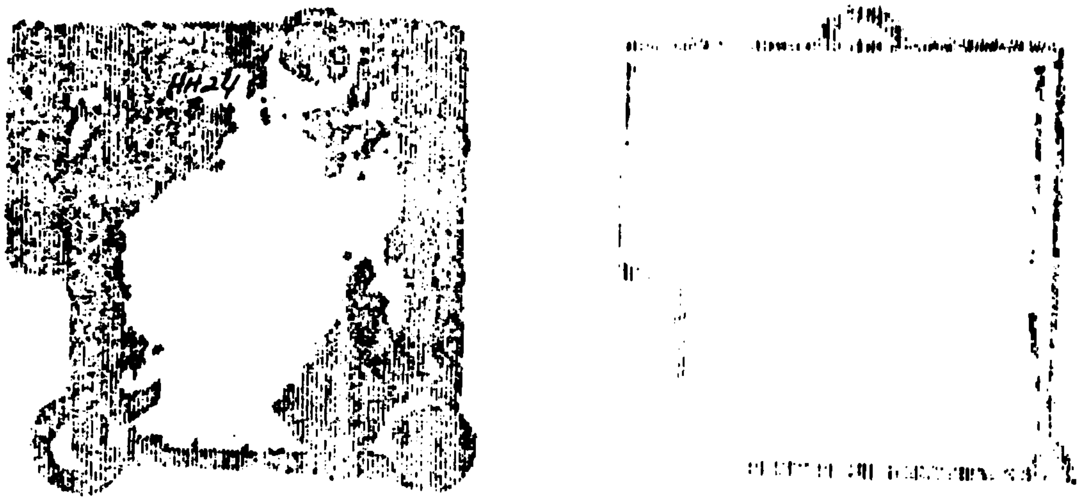

BEFORE POSTCURE

AFTER POSTCURE

Fig. 24 Ultrasonic C-scan of 7781E/HR600P laminate.

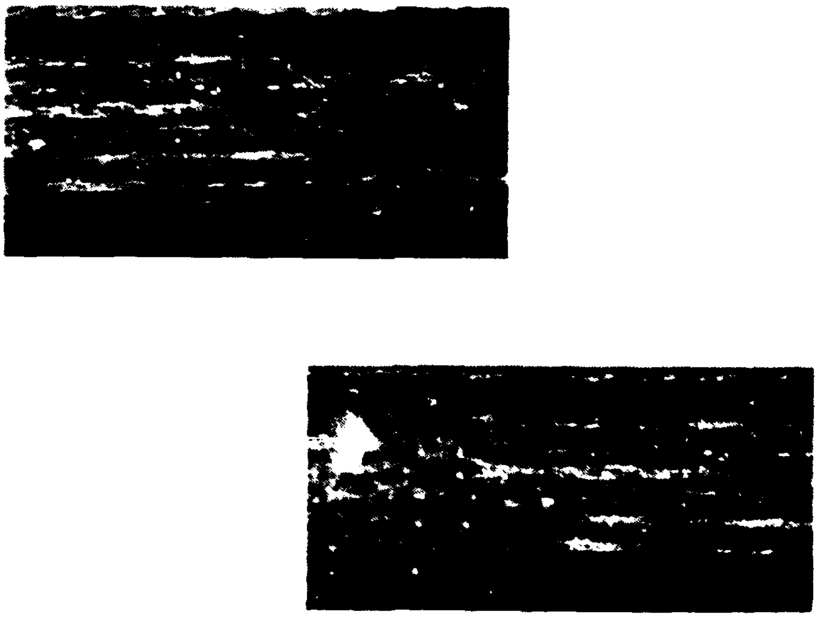

Fig. 25 Photomicrograph of 7781E/HR600P cross sections.

Table 11

Hughes HR600P/Celion 6K/P103 Graphite Composites - 13 Ply Unidirectional, In Situ Staging, No Bleeder 2 h 400°F or 500°F Cure in Autoclave 4 h 700°F Postcure in Oven

	Staging Conditions 2 in. Hg	150 psi Pressure Applied Full Vacuum	Autoclave Cure Temperature	Thickness Mils/Ply
HI1	30 min, 315°F	315°F	400°F	5.4-5.8
HI2	30 min, 315°F	315°F	400°F	5.5-5.7
HI3	30 min, 315°F	315°F	400°F	4.6-5.7
HI4	30 min, 315°F	315°F	400°F	5.0-5.8
HI5	30 min, 315°F	315°F	400°F	4.8-5.8
HI6	30 min, 315°F	315°F	400°F	5.4-5.9
HI7	30 min, 315°F	315°F	400°F	5.0-5.4

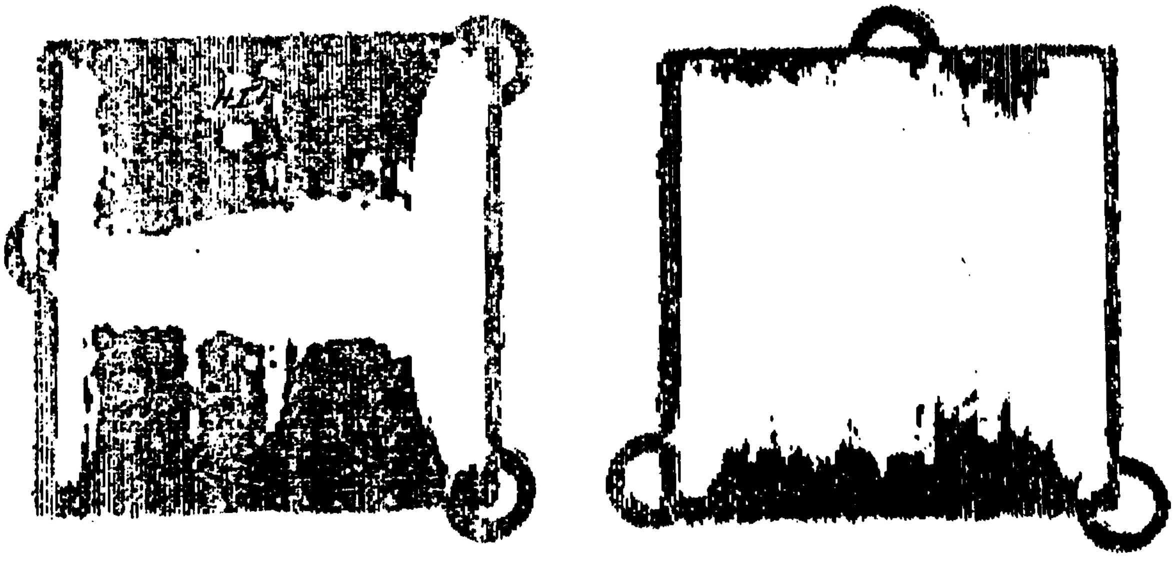
BEFORE POSTCURE

AFTER POSTCURE

Fig. 26 Ultrasonic C-scan of Celion 6K/HR600P laminate.

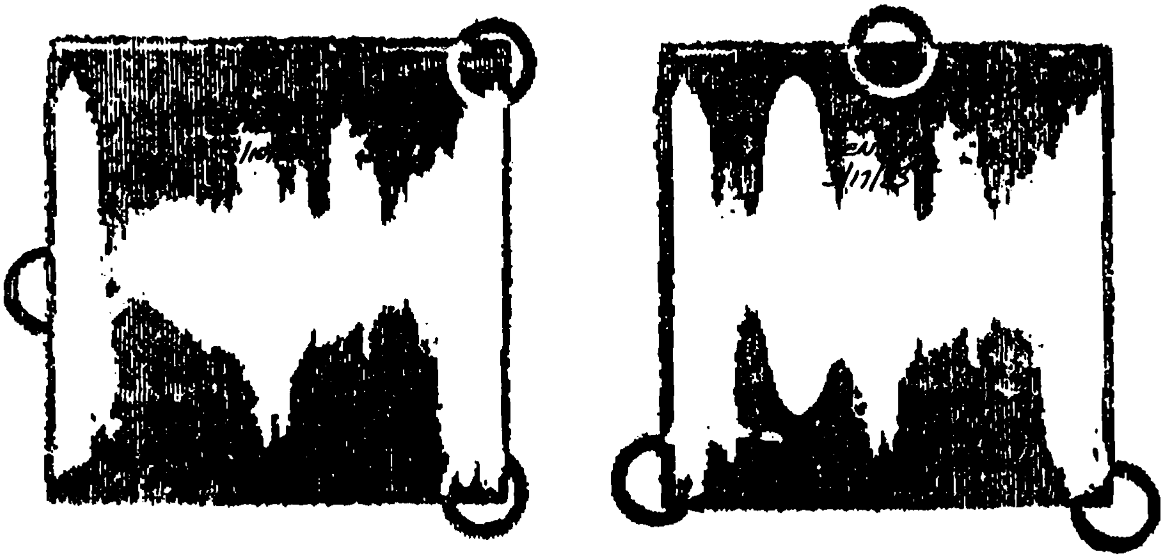

BEFORE POSTCURE AFTER POSTCURE

Fig. 27 Ultrasonic C-scan of Celion 6K/HR600P laminate.

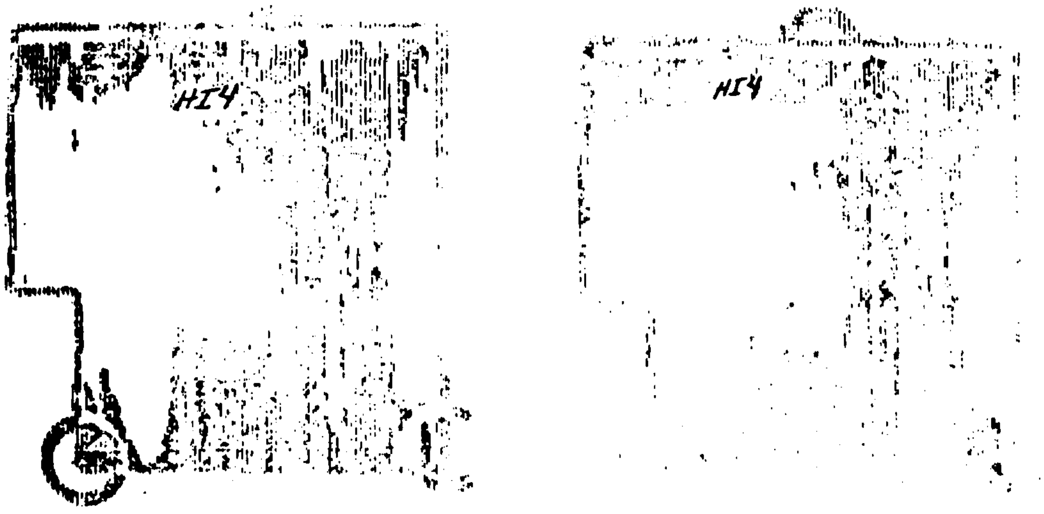

BEFORE POSTCURE AFTER POSTCURE

Fig. 28 Ultrasonic C-scan of Celion 6K/HR600P laminate.

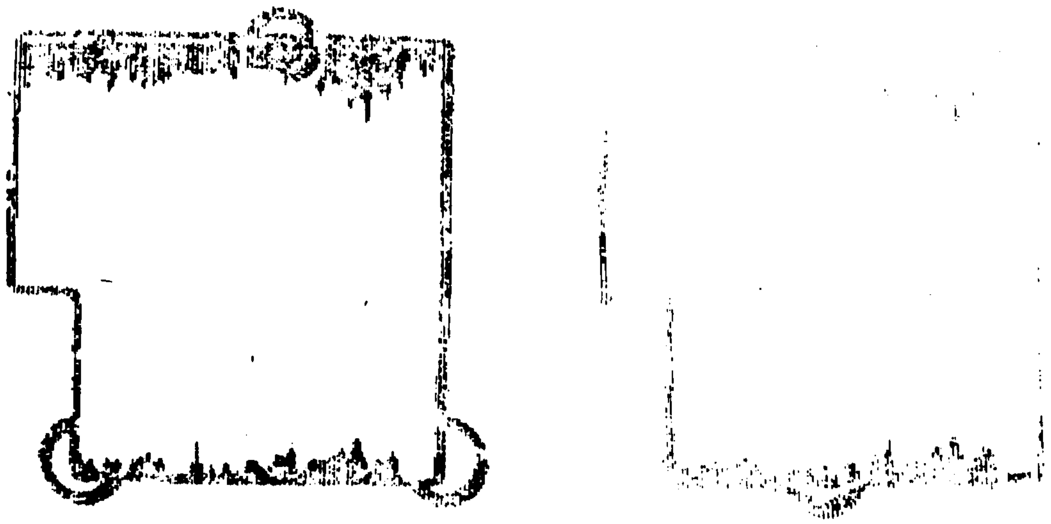

BEFORE POSTCURE

AFTER POSTCURE

Fig. 29 Ultrasonic C-scan of Celion 6K/HR600P laminate.

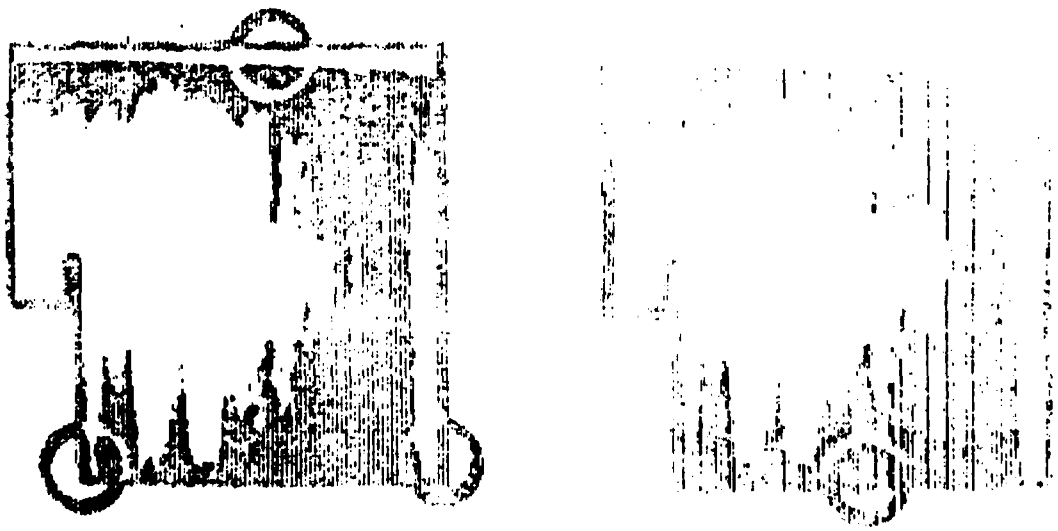

BEFORE POSTCURE

AFTER POSTCURE

Fig. 30 Ultrasonic C-scan of Celion 6K/HR600P laminate.

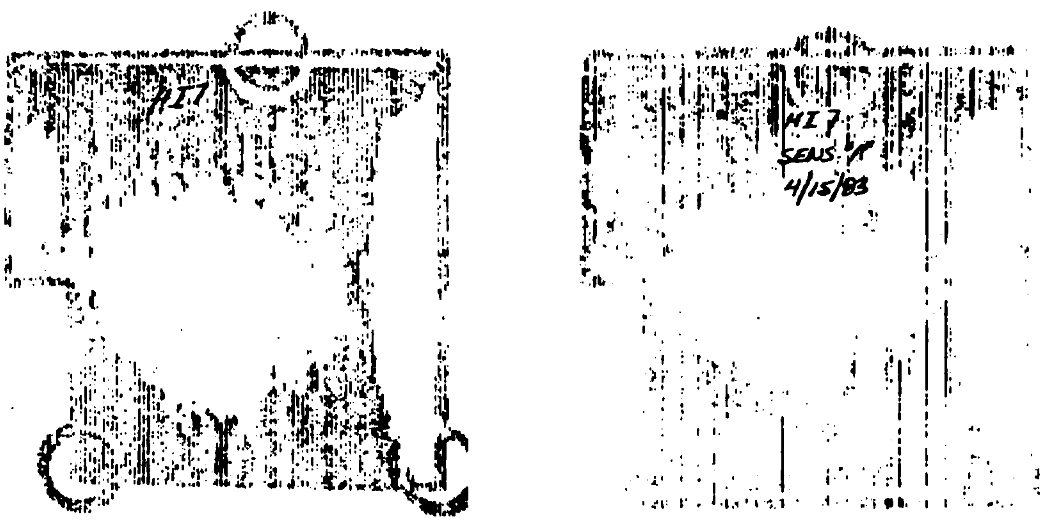

Fig. 31 Ultrasonic C-scan of Celion 6K/HR600P.

SC83-23039

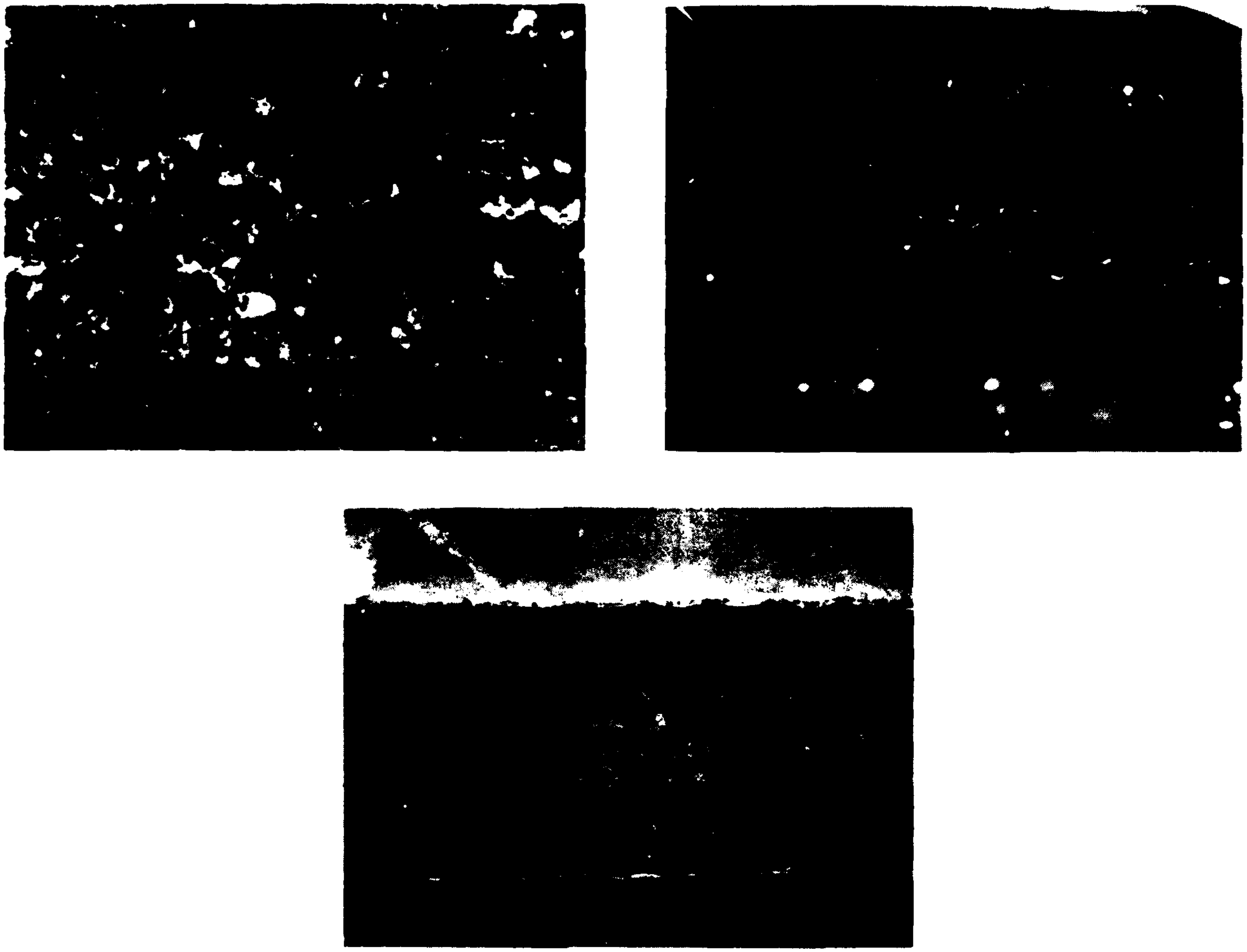

Fig. 32 Photomicrographs of Celion 6K/HR600P cross section.

Other specimens were molded according to the neat resin cure process described in Section 1.1.2. The interlaminar shear strength of these specimens was ~ 51 MPa (7.4 ksi). Photomicrographs of cross sections again revealed the presence of voids. The use of a higher molding pressure of 41 MPa (6.0 ksi) did not improve the interlaminar shear strength or the porosity. Two further four-point shear specimens were molded according to the neat resin cure procedure. One was postcured 4 h at 260°C (500°F) and the other 4 h at 371°C (700°F). The interlaminar shear strength of these was 54 MPa (7.8 ksi) and 38 MPa (5.6 ksi), respectively. They also contained porosity.

SEM characterization was made of the interlaminar shear fracture surfaces, and are shown in the micrographs of Figs. 33-34. The failure surfaces of the molded specimens were similar. The features appear somewhat different from those shown for the interlaminar shear surface of graphite/epoxy laminates by Browning.[3] The resin deformation in the Célion 6K/HR600P specimens does not show the platelet-like regularity seen in the epoxy composite failure surfaces. This may result from a lower ductility of HR600P. A greater amount of bare fiber surface is also evident in the HR600P composite. It is not understood whether these features are related to the low interlaminar shear strengths measured.

Work at this point was discontinued on HR600P composite fabrication. Several problems with the materials were later identified by Hughes Aircraft and National Starch Corporation. Evidence indicated that the early materials contained some amic acid form of the polymer due to moisture contamination. Conversion of the amic acid to isoimide or imide at high temperature may have been responsible for the persistent porosity observed. Recent work by others, with new IP600 resin materials has given good quality composite.

The graphite composite work may also have been influenced by the PI03 polyimide size used with the Celion 6K fiber. IR&D studies at Rockwell's Shuttle Orbiter Division in Downey, CA showed that Celion 6K/LARC-160 composite, prepared with fiber having the PI03 finish, had much lower interlaminar shear strength compared to composite in which the Celion 6K was sized with

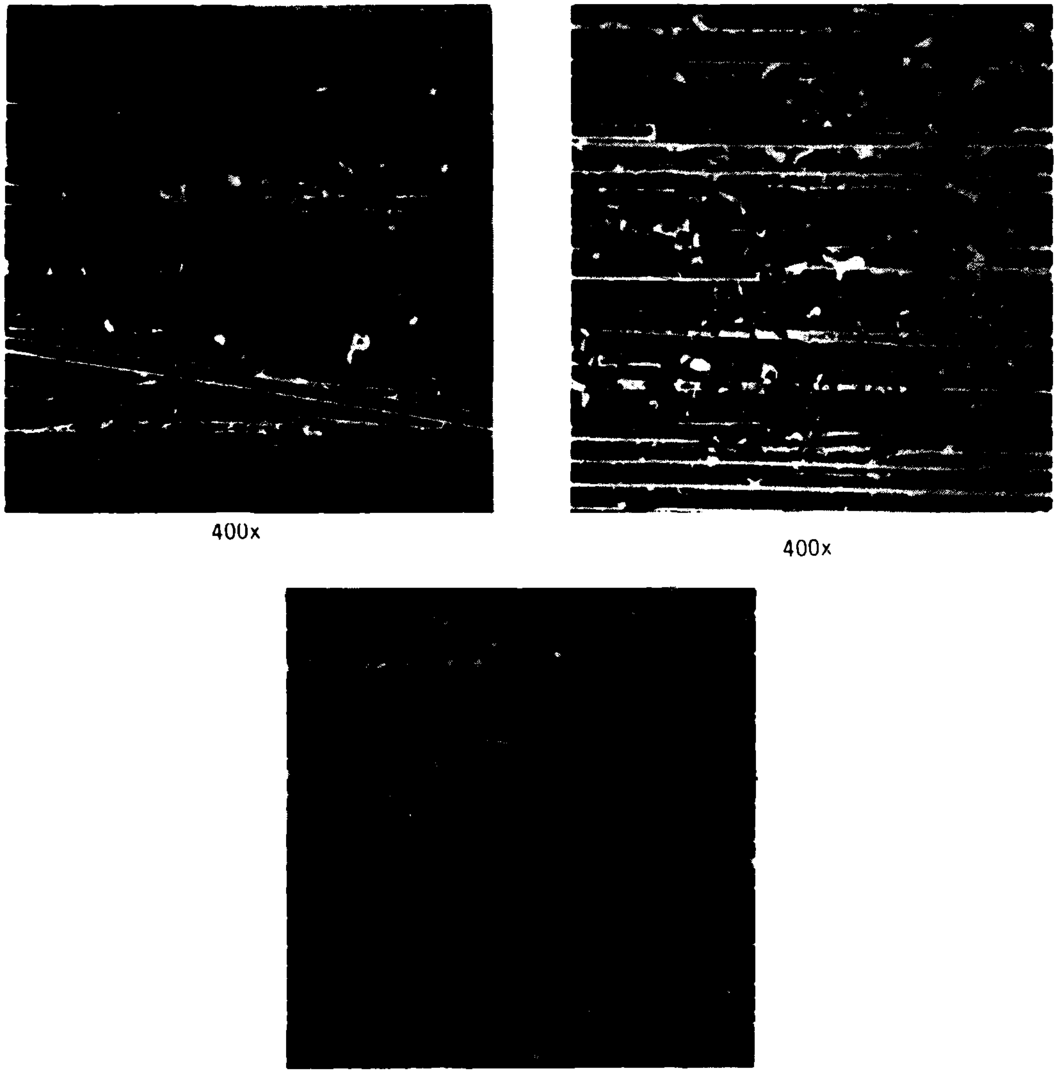

400x

400x

400x

Fig. 33 SEM micrographs of Celion 6K/HR600P interlaminar shear fracture surface.

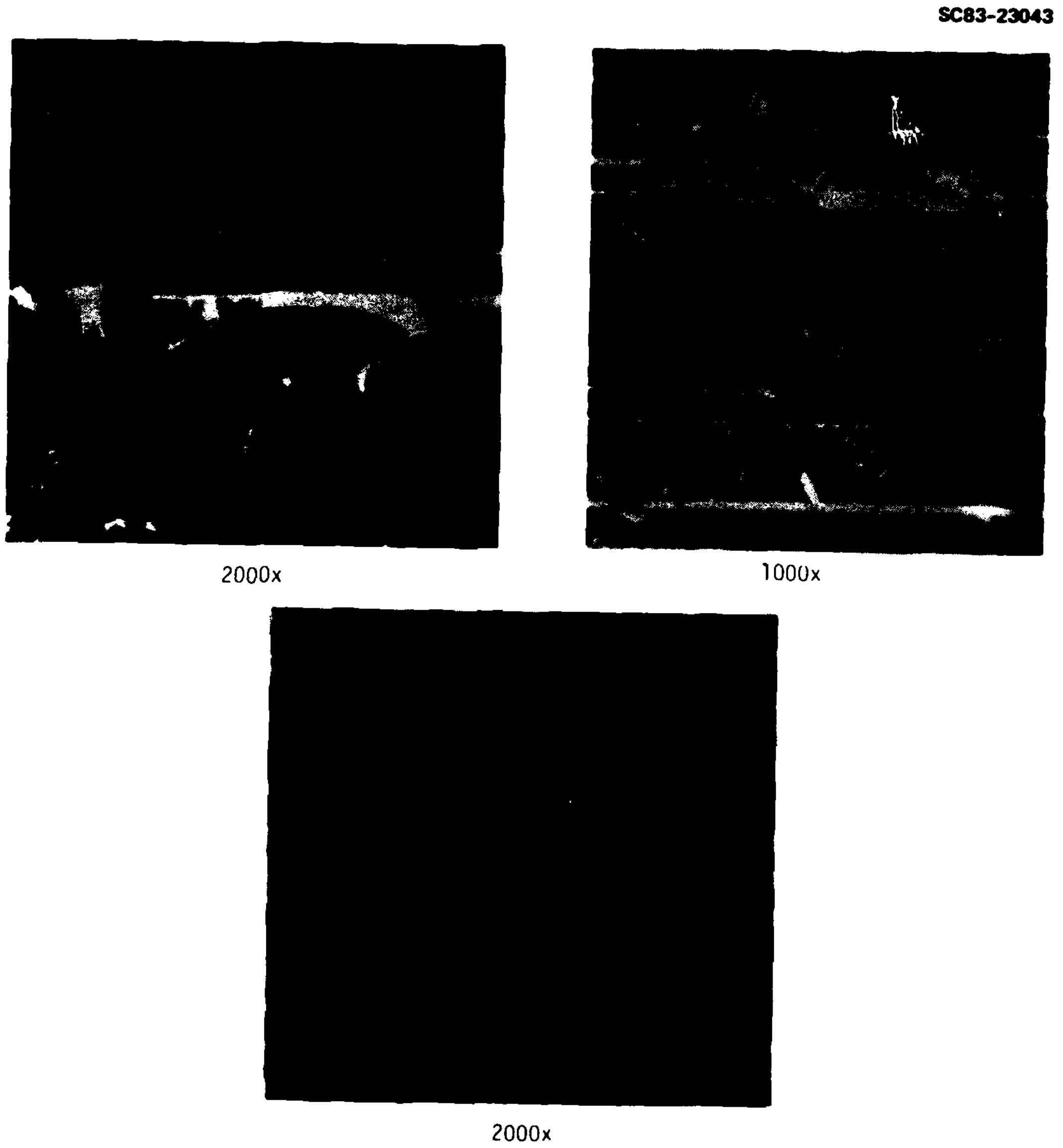

Fig. 34 SEM micrographs of Celion 6K/HR600P interlaminar shear fracture surface.

epoxy-compatible finish. Continued difficulties with this sizing led to its eventual removal from the market by Celanese.

The dynamic viscoelastic behavior of Celion 6K/HR600P is shown in Fig. 35. The modulus decreases continuously with temperature above about 100°C (212°F). A clear T_g was not indicated up to 350°C (662°F). TMA studies indicated T_g was well below 316°C (600°F) in all cases, and did not correlate well with neat resin data.

3.2 Air Force BATQ-H Resin

BATQ-H is one of a family of acetylene-terminated resins developed by the Air Force Wright Aeronautical Laboratories. The molecular structure of this material is shown in Fig. 36. The high molecular weight structure between the acetylene groups provides an increased fracture toughness, but the uncured T_g of 185°C (365°F) hinders processing. To improve the processability of this resin, a reactive diluent, 3 phenoxy 3' ethynyl-diphenyl ether (ATP), was *added. The structure of this liquid compound is also shown in Fig. 36.* The Air Force Materials Laboratory determined that a 95/5 weight ratio of

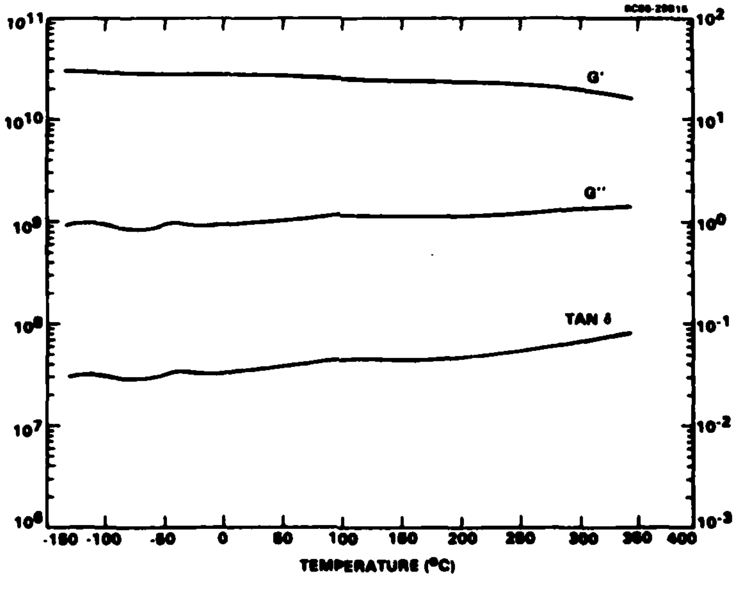

Fig. 35 Dynamic viscoelastic analysis fo Celion 6K/HR600P.

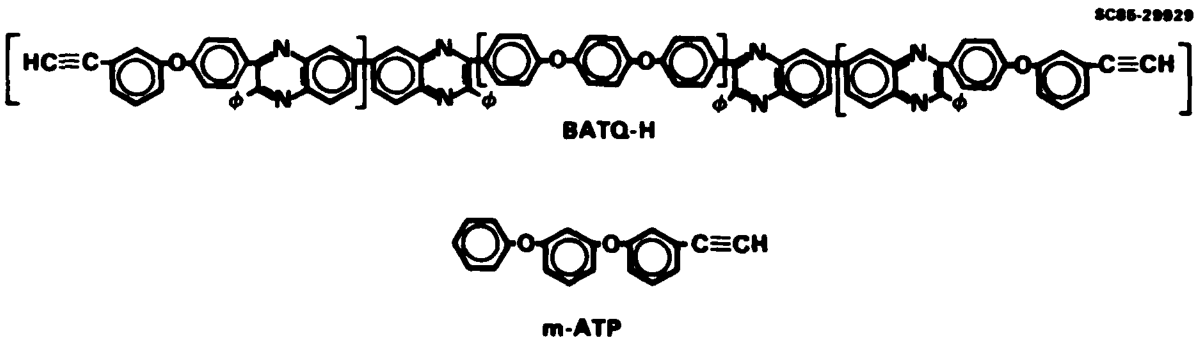

Fig. 36 Molecular structures of BATQ-H resin and ATP reactive diluent.

resin to diluent was sufficient to ensure adequate processability. This composition was used throughout the program for neat resin and composite studies. Gulf Research and Development Corporation synthesized the BATQ-H resin and it was further purified by the Air Force Materials Laboratory before delivery to Rockwell International. The composition of the BATQ-H was reported by the Air Force Materials Laboratory to be 48.8% monomer, 57.7% dimer, 20.7% trimer and 4.5% n = 0 product.

The formulated resin was prepared by dissolving the two ingredients in benzene to ensure complete mixing. Excess benzene was removed by evaporation to give a solution containing ~ 10% resin solids. This concentrated resin solution was frozen in liquid nitrogen and subsequently freeze-dried under vacuum at -15°C for 72 h to remove the benzene. The resin was then ground to a powder and dried at 140°C under vacuum for 2 h. Freeze-drying of the resin mixture is necessary to prevent phase separation of the ATP. Microtensile specimens, prepared from a BATQ-H/ATP mixture in which the benzene solvent was removed by evaporation, showed regions of what appeared to be a brittle phase, which was probably polymerized ATP.

3.2.1 Materials Validation

3.2.1.1 Differential Scanning Calorimetry

The cure behavior of BATQ-H/ATP is shown in Fig. 37. A single symmetric exotherm was found for all heating rate experiments. The effect of heating rate on the exotherm peak temperature, T_{max}, is plotted in Fig. 38 according to a modified Arrhenius expression developed by Duswalt.[1] The activation energy for polymerization of the uncured resin is 23.9 kcal/mole. The characteristic DSC parameters are given in Table 13. From these data, the resin would appear to require a higher temperature and longer time to cure compared to Hughes HR600P resin.

SC83-22841

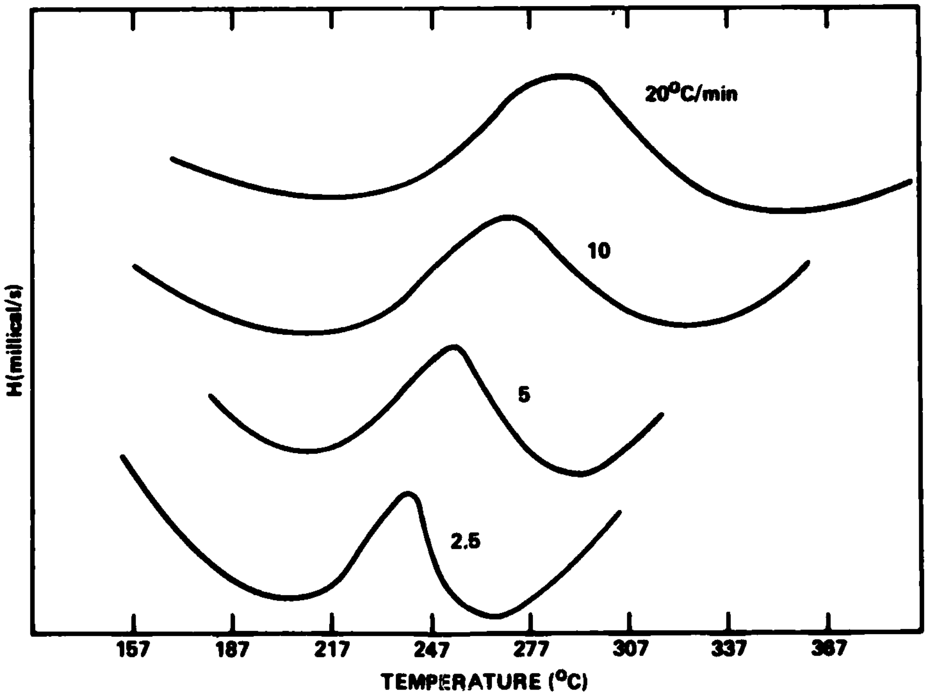

Fig. 37 DSC thermograms of BATQ-H (ATP) resin

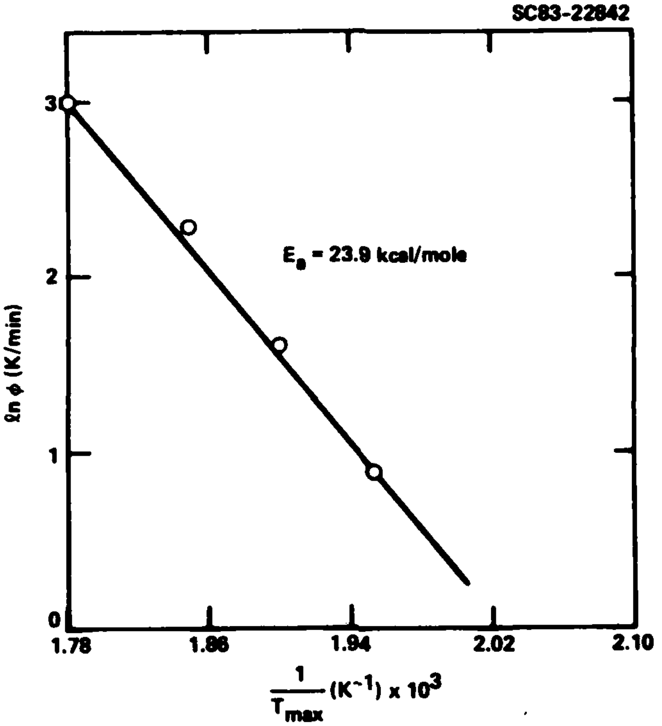

Fig. 38 Dependence of DSC exotherm peak temperature with heating rate from BATQ-H (ATP) resin.

Table 12

DSC Analysis of BATQ-H (ATP) Neat Resin

Uncured melt temperature		~ 180°C (356°F)
Exotherm onset temperature	(ϕ = 10°C/min)	207°C (405°F)
Exotherm peak temperature	(ϕ = 10°C/min)	269°C (516°F)
Exotherm completion temperature	(ϕ = 10°C/min)	325°C (617°F)
Heat of polymerization		35 cal/g
Activation energy for polymerization		23.9 kcal/mole

3.2.1.2 Cure Rheology

The rheological properties of BATQ-H (ATP) during cure were studied at several linear heating rates and are plotted in Fig. 39. The resin softens sufficiently by ~ 180°C (356°F) to begin parallel-plate measurements. The flow behavior is similar to that exhibited by HR600P resin in Fig. 4. Isothermal viscosity data are plotted in Fig. 40. Under isothermal conditions, the resin shows somewhat less flow than HR600P resin in Fig. 5.

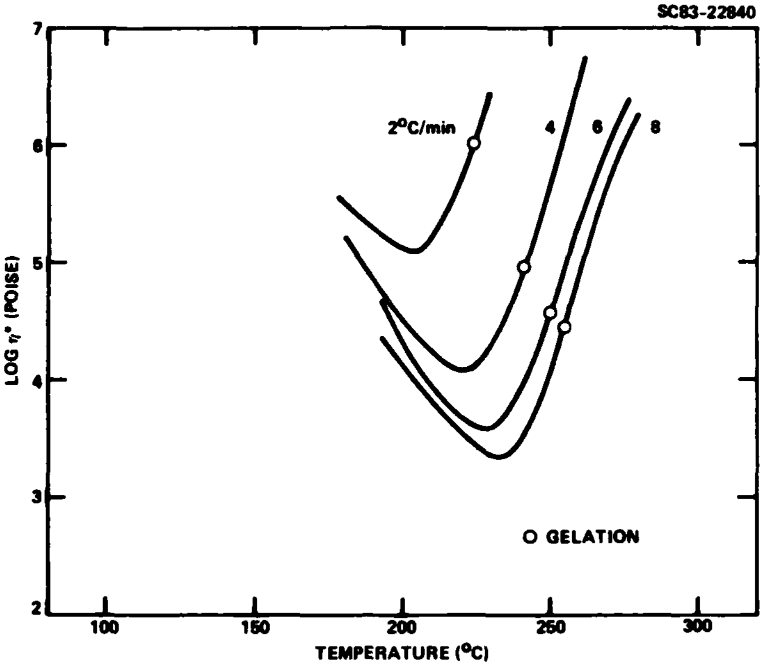

Fig. 39 Dynamic viscosity during cure of BATQ-H (ATP) resin at different heating rates.

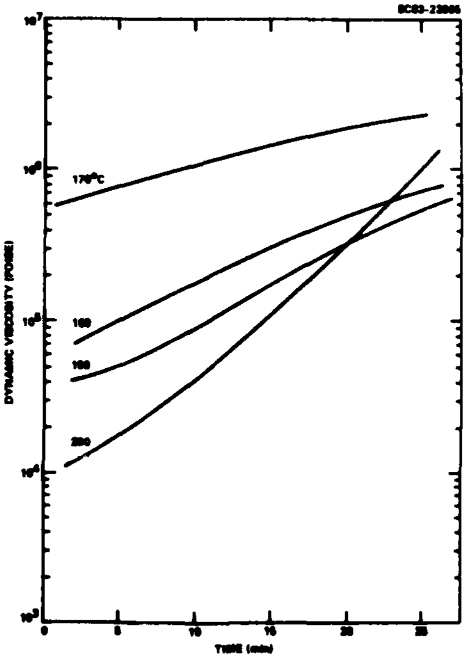

Fig. 40 Dynamic viscosity during cure of BATQ-H (ATP) resin at different heating rates.

3.2.2 Neat Resin Cure Cycle Development

3.2.2.1 Microtensile Specimen Preparation

BATQ-H(ATP) is a low flow resin requiring the use of compression molding to prepare neat resin microtensile specimens. A three-step molding process, similar to that used for molding HR600P, was required to prepare void-free specimens. It consisted of a devolatilization, followed by consolidation and a final curing step. The molding procedure is outlined in Table 13. Specimens were 40-50 mils in thickness having a tensile strength of about 110 MPa (16 ksi) with an ultimate elongation over 6%.

Table 13
Compression Molding Procedure for Air Force BATQ-H/ATP
Neat Resin Microtensile Specimens

1. Change mold at room temperature and wrap with shrink tape.
2. Degas for 15 min at 150°C (302°F).
3. Cure at 10-20 ksi for 1 h at each of the following temperatures: 150, 170, 190, 210 and 225°C (302, 338, 374, 410 and 437°F).
4. Remove from mold while hot.

3.2.2.2 Thermomechanical Analysis

The second step in the development of a neat resin cure cycle for BATQ-H(ATP) resin was to select an appropriate postcure cycle. Glass transition temperatures were measured by thermomechanical analysis for postcures of 250°C (482°F), 316°C (600°F) and 371°C (700°F). The results are summarized in Table 14.

Table 14

The Effect of Postcure Conditions on the Glass Transition Temperature of BATQ-H(ATP) Resin

Postcure		T_g (°C)	T_g (°F)
None, Molded Only		255 ± 11	491 ± 20
4.5 h	250°C	277 ± 2	531 ± 4
9 h	250°C	289 ± 2	551 ± 4
13.5 h	250°C	290 ± 4	554 ± 7
4.5 h	316°C	305 ± 4	581 ± 7
9 h	316°C	299 ± 2	571 ± 4
13.5 h	316°C	298 ± 5	570 ± 9
4.5 h	371°C	296 ± 4	565 ± 7
9 h	371°C	297 ± 7	567 ± 13
13.5 h	371°C	287 ± 2	549 ± 4

Each measurement was the average of three determinations. The data are unusual in that higher temperatures or longer postcures do not increase the cured glass transition temperature beyond ~ 300°C (572°F). Based on these results, it appears that BATQ-H (ATP) would at most be a 260°C (500°F) service resin. Other factors, such as thermal stability and high temperature mechanical properties, however, were also considered in selecting a cure cycle.

3.2.2.3 Thermogravimetric Analysis

The thermogravimetric analysis of uncured and postcured (4.5 h 250°C (482°F)) BATQ-H (ATP) in air is shown in Fig. 41. The uncured resin loses about 1.3% of its weight between 180°C (356°F) and the onset temperature of degradation of ~ 460°C (860°F). The "knee" or temperature inflection point for major degradation is ~ 530°C (986°F).

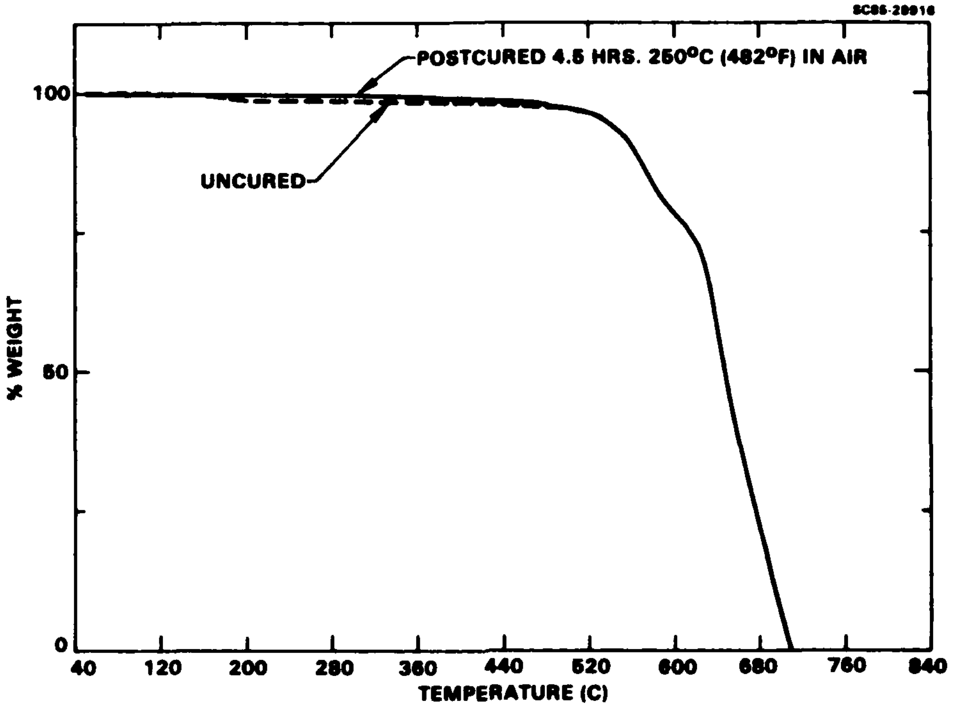

Fig. 41 Thermogravimetric behavior of BATQ-H (ATP) resin in air.

The effect of environment on the thermal stability of 4 h 250°C (482°F) postcured resin is shown in Fig. 42. The resin has a high char yield of 73% to 800°C (1472°F) in nitrogen. In air, the "knee" temperature for major degradation is slightly higher prior to its rapid loss above ~ 600°C (1112°F).

The thermal stability in nitrogen of resin cured 13.5 h at 316°C (600°F) is compared to that cured 4.5 h at 250°C (482°F) in Fig. 43. The higher temperature postcured material shows a slightly higher char yield of 75%. The thermal stability of the two materials in air are shown in Fig. 44. The results are almost identical.

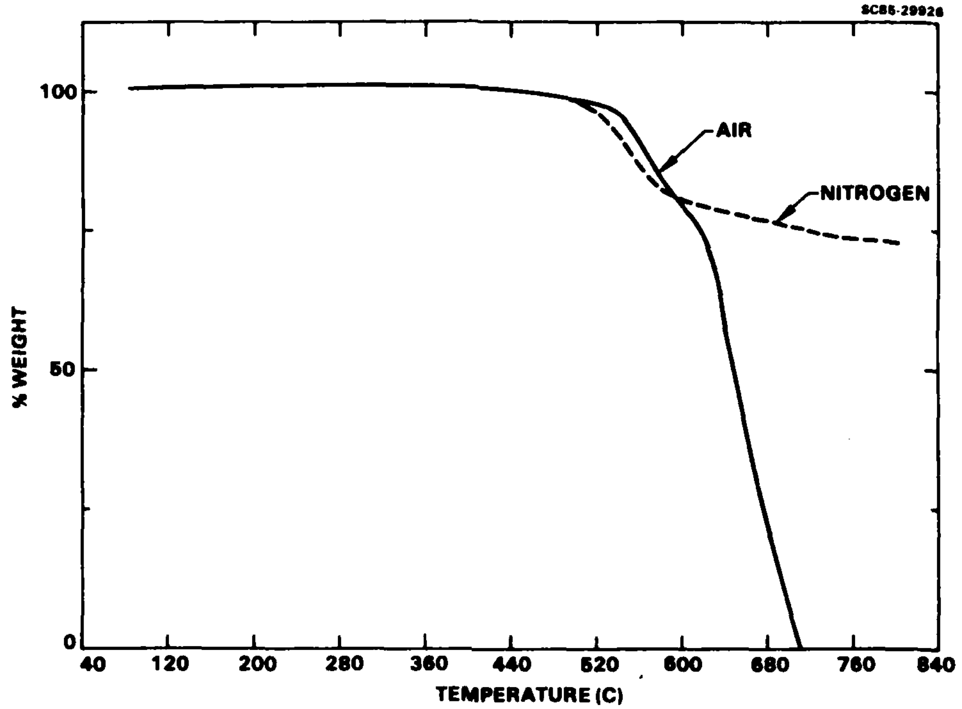

Fig. 42 The effect of environment on the thermograviometric behavior of BATQ-H (ATP) resin postcured 4.5 h at 250°C (482°F) in air.

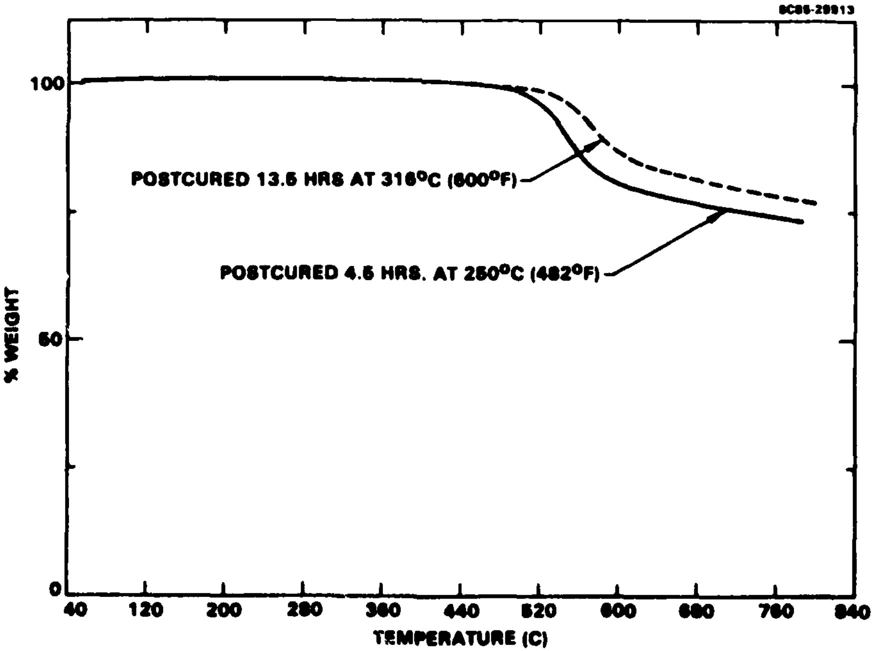

Fig. 43 The effect of postcure conditions on the thermogravimetric behavior of BATQ-H (ATP) resin in nitrogen.

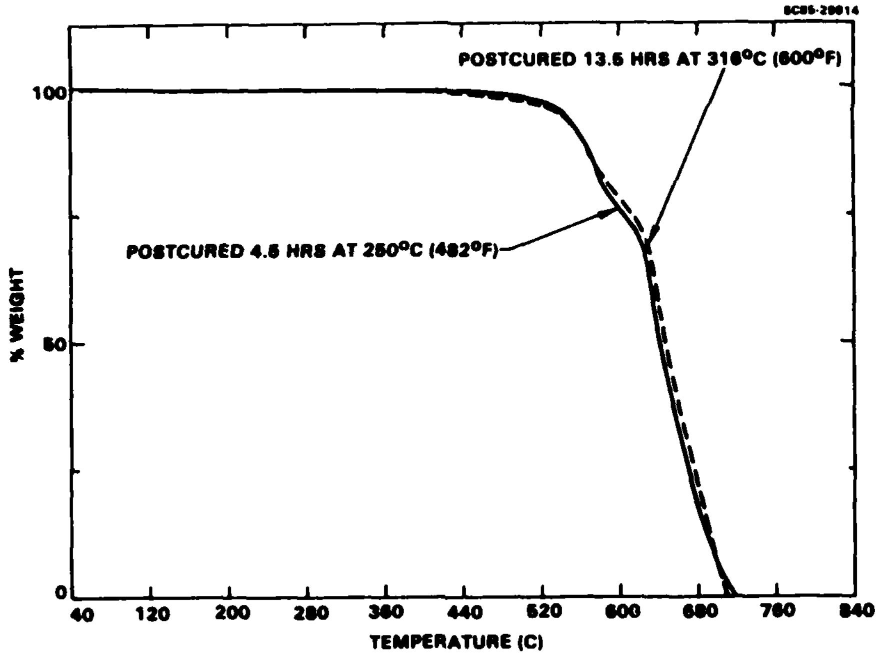

Fig. 44 The effect of postcure conditions on the thermogravimetric behavior of BATQ-H (ATP) resin in air.

3.2.2.4 Mechanical Properties

Three postcure conditions were selected for evaluation by microtensile neat resin testing. They were: 1) 4.5 h at 250°C (482°F), 2) 4.5 h at 316°C (600°F), and 3) 9.0 h at 316°C (600°F). The room temperature mechanical property data for these three postcure conditions are given in Table 15. The three postcure conditions show no clear trend. Elevated temperature tensile testing was conducted at 177°C (350°F) and 260°C (500°F) for evaluation by the failure envelope method. A summary of the tensile tests carried out at these temperatures is given in Tables 16 and 17. The failure envelopes based on these data are given in Fig. 45. The three postcures result in similar mechanical properties at room temperature and 177°C (350°F). At 260°C (500°F),

Table 15

23°C (73°F) Mechanical Properties of Hughes BATQ-H (ATP) Molded Neat Resin Microtensile Specimens

Postcure (In Air)	Tensile Strength MPa (ksi)	Tensile Modulus GPa (ksi)	Elongation To Failure (%)
4 h at 250°C (482°F)	109.0 (15.8) ± 7.6 (1.1)	2.86 (414) ± 0.18 (25)	6.57 ± 0.07
4.5 h at 316°C (600°F)	96.5 (14.0) ± 8.3 (1.2)	2.75 (398) ± 0.08 (11)	6.17 ± 0.24
9 h at 316°C (600°F)	95.2 (13.8) ± 11.7 (1.7)	2.60 (378) ± 0.20 (29)	6.25 ± 0.95

Table 16

177°C (350°F) Mechanical Properties of Hughes BATQ-H (ATP) Molded Neat Resin Microtensile Specimens

Postcure (In Air)	Tensile Strength MPa (ksi)	Tensile Modulus GPa (ksi)	Elongation To Failure (%)
4.5 h at 250°C (482°F)	55.0 (7.98) ± 0.6 (0.08)	1.99 (289) ± 0.13 (19)	6.8 ± 0.8
4.5 h at 316°C (600°F)	63.1 (9.15) ± 4.1 (0.59)	2.40 (349) ± 0.11 (16)	8.4 ± 2.1
9 h at 316°C (600°F)	59.7 (8.66) ± 1.5 (0.22)	1.99 (312) ± 0.17 (24)	7.4 ± 0.1

Table 17

260°C (500°F) Mechanical Properties of Hughes BATQ-H (ATP) Molded Neat Resin Microtensile Specimens

Postcure (In Air)	Tensile Strength MPa (ksi)	Tensile Modulus GPa (ksi)	Elongation To Failure (%)
4.5 h at 250°C	37.4 (5.43)	1.74 (252)	28
(482°F)	± 1.8 (0.26)	± 0.16 (22)	± 4
4.5 h at 316°C	35.0 (5.08)	2.18 (316)	22
(600°F)	± 5.6 (0.81)	± 0.19 (27)	± 1
9 h at 316°C	38.3 (5.56)	1.53 (221)	17
(600°F)	± 0.8 (0.12)	± 0.18 (26)	± 2

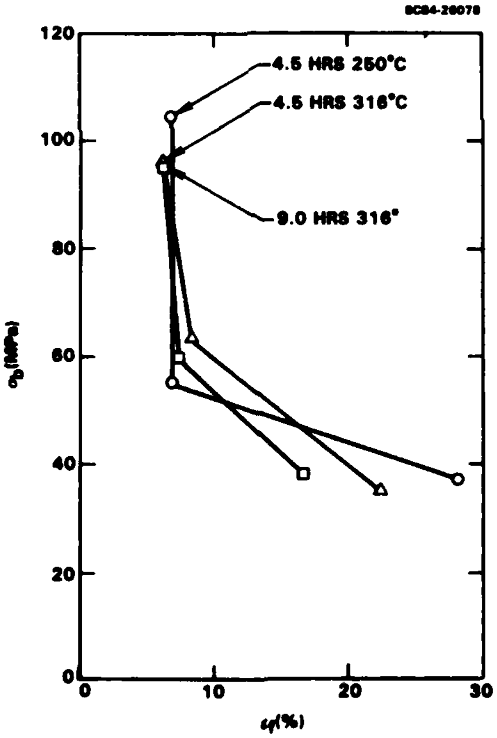

Fig. 45 The effect of postcure conditions in air on the tensile failure envelopes of BATQ-H (ATP) resin.

the resin is rubbery with very high elongations to failure measured for all three postcures. The elongations to failure of the microtensile specimens were measured by a water-cooled strain gauge extensiometer. Specimens showing strains to failure greater than 10% were estimated by direct measurement of the permanent elongation. Based on these results, it was decided to test BATQ-H (ATP) at 232°C (450°F) rather than 260°C (500°F).

3.2.2.5 Tensile Fracture Surface Analysis

SEM photomicrographs of the fracture surfaces of neat resin microtensile specimens tested at room temperature are shown in Figs. 46 and 47. The rough distorted surface features present are indications of the greater toughness of this resin compared to Hughes HR600P or Air Force ATB and m-ATS resins, which will be described in Sections 3.3 and 3.4, respectively. In those materials, the failure surfaces were predominantly smooth, which is typical of brittle resins.

3.2.3 Composite Cure Cycle Development

3.2.3.1 Prepreg Preparation

Several problems were encountered in preparing prepreg of BATQ-H (ATP) resin. Because of its low flow character, solvent impregnation must be used. The resin, however, forms a reversible gel with many common solvents at the high concentrations required for use with the single tow pultrusion technique described in Appendix A. It was found, however, that concentrated solutions of the resin in dioxane could be prepared without gel formation. The combination of a 20% solution of resin in dioxane with an enlarged die in the pultrusion prepregger gave good quality prepreg. Most importantly, fiber tows retained enough solvent so that they held together to give a continuous tape. A disadvantage of this approach is that excess solvent must be removed prior to layup and cure. Dioxane is also environmentally undesirable, as it is a

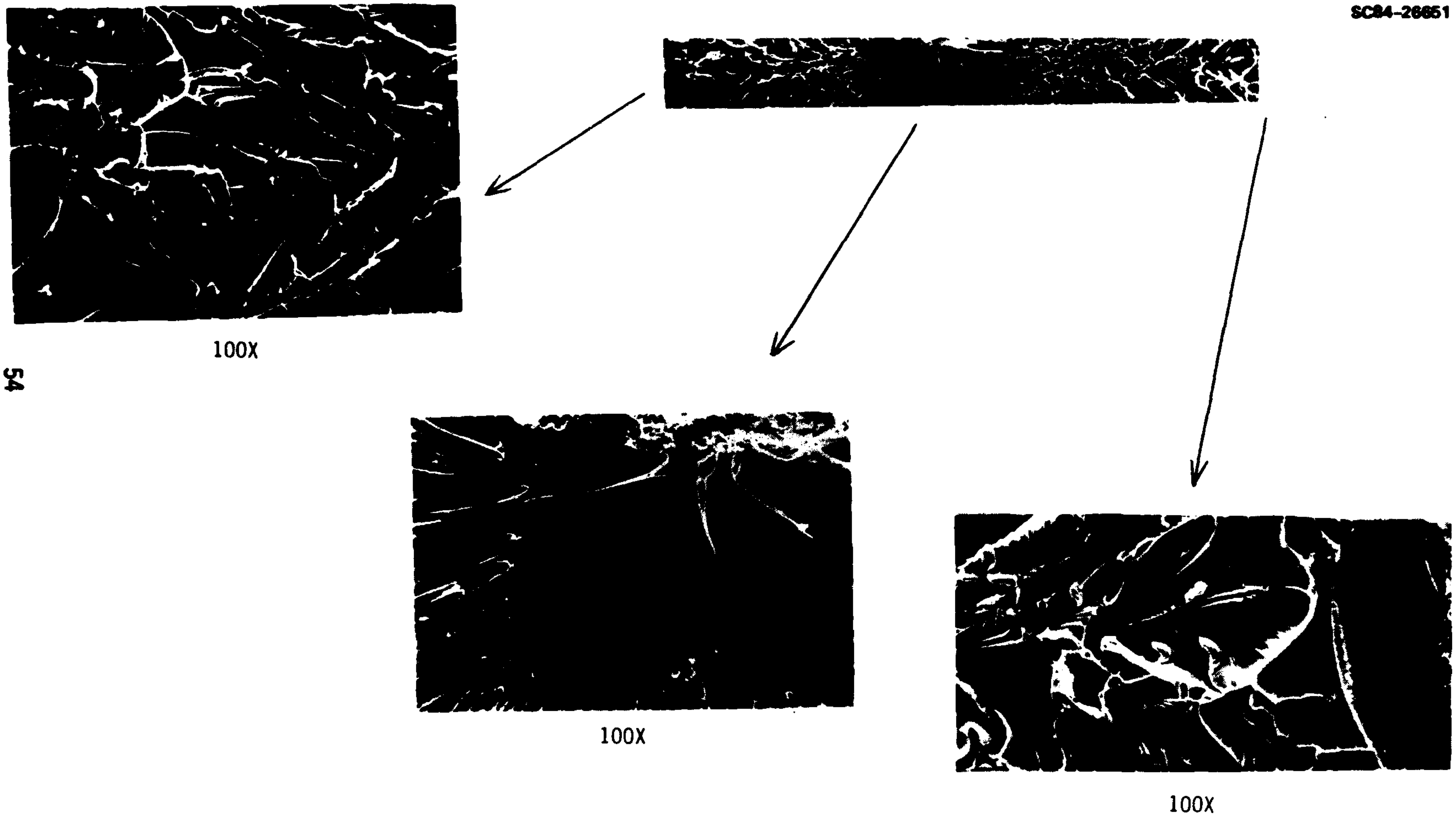

Fig. 46 SEM micrographs of BATQ-H (ATP) neat resin tensile fracture surface.

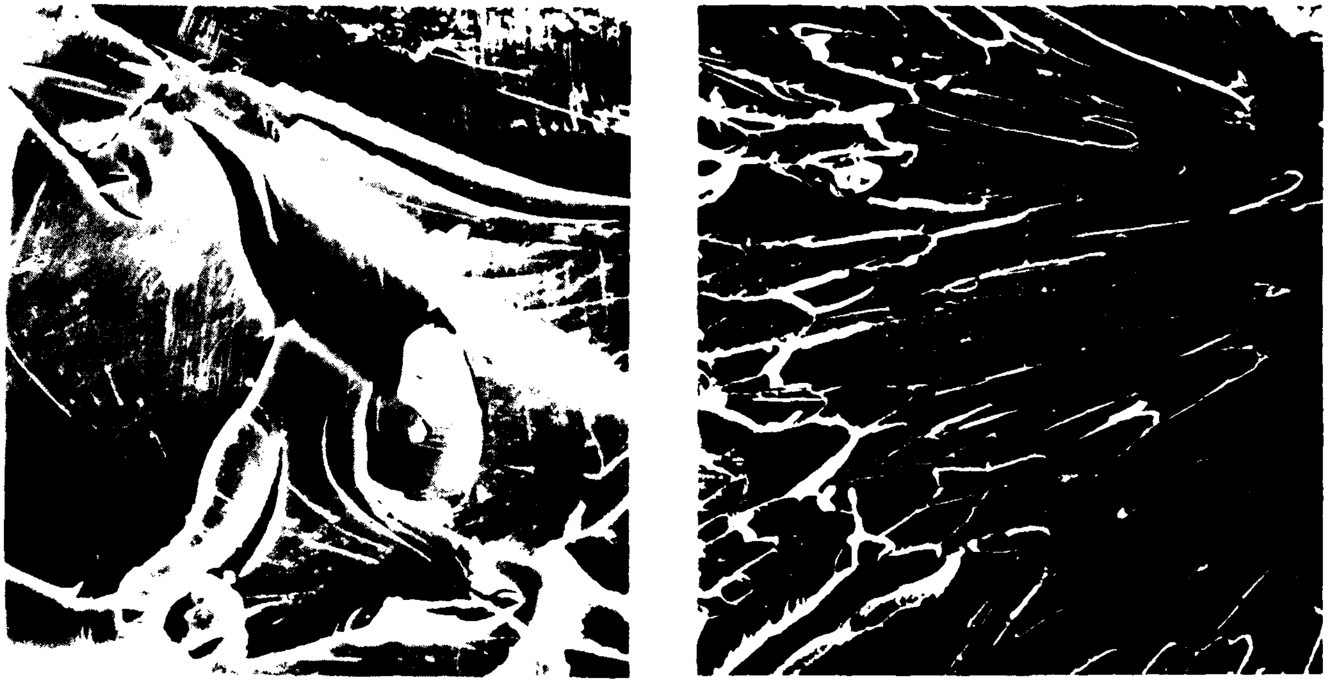

400X

170X

Fig. 47 SEM micrographs of BATQ-H (ATP) neat resin tensile fracture surface.

cancer suspect material. Freshly prepared prepreg was stored overnight under nitrogen purge and then dried 24 h under vacuum, followed by another 2 h at 80°C. Slow drying was necessary to prevent blistering of the surface of the prepreg. Slow drying would also be expected to favor phase separation of the resin from the ATP plasticizer. No evidence of phase separation was found. A summary of the prepreg's characteristics is given in Table 18.

3.2.3.2 Laminate Fabrication

AS4/BATQ-H (ATP) laminates were press-molded in a simple arrangement, shown schematically in Fig. 48. The sequence of steps used in the press molding cycle is given in Table 19. The physical properties of 16-ply unidirectional laminates prepared by this procedure are given in Table 20. Photomicrographs of composite cross sections are shown in Fig. 49.

Table 18

AS4/BATQ-H (ATP) Prepreg Properties

Resin	20% 95/5 BATQ-H/ATP in Dioxane
Fiber	AS4 12K, unsized
Pultrusion Die	0.0343 cm x 0.559 cm
Prepregging Temperature	70°C (158°F)
Pultrusion Viscosity	~ 10 Poise
Pultrusion Rate	120 cm/min
Tows Per Inch	5
Resin Content	29-35%
Areal Fiber Weight	174g/m^2
Fiber Collimation	Fair
Resin Uniformity	Fair
Tack	None
Drape	None

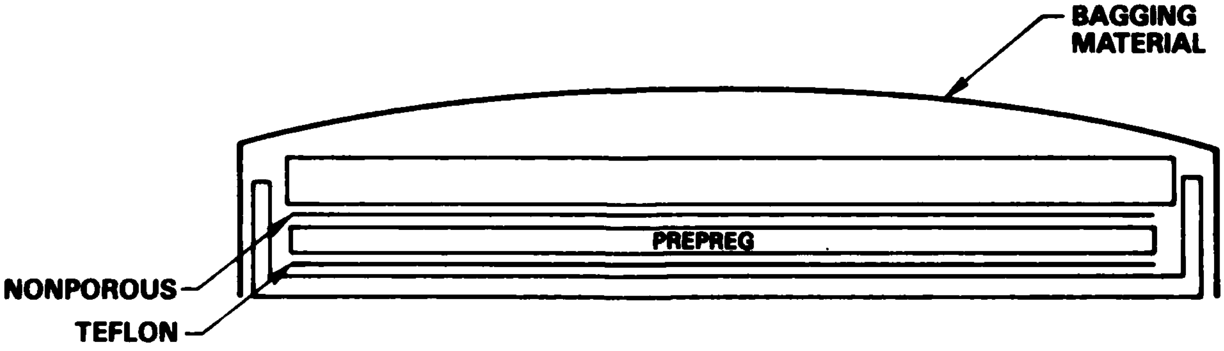

Fig. 48 Schematic of compression molding layput for AS4/BATQ-H (ATP) laminates.

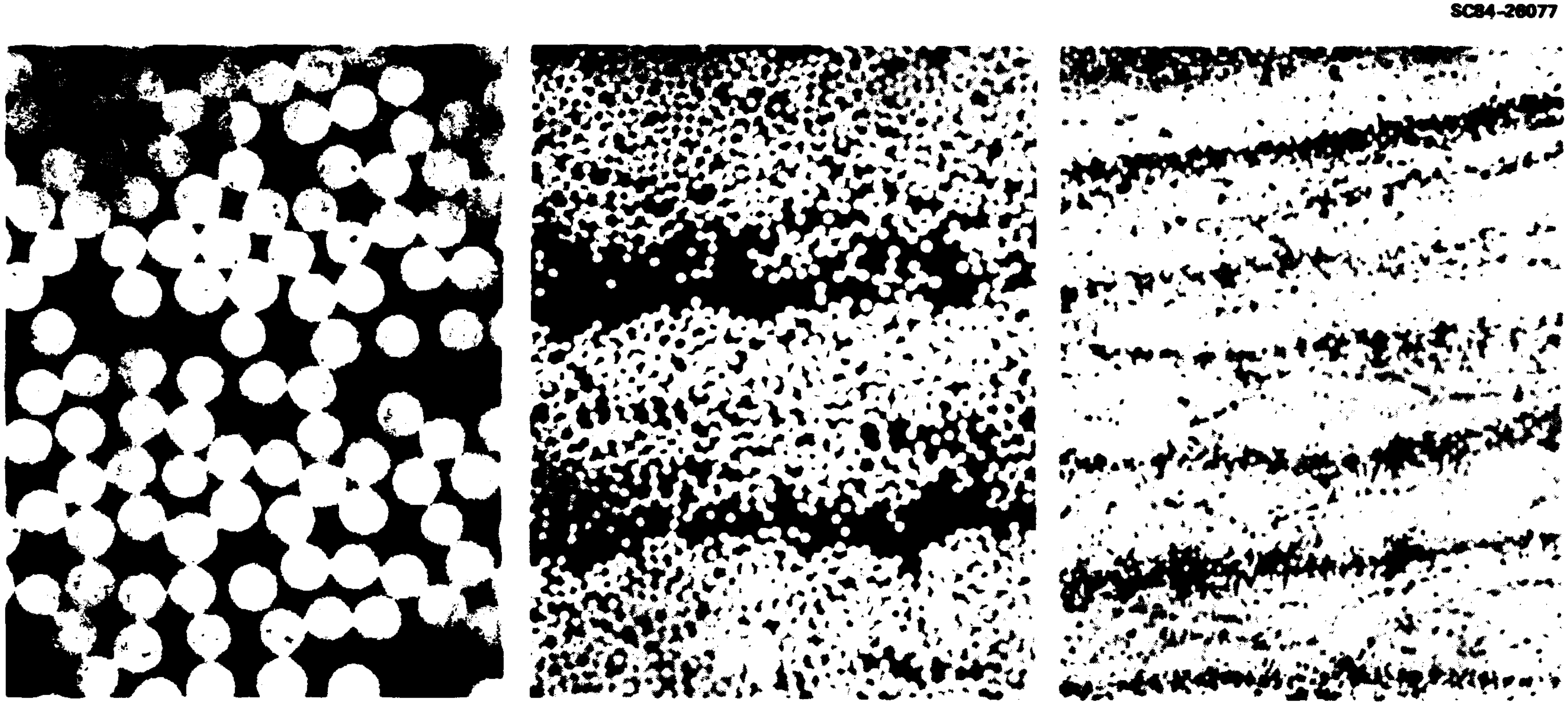

Fig. 49 Photomicrographs of AS4/BATQ-H (ATP) cross sections.

Table 19

AS4/BATQ-H (ATP) Press Molding Cure and Postcure Cycles

1. Degas prepreg 16 h at RT and 2 h at 80°C (176°F) under vacuum.
2. Place in mold, apply vacuum and 50 psi pressure.
3. Ramp to 150°C (302°F) and hold 1 h.
4. Release vacuum.
5. Cure with 500 psi pressure for 1 h at 150°C (302°F), 170°C (338°F), 190°C (374°F), 210°C (410°F) and 225°C (437°F).
6. Postcure 4.5 h at 250°C (482°F) under pressure in air.

Table 20

Physical Properties of 16-Ply Unidirectional AS4/BATQ-H (ATP) Laminates

Ply Thickness	6.3 mil/ply
Density	1.55 g/cm^3
Resin Content	34.4%
Fiber Volume	58%
T_g (Rheometrics)	257°C (495°F)

3.2.4 Composite Testing and Evaluation

3.2.4.1 Dynamic Viscoelastic Analysis

The dynamic mechanical behavior of AS4/BATQ-H (ATP) composite is shown in Fig. 50. A glass transition temperature of 257°C (495°F) is indicated by the peak maximum in the dynamic shear loss modulus, G". The occurrence of a small decrease in shear modulus around room temperature reported by

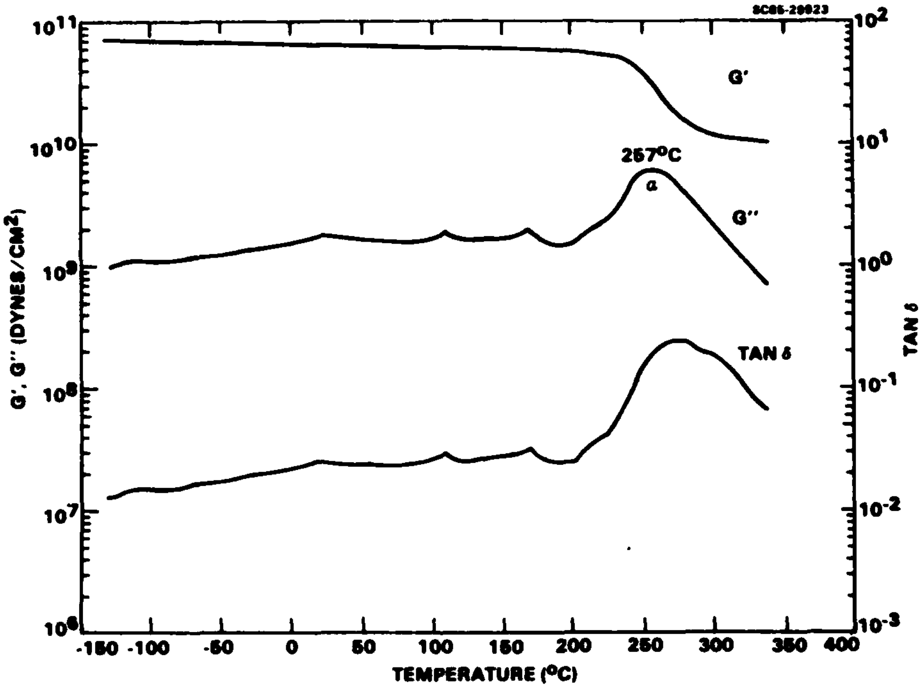

Fig. 50 Dynamic viscoelastic analysis of AS4/BATQ-H (ATP).

the Air Force Materials Laboratory[4] is not clearly seen in this composite dynamic mechanical test.

3.2.4.2 Four-Point Shear Strength

The interlaminar shear strength of AS4/BATQ-H (ATP) was evaluated by the four-point shear test developed by Browning et al.[3] This method has been shown to produce true interlaminar shear failures. The ASTM test for "Apparent Interlaminar Shear Strength of Parallel Fiber Composites by Short-Beam Method" (D2344) was also carried out for comparison purposes. Testing was made on 16-ply unidirectional specimens cured by the cycle described in Table 19. The effect of moisture on shear strength was studied for specimens equilibrated at 71°C (160°F) and 95% RH. The four-point shear data for temperatures of 24°C (75°F), 177°C (350°F) and 232°C (450°F) are given in Table 21.

Table 21

Four-Point Shear Strength of AS4/BATQ-H (ATP) Molded Composite

Test Temperature °C (°F)	Shear Strength Dry MPa (ksi)	Shear Strength Wet MPa (ksi)	Failure Mode
24 (75)	69.6 (10.1) ± 2.1 (0.3)	67.6 (9.8) ± 1.4 (0.2)	Interlaminar
177 (350)	47.9 (6.94) ± 1.4 (0.21)	46.9 (6.8) ± 2.1 (0.3)	Compression
232 (450)	41.2 (5.98) ± 1.0 (0.15)	31.7 (4.6) ± 2.1 (0.3)	Compression

3.2.4.3 Short-Beam Shear Strength

Short-beam shear strength data for the same conditions are given in Table 22. Of both shear tests, only the room temperature four-point specimens showed a true interlaminar shear failure mode. The elevated temperature four-point shear specimens were observed to creep and finally break in a compressive mode. The cause of this effect may relate to a small modulus drop near 100°C (212°F) reported by the Air Force Materials Laboratory. The interlaminar shear strength of those specimens which failed in true shear was only about 80% of that reported for AS 1/3502 graphite/epoxy composites.[6] The effect of moisture on the apparent shear strengths is small except at 232°C (450°F) where a significant decrease is noted. The elevated temperature tests, however, are invalid and therefore this is of little significance.

Table 22

Short-Beam Shear Strength of AS4/BATQ-H (ATP) Molded Composite Laminates

Test Temperature °C (°F)	Shear Strength Dry MPa (ksi)	Shear Strength Wet MPa (ksi)	Failure Mode
24 (75)	95.8 (13.9) ± 1.4 (0.2)	92.4 (13.4) ± 0.7 (0.1)	None apparent
177 (350)	72.4 (10.5) ± 2.1 (0.3)	64.1 (9.30) ± 0.1 (0.01)	None apparent
232 (450)	57.9 (8.40) ± 2.8 (0.40)	48.1 (6.98) ± 1.2 (0.17)	None apparent

The fracture surfaces of the room temperature four-point specimens were examined by SEM. The region of the specimens studied was that in which failure initiated. This region was generally under one of the two loading pins in the four-point test. It is distinguished by having a "whitish" cast compared to failure regions which are induced later by the test or caused by manually breaking the specimen apart.[3] Several SEM micrographs are shown in Figs. 51-53 for various magnifications. The surfaces show the presence of resin deformation or "hackles" formed during failure. The extent of this effect, however, is much less than shown for state-of-the-art 177°C (350°F) graphite/epoxy composite failure surfaces.[3] The SEM micrographs also reveal a large amount of fiber in which striations are evident, indicative of unbonded fiber due to poor fiber/matrix adhesion.

SC84-26654

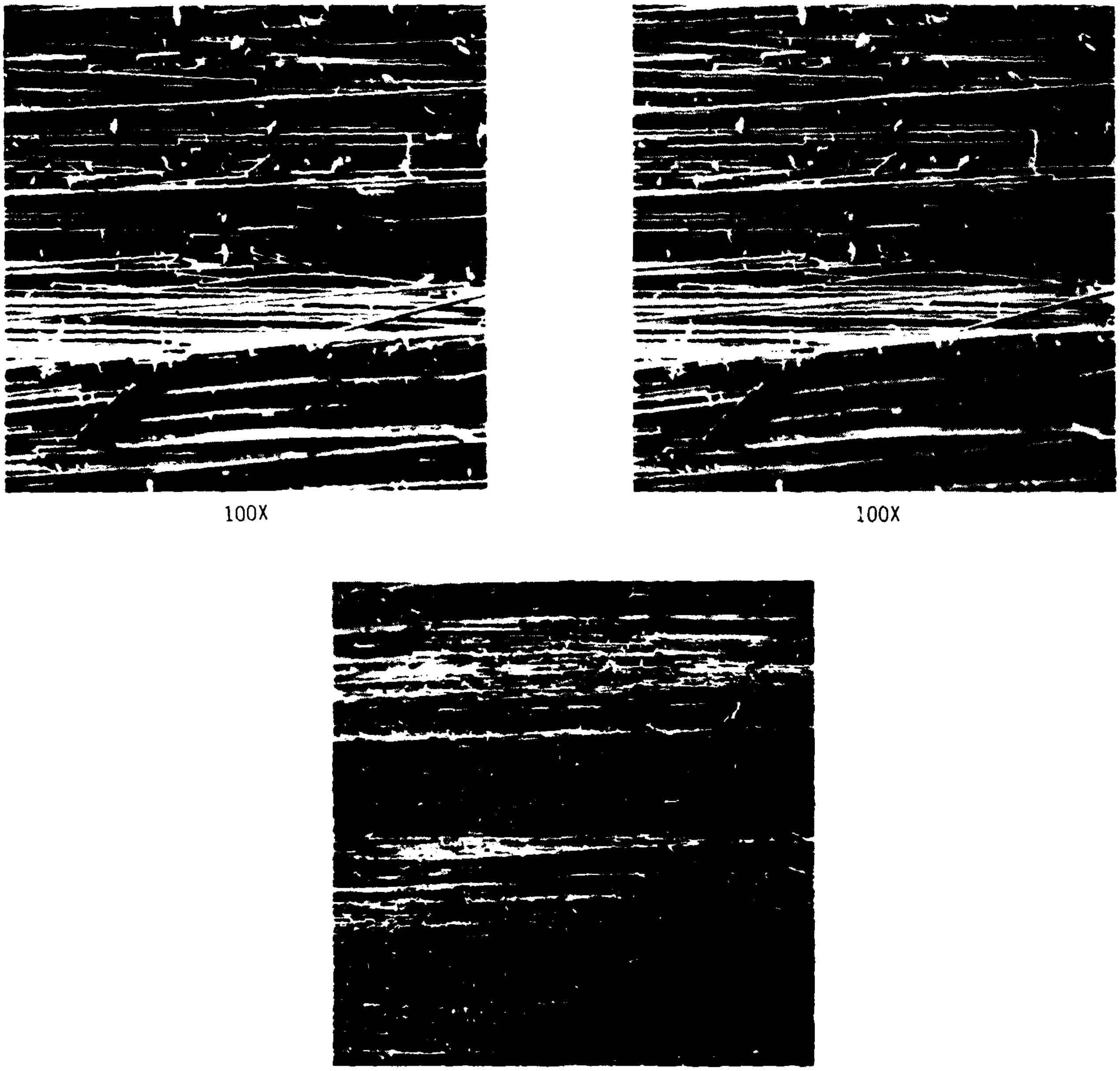

100X

100X

30X

Fig. 51 SEM micrographs of AS4/BATQ-H (ATP) interlaminar shear fracture surface.

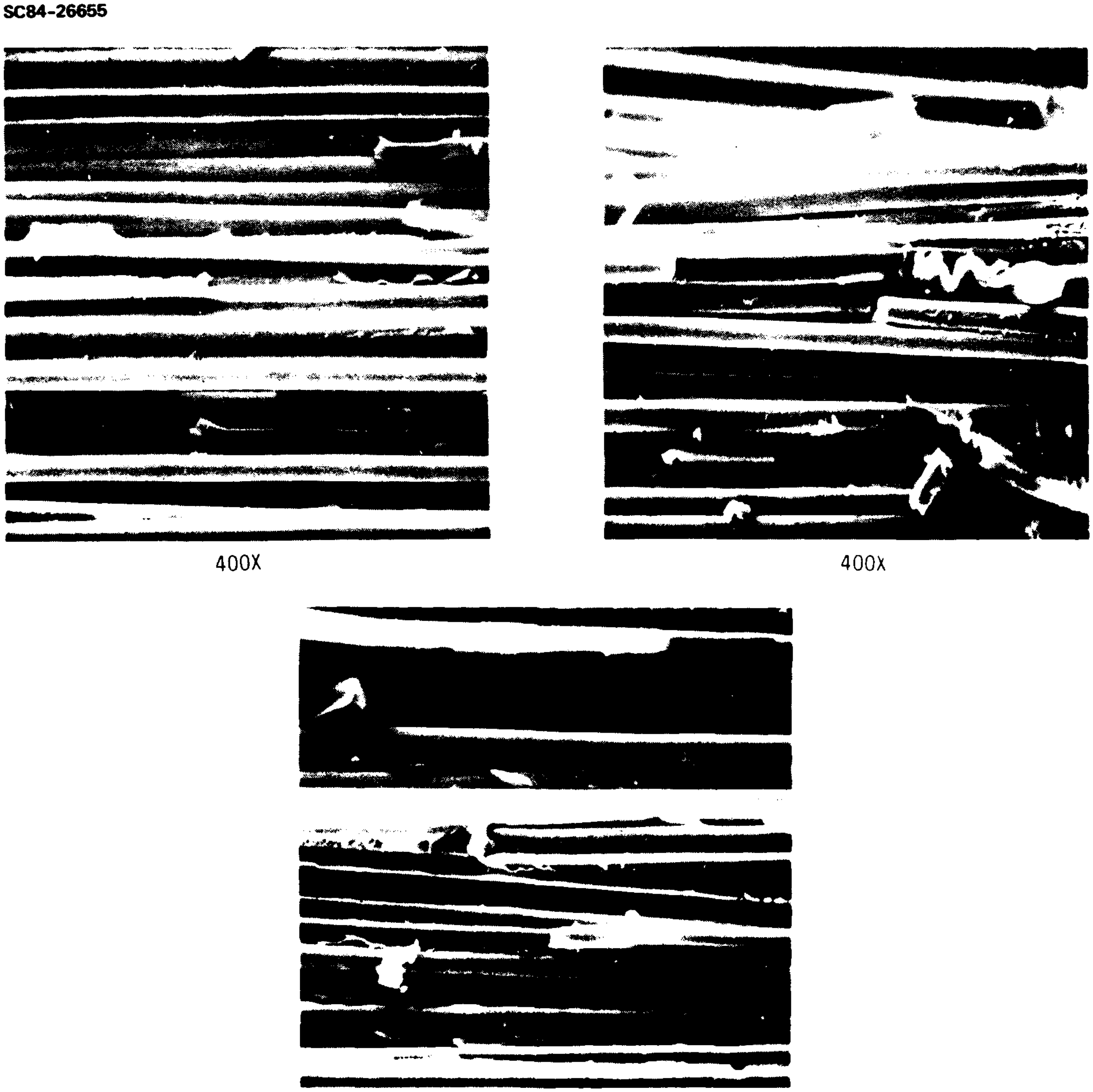

400X

400X

400X

Fig. 52 SEM micrographs of AS4/BATQ-H (ATP) interlaminar shear fracture surface.

SC84-26656

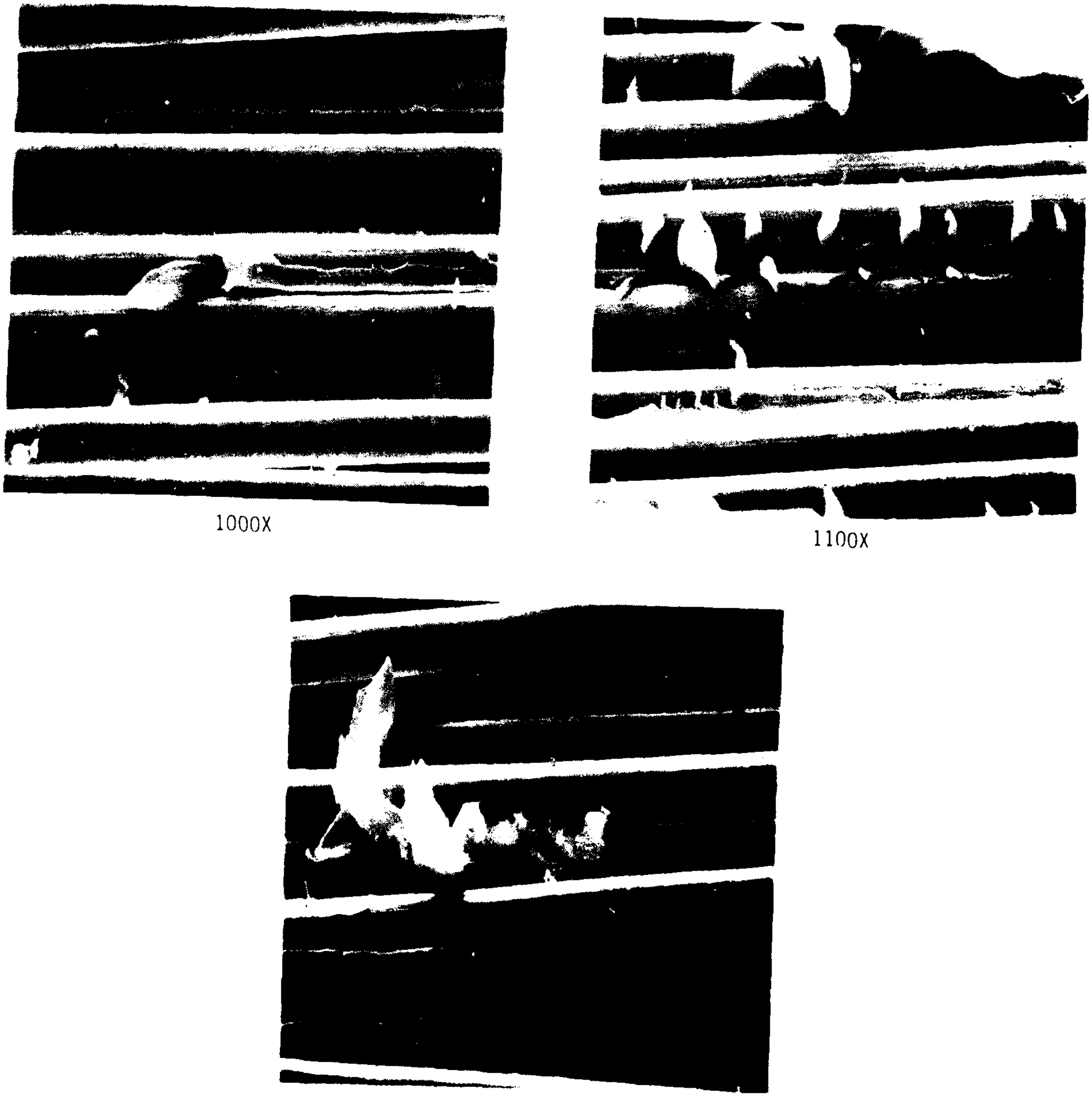

1000X

1100X

1100X

Fig. 53 SEM micrographs of AS4/BATQ-H (ATP) interlaminar shear fracture surface.

3.2.4.4 Flexural Strength and Modulus

Three-point 0° flexural properties of AS4/BATQ-H (ATP) are given in Tables 23 and 24. The values have been normalized to 60% fiber volume. Failure in the flexural specimens appeared to be in compression for both the dry and wet tests. Little difference was found for specimens conditioned to equilibrium at 71°C (160°F) and 95% RH. Equilibration occurred in approximately 14 days to give an average moisture uptake of 0.78%. The material shows a 72% flexural strength retention at 177°C (350°F) and 59% at 232°C (450°F).

3.2.4.5 Transverse Flexural Strength

The transverse four-point 90° flexural properties of AS4/BATQ-H (ATP) are given in Table 25. Specimens were tested with a strain gauge bonded on the tensile side. Stress-strain data for one experiment is plotted in Fig. 54. The strain-to-failure values are about twice that reported for state-of-the-art 177°C (350°F) graphite/epoxy materials.

Table 23

Three-Point Flexural Properties of AS4/BATQ-H (ATP)Molded Composite

Test Temperature °C (°F)	Flexural Strength GPa (msi)	Flexural Modulus GPa (msi)	Failure Mode
24 (75)	1.92 (279) ± 0.11 (14)	148 (21.4) ± 30 (4.4)	Compression
177 (350)	1.39 (201) ± 0.05 (7)	164 (23.8) ± 4 (0.6)	Compression
232 (450)	1.13 (164) ± 0.04 (6)	171 (24.9) ± 1 (0.2)	Compression

Table 24

Three-Point Flexural Properties of AS4/BATQ-H (ATP)Molded Composite, Moisture Conditioned at 71°C (160°F) and 95% RH

Test Temperature °C (°F)	Flexural Strength GPa (msi)	Flexural Modulus GPa (msi)	Failure Mode
24 (75)	1.86 (270) ± 0.01 (1)	151 (21.9) ± 5 (0.8)	Compression
177 (350)	1.33 (193) ± 0.04 (6)	150 (21.7) ± 2 (0.3)	Compression
232 (450)	1.08 (157) ± 0.05 (7)	152 (22.1) ± 5 (0.7)	Compression

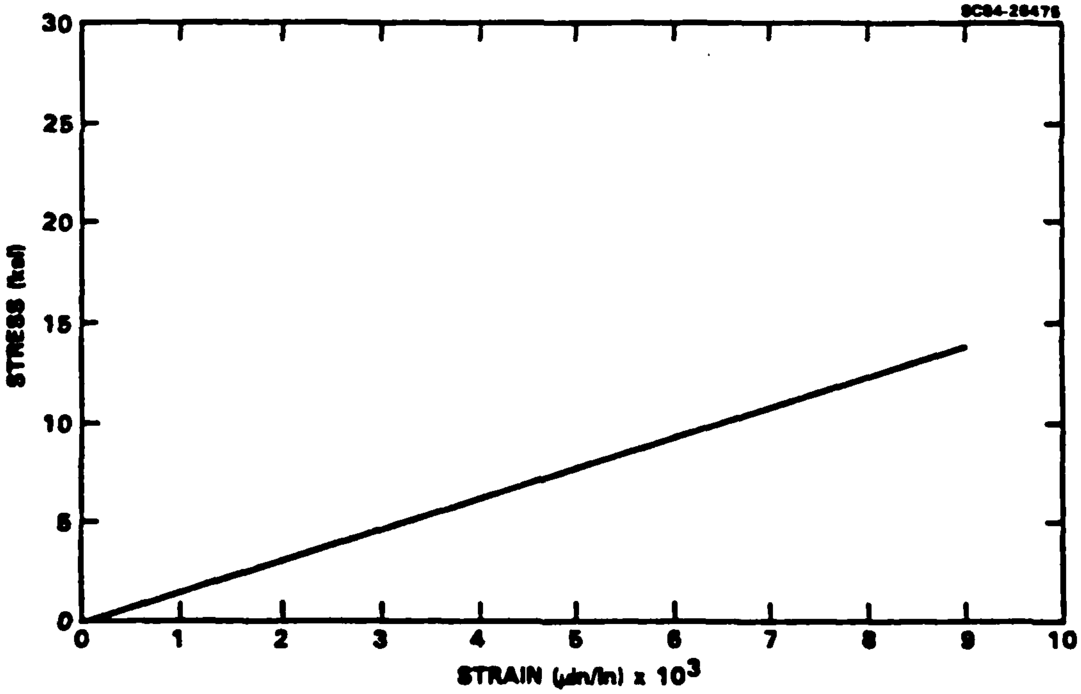

Fig. 54 Stress-strain curve for 90° flexural test of AS4/BATQ-H (ATP).

Table 25

Transverse Flexural Properties of AS4/BATQ-H (ATP)

Specimen	Flexural Strength (Dry) MPa (ksi)	Strain-to-Failure μin./in.	Flexural Modulus (Dry) GPa (msi)
1	102 (14.8)	9700	10.5 (1.53)
2	106 (15.4)	10300	10.3 (1.50)

3.2.4.6 Fracture Toughness

The Mode I delamination fracture toughness G_{1c} of unidirectional AS4/BATQ-H (ATP) composite was determined by the procedure developed by Devitt et al.[5] Three reference composite materials were tested for comparative purposes. Data for the duplicate tests are given in Table 26. The values given are the average of 10-15 determinations taken along the crack length of individual specimens.

Table 26

G_{1c} Fracture Toughness of AS4/BATQ-H (ATP)

Composite Material	G_{1c} (N/m)
As4/BATQ-H (ATP)	552 ± 40 534 ± 88
AS1/3501-5A	219 ± 25 190 ± 10
XAS/PEEK (MG-1)	1846 ± 25 1640 ± 11

The G_{1c} values obtained for Hercules, Inc. AS1/3501-5A graphite/epoxy and Imperial Chemical Industries XAS/PEEK (MG-1) graphite/thermoplastic composites are close to those reported by Hartness.[6] The values determined for AS4/BATQ-H (ATP) are significantly higher than those of graphite/epoxy, but still far below that of the thermoplastic PEEK composite. Examination of the fracture surfaces of these materials, however, indicates that AS4/BATQ-H (ATP) failed in multiple crack fronts, thus giving an artificially high fracture toughness. A low magnification SEM micrograph illustrates this in Fig. 55.

The fracture surface of AS1/3501-5A and XAS/PEEK (MG-1) shown in Figs. 56 and 57 are smooth as a result of delamination occurring within a single ply. The AS4/BATQ-H (ATP) surface is rough as a result of failure occurring in more than one ply. This produces a larger effective fracture area than the geometrical size used to calculate G_{1c}.

SC84-27959

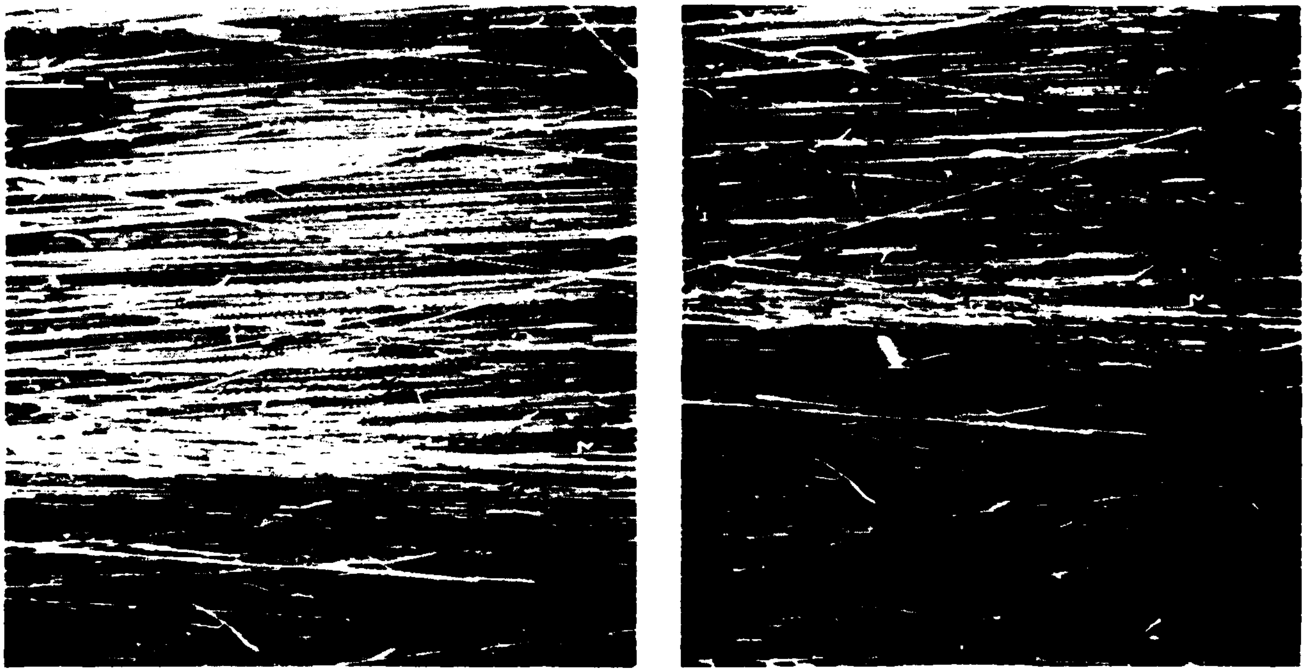

Fig. 55 SEM micrographs of AS4/BATQ-H (ATP) G_{1c} fracture surface, 40X.

SC84-27960

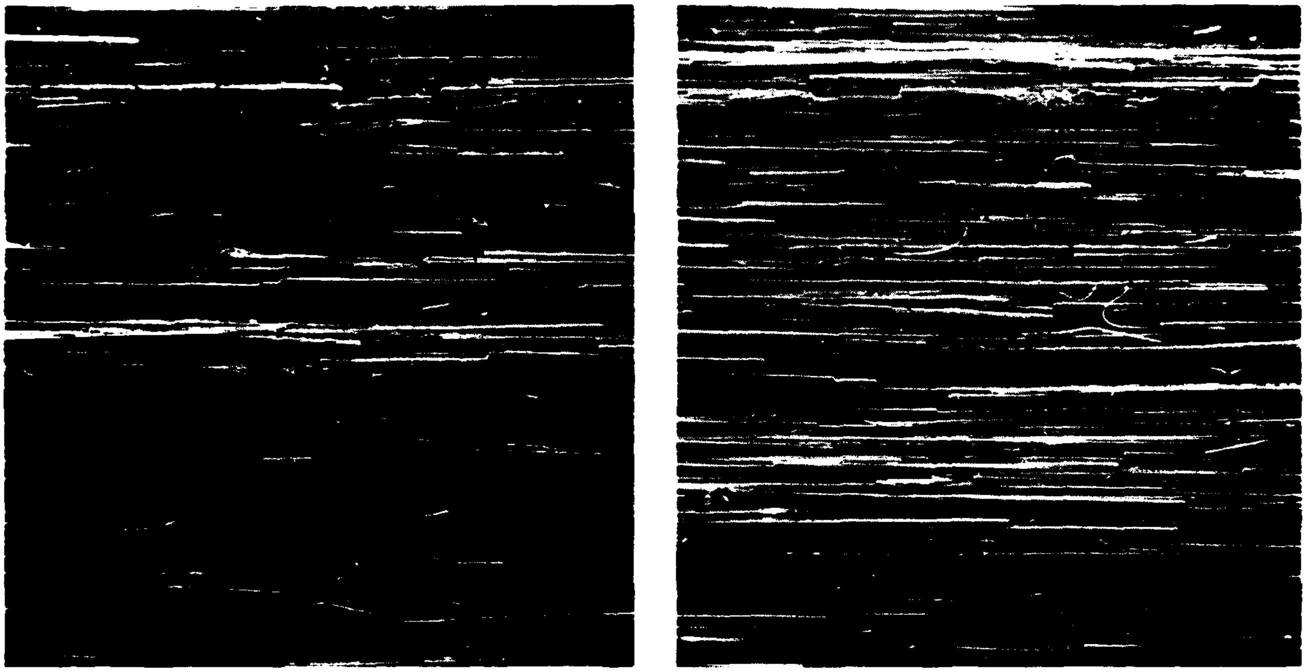

Fig. 56 SEM micrographs of AS1-3501-5A G_{1c} fracture surface, 40X.

SC84-27961

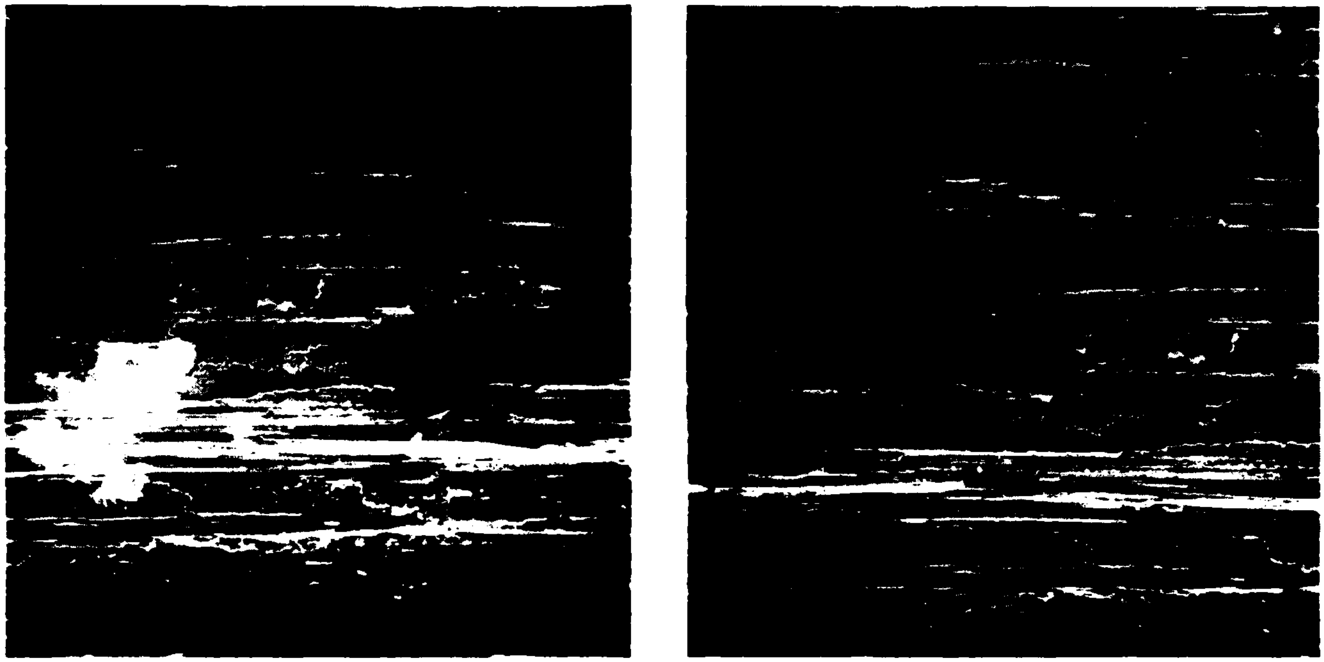

Fig. 57 SEM micrographs of XAS/PEEK (MG-1) G_{1c} fracture surface, 40X.

Some further aspects of the G_{1c} failure modes are shown in 400X micrographs in Fig. 58-60. The AS4/BATQ-H (ATP) failure surface again appears rougher than that for AS1/3501-5A or XAS/PEEK (MG-1). Another feature which is shown in the 400X micrographs is the greater degree of unbonded fiber surface in AS4/BATQ-H (ATP) compared to the other two materials.

3.3 Air Force ATB Resin

ATB resin is another acetylene-terminated matrix resin developed by the Air Force Wright Aeronautical Laboratories. The molecular structure of this material is shown in Fig. 61. The bisphenol-A backbone imparts excellent moisture resistence and processability, with the potential of providing good retention of properties at 177°C (350°F). A 1 lb sample of the resin (Lot FC-MATB-123) was received from the Air Force Materials Laboratory. The resin was a viscous liquid with a composition estimated from liquid chromographic analysis to be ~ 75% ATB monomer, the remainder being oligomeric products.

SC84-27963

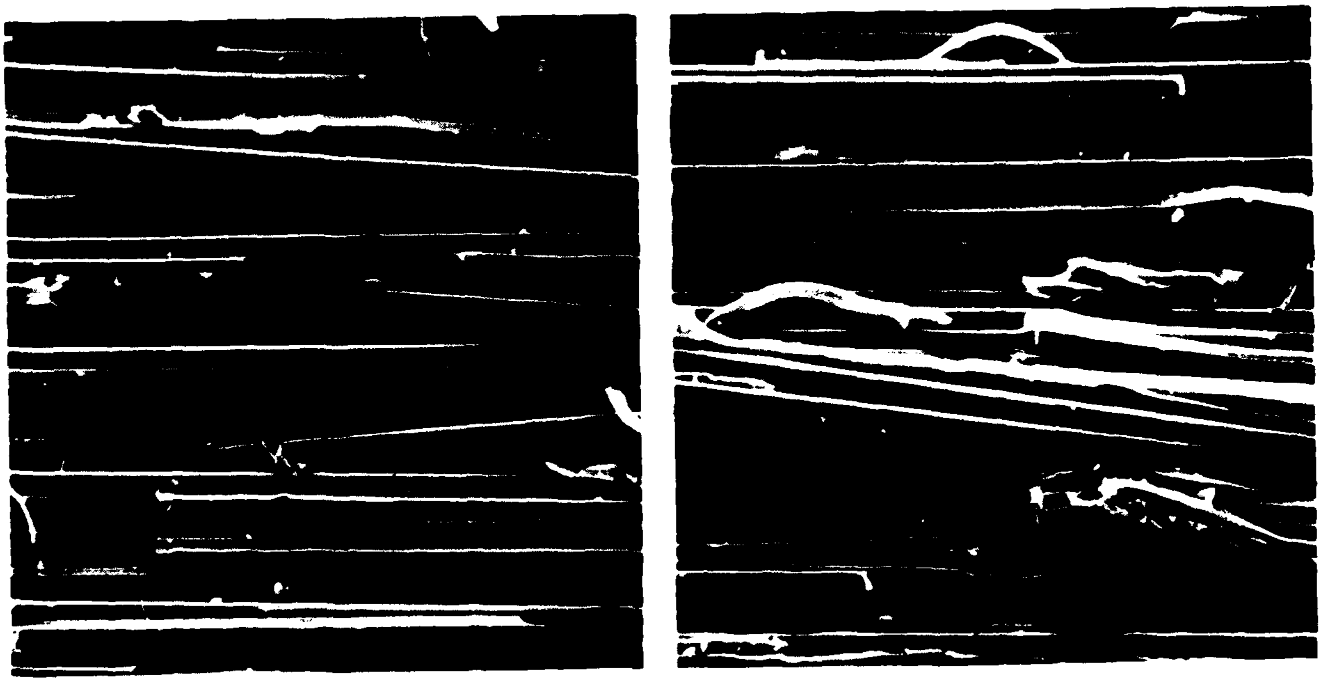

Fig. 58 SEM micrographs of AS4/BATQ-H (ATP) G_{1c} fracture surface, 400X.

SC84-27964

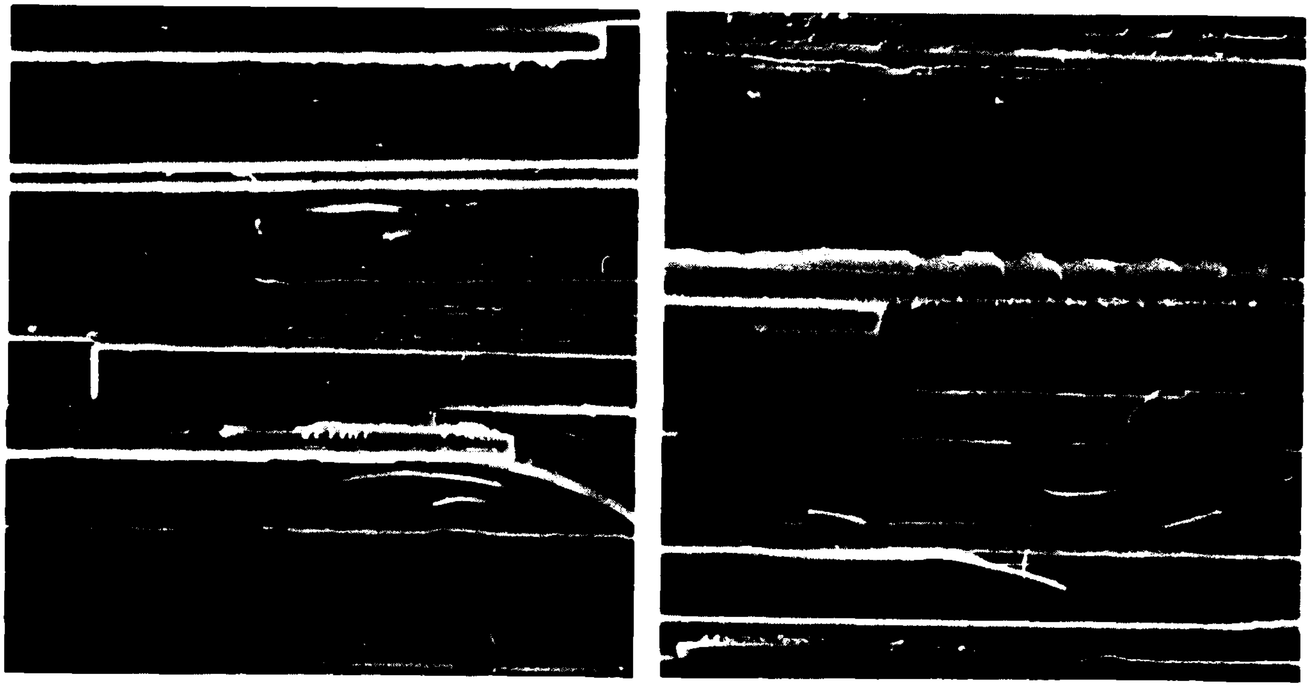

Fig. 59 SEM micrographs of AS1/3501-5A G_{1c} fracture surface, 400X.

SC84-27965

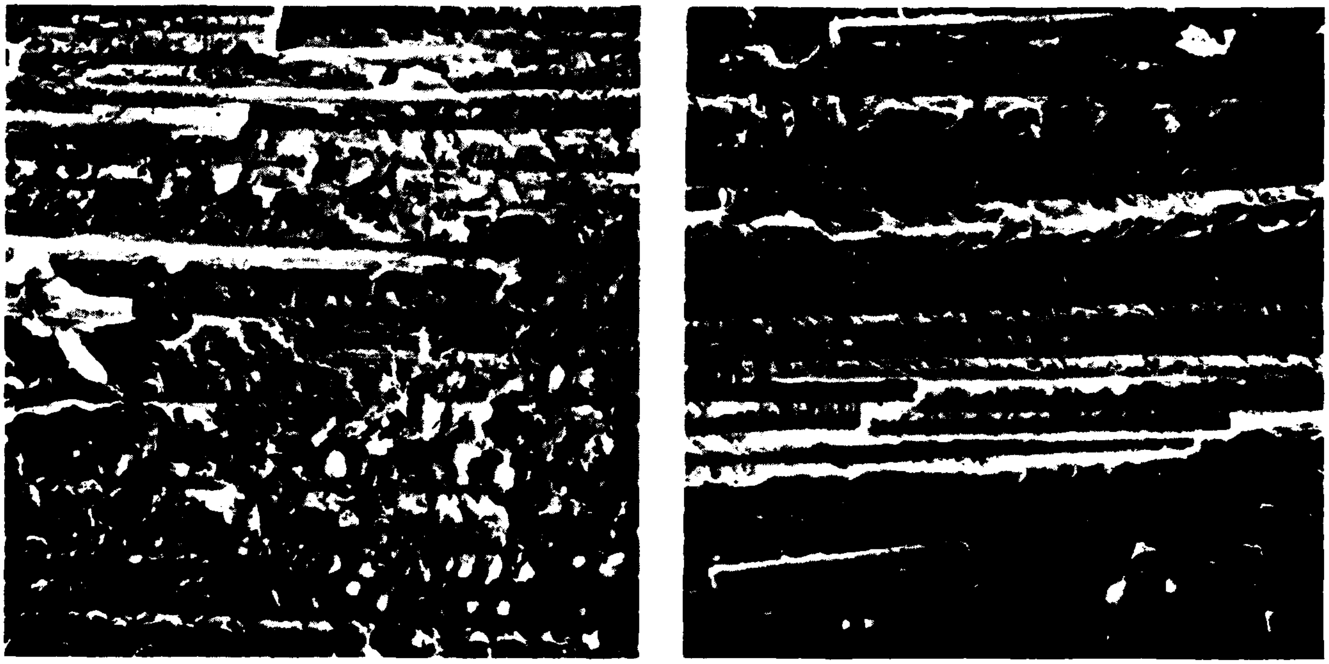

Fig. 60 SEM micrographs of XAS/PEEK (MG-1) G_{1c} fracture surface, 400X.

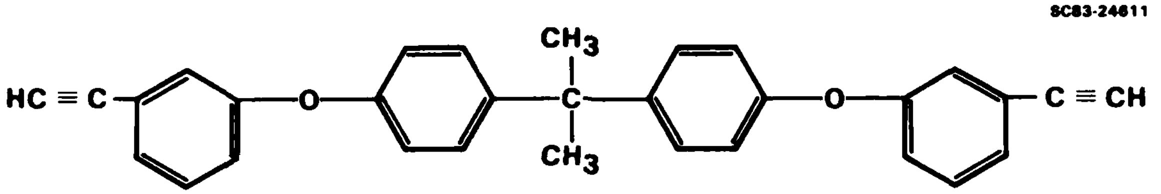

Fig. 61 Molecular structure of ATB resin

3.3.1 Materials Validation

3.3.1.1 Differential Scanning Calorimetry

The DSC thermograms for the cure of ATB resin at various heating rates are shown in Fig. 62. The exotherms consist of a single symmetric peak. The standard kinetic analysis[1] involving the dependence of the peak exotherm temperature on heating rate is plotted in Fig. 63, where an activation energy of 28.1 kcal/mole is defined. A summary of the DSC data is given in Table 27.

3.3.1.2 Cure Rheology

The rheological behavior of ATB resin during various linear heating rate experiments is shown in Fig. 64. The dynamic viscosity of the resin is very low through much of these cure cycles and below the sensitivity of the Rheometrics 2000 g•cm torque load cell. Gelation occurred at ~ 200°C (392°F) in these cure cycles. Due to the very high flow behavior of this resin, it is not sensitive to variations in heating rate.

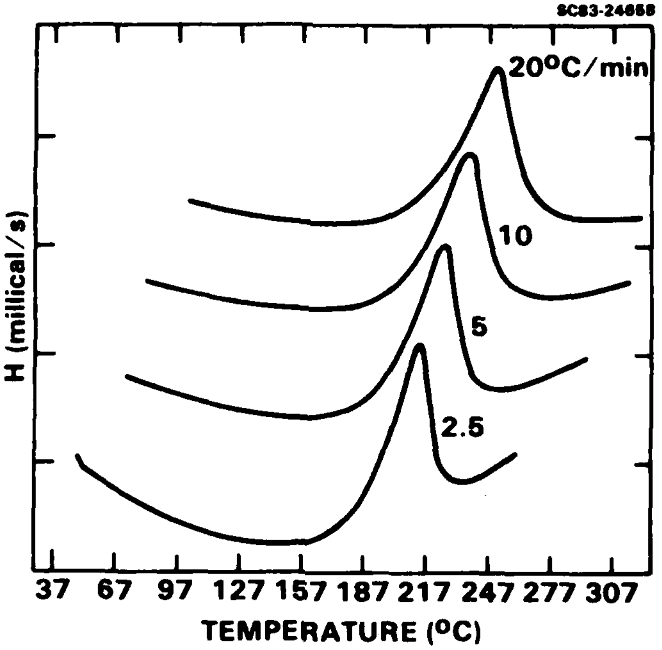

Fig. 62 DSC thermograms of ATB resin.

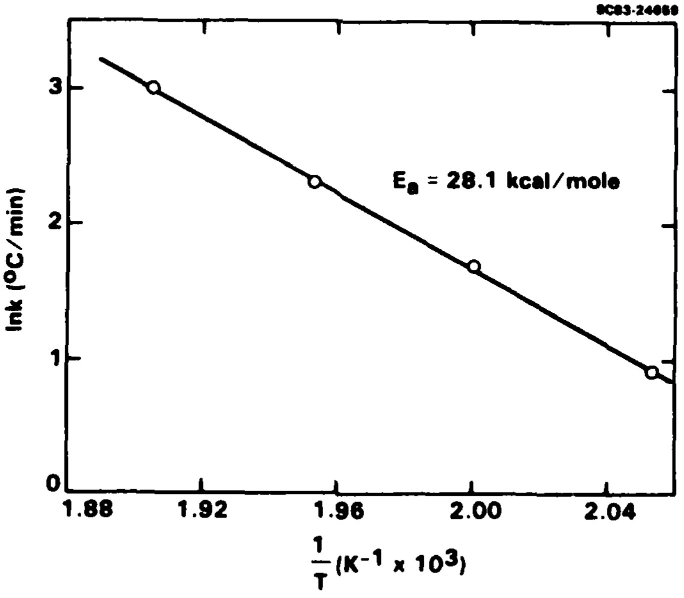

Fig. 63 Dependence of DSC exotherm peak temperature with heating rate for ATB resin.

Table 27

DSC Analysis of ATB Neat Resin

Uncured melt temperature		-11°C (12°F)
Exotherm onset temperature	(ϕ = 10°C/min)	171°C (340°F)
Exotherm peak temperature	(ϕ = 10°C/min)	239°C (462°F)
Exotherm completion temperature	(ϕ = 10°C/min)	273°C (523°F)
Heat of polymerization		128 cal/g
Activation energy for polymerization		28 kcal/mole

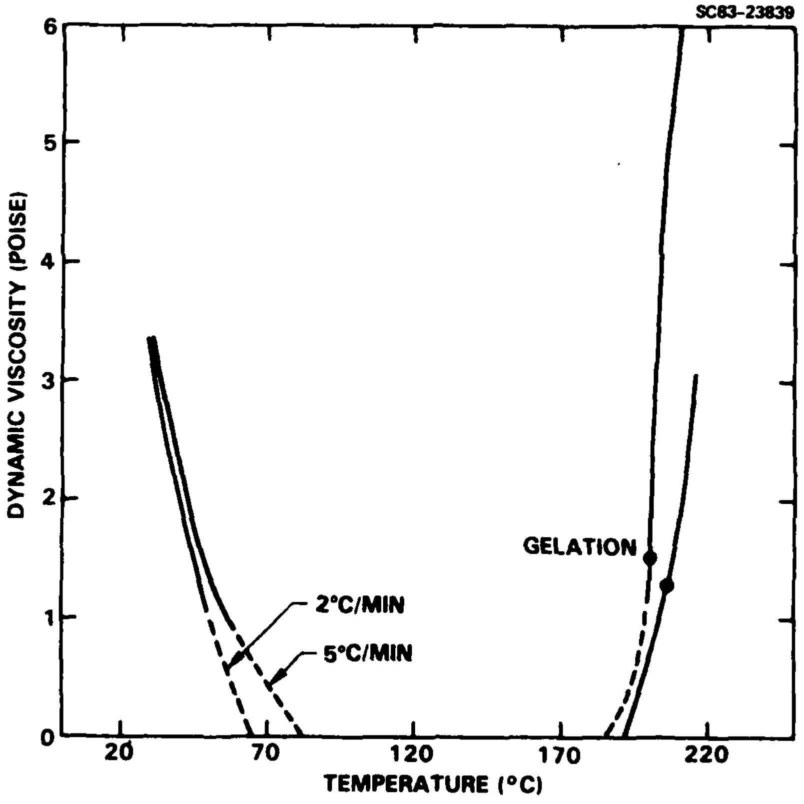

Fig. 64 Dynamic viscosity during cure of ATB resin at different heating rates.

The isothermal cure behavior for ATB resin is plotted in Fig. 65. The viscoelastically defined gelation times are given in Table 28.

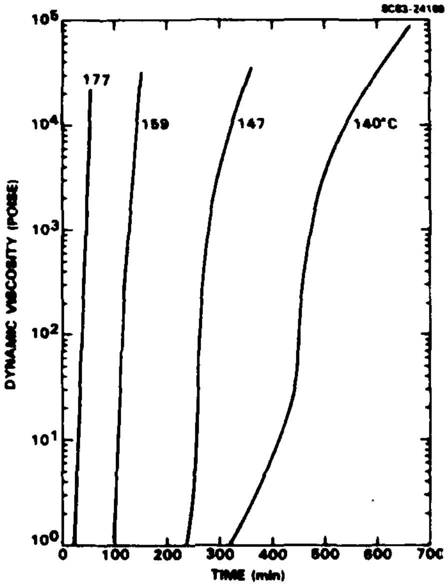

Fig. 65 Dynamic viscosity during cure of ATB resin at different temperatures.

Table 28

Dynamic Viscoelastic Analysis of Gelation for ATB Resin

T (°C)	T (°F)	$t_{G' = G''}$ (min)
140	284	420
147	300	252
159	318	110
177	350	36

AD-A158 648 EVALUATION OF NEW RESIN SYSTEMS(U) ROCKWELL 2/2
INTERNATIONAL THOUSAND OAKS CA SCIENCE CENTER
P J DYNES MAY 85 SC5338.85FR AFWAL-TR-85-4053
UNCLASSIFIED F33615-82-C-5064 F/G 11/4 NL

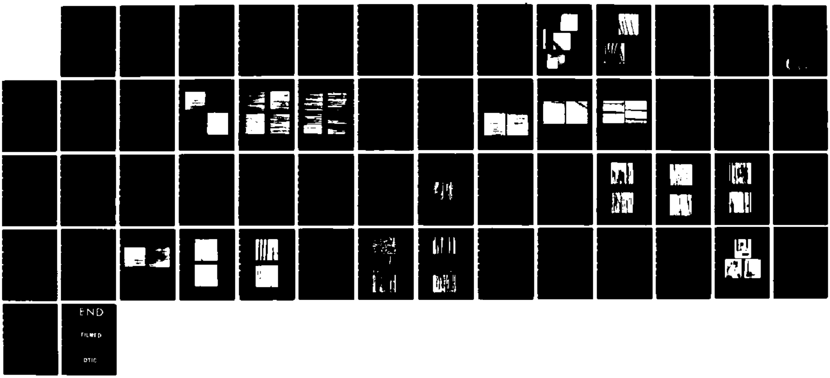

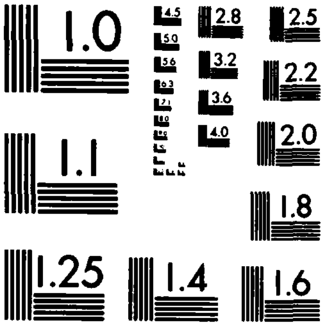

MICROCOPY RESOLUTION TEST CHART
NATIONAL BUREAU OF STANDARDS-1963-A

The 177°C (350°F) gel time of 36 min is comparable to state-of-the-art 177°C (350°F) curing epoxy systems. The temperature dependence of the gel times is plotted in Fig. 66, where an activation energy to gelation of 25.4 kcal/mole is defined. The viscoelastic properties of ATB are very different from HR600P or BATQ-H/ATP. For example, the dynamic viscosity of ATB at the point of gelation is ~ 5-50 Poise, whereas HR600P and BATQ-H (ATP) is near 10^6 Poise.

3.3.2 Neat Resin Cure Cycle Development

3.3.2.1 Microtensile Specimen Preparation

Neat resin microtensile specimens were prepared in silicone rubber molds. The Air Force Materials Laboratory had previously developed an optimum cure cycle for ATB which consisted of 15 h at 140°C (285°F) and 5 h at 170°C (338°F) in air. Given this cure cycle, only the optimum postcure cycle needed to be determined. The silicone rubber mold technique for preparing tensile

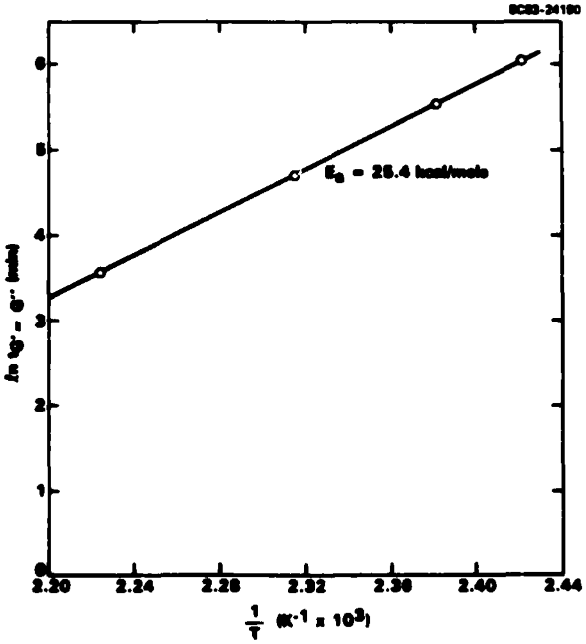

Fig. 66 Dependence of dynamic moduli crossover time with cure temperature for ATB resin.

specimens worked very well for ATB due to the high flow behavior of this resin. Prior to postcure, the microtensile specimens were sanded flat to uniform thickness with 600 grit paper. Specimens prepared in this manner were void-free with a tensile strength of near 69 MPa (10 ksi) and an ultimate elongation of ~ 3%.

3.3.2.2 Thermomechanical Analysis

Thermomechanically determined T_g measurements were used to aid in selection of a postcure cycle for ATB resin. Postcure temperatures of 250°C (482°F), 275°C (527°F) and 300°C (572°F) were studied. The results of these experiments is given by the T_g data in Table 29. The data in this table show that a substantial increase in the T_g of ATB resin can be obtained by higher temperature postcures. Longer postcures at a given temperature generally resulted in higher T_g values also, but was not as efficient as higher temperatures for raising T_g. Based on these T_g results, three postcure cycles were selected for further experimentation: 4 h at 250°C (482°F), 4 h at 275°C (527°F) and 4 h at 300°C (572°F).

Table 29

The Effect of Postcure Conditions on the Glass Transition Temperature of ATB Resin

Postcure Time	Postcure Temperature 250°C (482°F)	275°C (527°F)	300°C (572°F)
None	155 ± 6°C (311 ± 11°F)	155 ± 6°C (311 ± 11°F)	155 ± 6°C (311 ± 11°F)
1 h	184 ± 2°C (363 ± 4°F)	-----	224 ± 2°C (435 ± 4°F)
2 h	207 ± 2°C (405 ± 4°F)	210 ± 1°C (410 ± 2°F)	231 ± 2°C (448 ± 4°F)
4 h	207 ± 4°C (405 ± 7°F)	225 ± 5°C (437 ± 9°F)	255 ± 4°C (491 ± 8°F)
6 h	211 ± 2°C (412 ± 4°F)	-----	253 ± 4°C (487 ± 8°F)
8 h	221 ± 3°C (430 ± 5°F)	249 ± 10°C (480 ± 18°F)	254 ± 7°C (489 ± 13°F)
24 h	227 ± 2°C (441 ± 4°F)	-----	310 ± 7°C (590 ± 12°F)

3.3.2.3 Thermogravimetric Analysis

A comparison of the thermal stability of resin cured by the three postcure cycles studied is shown in Fig. 67. The data indicate that the standard 4 h 250°C (482°F) air postcure results in a product with a somewhat lower char yield (52%) relative to either the 4 h 275°C (527°F) or 300°C (572°F) postcures with char yields of 63 and 61%, respectively. The thermal stability in air and nitrogen of ATB resin cured for 4 h at 250°C (482°F) is shown in Fig. 68. In a nitrogen atmosphere, the char yield to 800°C (1472°F) is 52% and the onset temperature ~ 496°C (925°F). The onset temperature in air is somewhat higher at 531°C (988°F) due to apparent oxidative weight gain at intermediate temperatures.

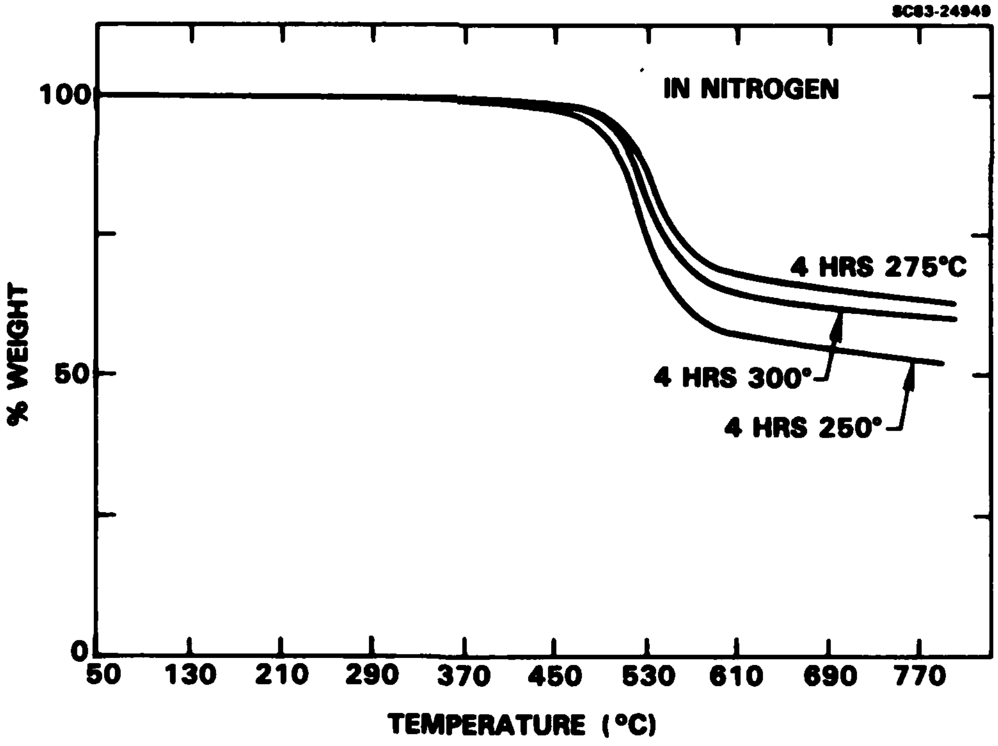

Fig. 67 The Effect of postcure conditions in air on the thermogravimetric behavior of ATB resin in nitrogen.

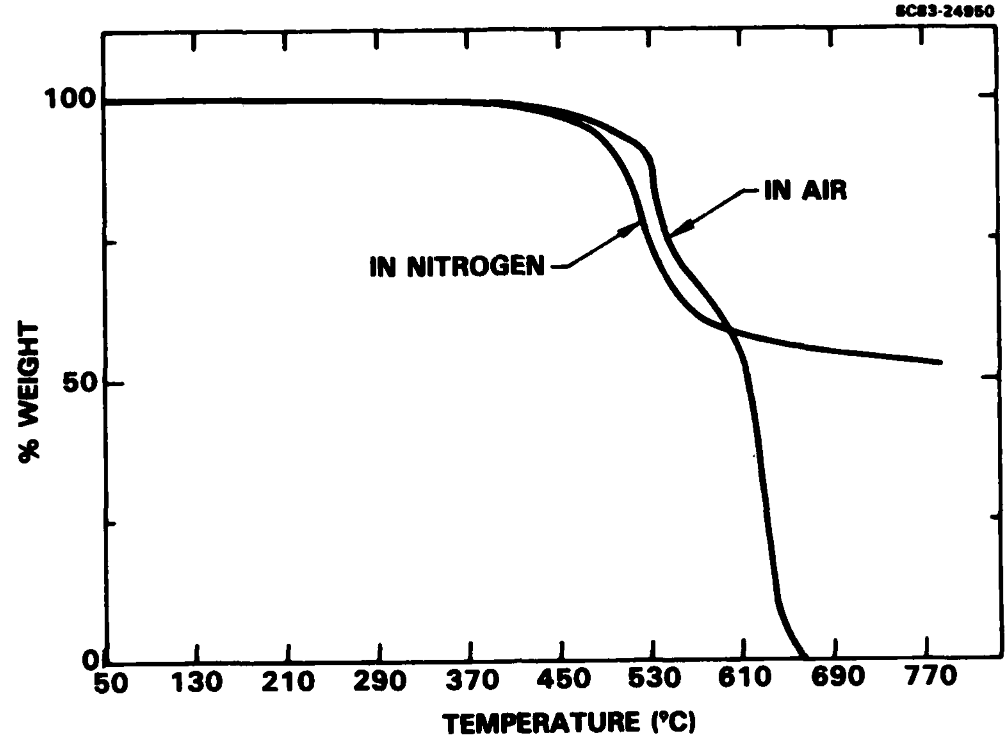

Fig. 68 The effect of environment on the thermogravimetric behavior of ATB resin cured 4 h at 250°C (482°F) in air.

3.3.2.4 Mechanical Properties

Based on previous glass transition temperature data, three postcure conditions for ATB resin were chosen for further investigation. They are each 4 h at 250°C (482°F), 275°C (527°F) or 300°C (572°F). The baseline cure cycle of 15 h at 140°C and 5 h at 170°C was used prior to postcure. The room temperature tensile mechanical data for these three postcure conditions is summarized in Table 30. The tensile properties at 121°C (250°F) and 177°C (350°F) are given in Tables 31 and 32, respectively. The tensile strengths and elongations to failure from Tables 30, 31 and 32 are plotted in Fig. 69. Although the neat resin tensile data showed a large scatter, the failure envelopes in Fig. 77 indicate that the 4 h 250°C (482°F) postcure provides the best tensile properties.

Table 30

23°C (73°F) Mechanical Properties of ATB Molded Neat Resin Microtensile Specimens

Postcure (In Air)	Tensile Strength MPa (ksi)	Tensile Modulus GPa (ksi)	Elongation To Failure (%)
4 h at 250°C	92.4 (13.4)	2.02 (438)	5.4
(482°F)	± 0.7 (0.1)	± 0.25 (36)	± 0.6
4 h at 275°C	73.1 (10.6)	2.92 (424)	3.7
(527°F)	± 0.7 (0.1)	± 0.17 (25)	± 0.6
4 h at 300°C	60.8 (8.82)	3.00 (435)	2.4
(572°F)	± 8.5 (1.24)	± 0.28 (41)	± 0.2

Table 31

121°C (250°F) Mechanical Properties of ATB Molded Neat Resin Microtensile Specimens

Postcure (In Air)	Tensile Strength MPa (ksi)	Tensile Modulus GPa (ksi)	Elongation To Failure (%)
4 h at 250°C	73.1 (10.6)	2.39 (347)	7.2
(482°F)	± 2.8 (0.4)	± 0.13 (19)	± 0.2
4 h at 275°C	67.2 (9.74)	2.28 (330)	5.2
(527°F)	± 2.8 (0.410	± 0.15 (22)	± 0.3
4 h at 300°C	48.3 (7.00)	2.32 (337)	2.6
(572°F)	± 4.6 (0.66)	± 0.08 (11)	± 0.4

Table 32

177°C (350°F) Mechanical Properties of ATB Molded Neat Resin Microtensile Specimens

Postcure (In Air)	Tensile Strength MPa (ksi)	Tensile Modulus GPa (ksi)	Elongation To Failure (%)
4 h at 250°C (482°F)	51.4 (7.46) ± 2.3 (0.33)	2.07 (300) ± 0.08 (12)	9.4 ± 1.0
4 h at 275°C (527°F)	50.8 (7.37) ± 1.8 (0.26)	2.07 (300) ± 0.19 (27)	5.8 ± 2.0
4 h at 300°C (572°F)	45.5 (6.60) ± 3.4 (0.50)	1.95 (283) ± 0.17 (24)	3.7 ± 0.1

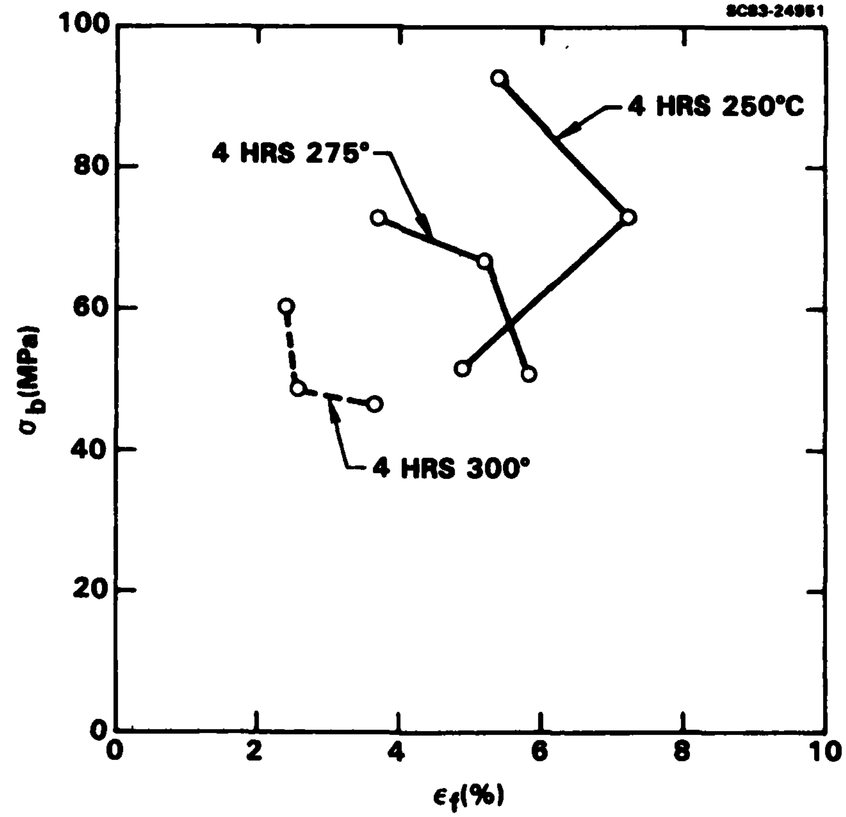

Fig. 69 The effect of postcure on the tensile failure envelopes of ATB resin.

3.3.2.5 Tensile Fracture Surface Analysis

SEM photomicrographs of the fracture surfaces of microtensile specimens tested at room temperature are shown in Figs. 70 and 71. The upper photomicrograph in Fig. 70 shows the cross section of an ATB neat resin tensile specimen. Below it in Fig. 70, three areas are shown at higher magnification. These photomicrographs and those in Fig. 71 show the smooth cleavage planes characteristic of a very brittle glassy material.

3.3.3 Composite Cure Cycle Development

3.3.3.1 Prepreg Preparation

Impregnation of unsized Hercules AS4 12K fiber was carried out using a single tow hot-melt pultrusion technique described in Appendix A. A prepregging temperature of 40°C, which produces a viscosity of ~ 300 Poise, was found suitable. A summary of the prepreg preparation and its properties are given in Table 33.

3.3.3.2 Laminate Fabrication

Autoclave processing of AS4/ATB was carried out using the Air Force Materials Laboratory fabrication procedure. Prepreg was vacuum-dried at room temperature for 12 h prior to layup. The laminates were precompacted in a vacuum bag for 4 h prior to autoclave processing. A schematic of the precompaction layup is shown in the upper portion of Fig. 72. Laminates were cured using the "no bag" technique shown in the lower portion of Fig. 72. A laminate is simply placed on a caul plate with a single ply of porous Teflon release ply on each side and cured under a constant air pressure of 100 psi. This technique was found to be very effective for processing resins like ATB which have excessive flow characteristics. A summary of the cure cycle is given in Table 34.

SC85-30272

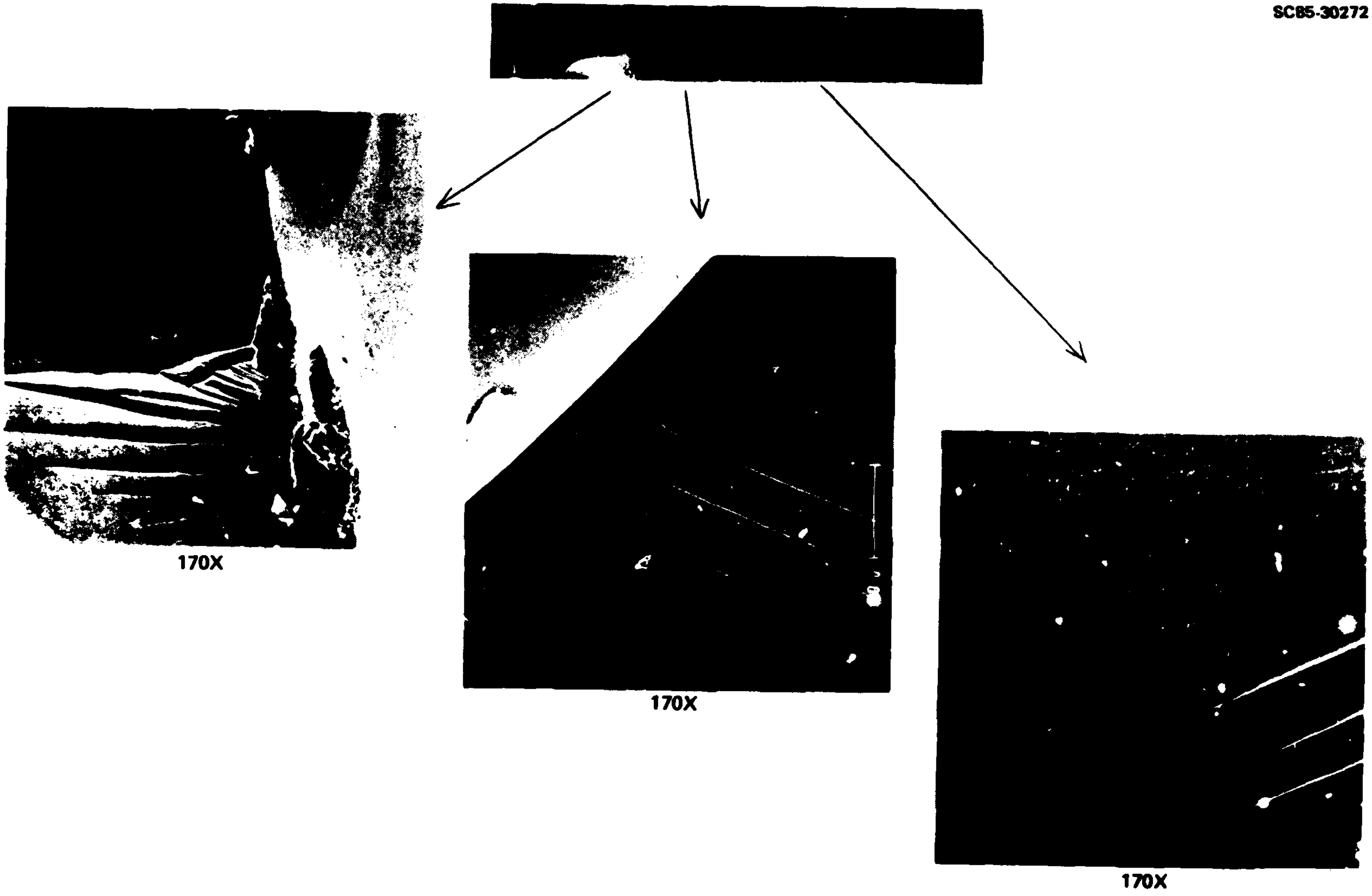

Fig. 70 SEM micrographs of ATB neat resin tensile fracture surfaces.

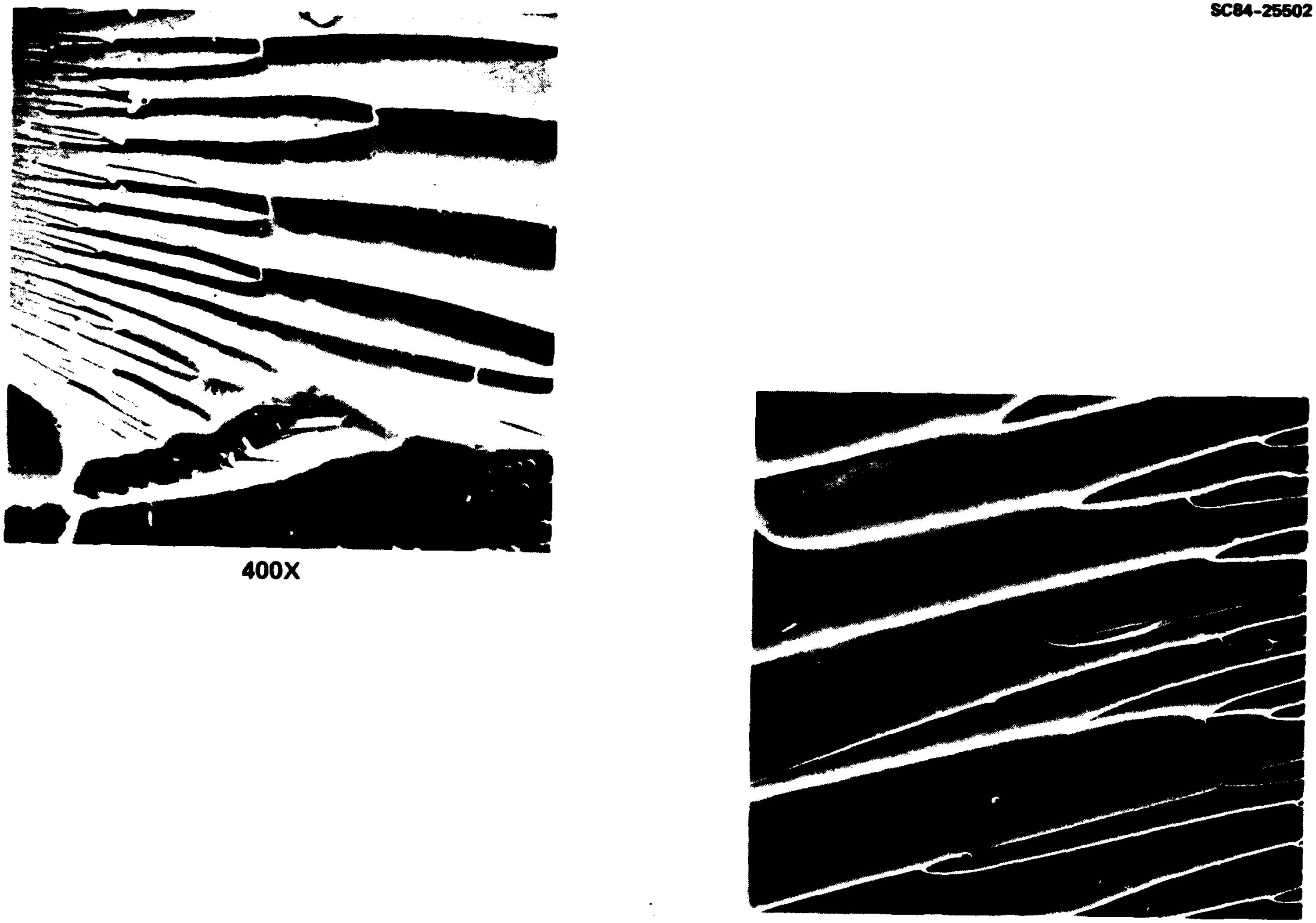

400X

400X

Fig. 71 SEM micrographs of ATB neat resin tensile fracture surfaces.

Table 33

AS4/ATB Prepreg Properties

Resin	Neat ATB
Fiber	AS4 12K, unsized
Pultrusion Die	0.147 cm x 0.559 cm
Prepregging Temperature	40°C
Pultrusion Viscosity	~ 300 Poise
Pultrusion Rate	5 cm/min
Tows Per Inch	5
Resin Content	35-36%
Areal Fiber Weight	174 g/m^2
Fiber Collimation	Good
Resin Uniformity	Good
Tack	Good
Drape	Good

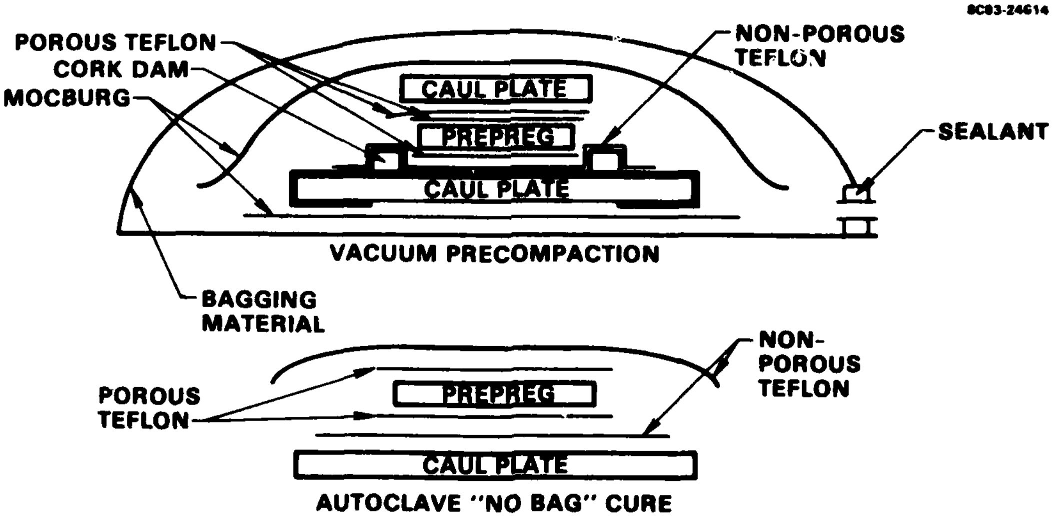

Fig. 72 Schematic of vacuum precompaction and "no bag" autoclave process for AS4/ATB.

Table 34

AS4/ATB Autoclave Cure Cycle

1. Place laminate on cool plate and apply 100 psi air.
2. Ramp to 140°C (284°F) at ~ 2°C/min (3.6°F/min).
3. Hold 15 h at 140°C (284°F).
4. Ramp to 170°C (338°F) at ~ 2°C/min (3.6°F/min).
5. Hold 5 h at 170°C (338°F).
6. Cool to RT at ~ 2°C/min (3.6°F/min).

The physical properties of 16-ply unidirectional laminates prepared by this procedure are given in Table 35. Photomicrographs of laminate cross sections are shown in Fig. 73. No evidence of delamination or porosity is indicated.

Table 35

Physical Properties of 16-Ply Unidirectional AS4/ATB Laminate

Ply Thickness	6.9 mils/ply
Density	1.51 g/cm^3
Resin Content	34.1%
Fiber Volume	55.4%
T_g (Rheometrics)	265°C (509°F)
NDI C-Scan	100%

3.3.4 Composite Testing and Evaluation

3.3.4.1 Dynamic Viscoelastic Analysis

The dynamic mechanical behavior of AS4/ATB composite is shown in Fig. 74. The T_g is not well defined by a maximum in the dynamic properties G" or tanδ. The dynamic shear modulus, G', however, begins to drop significantly by 250°C (482°F).

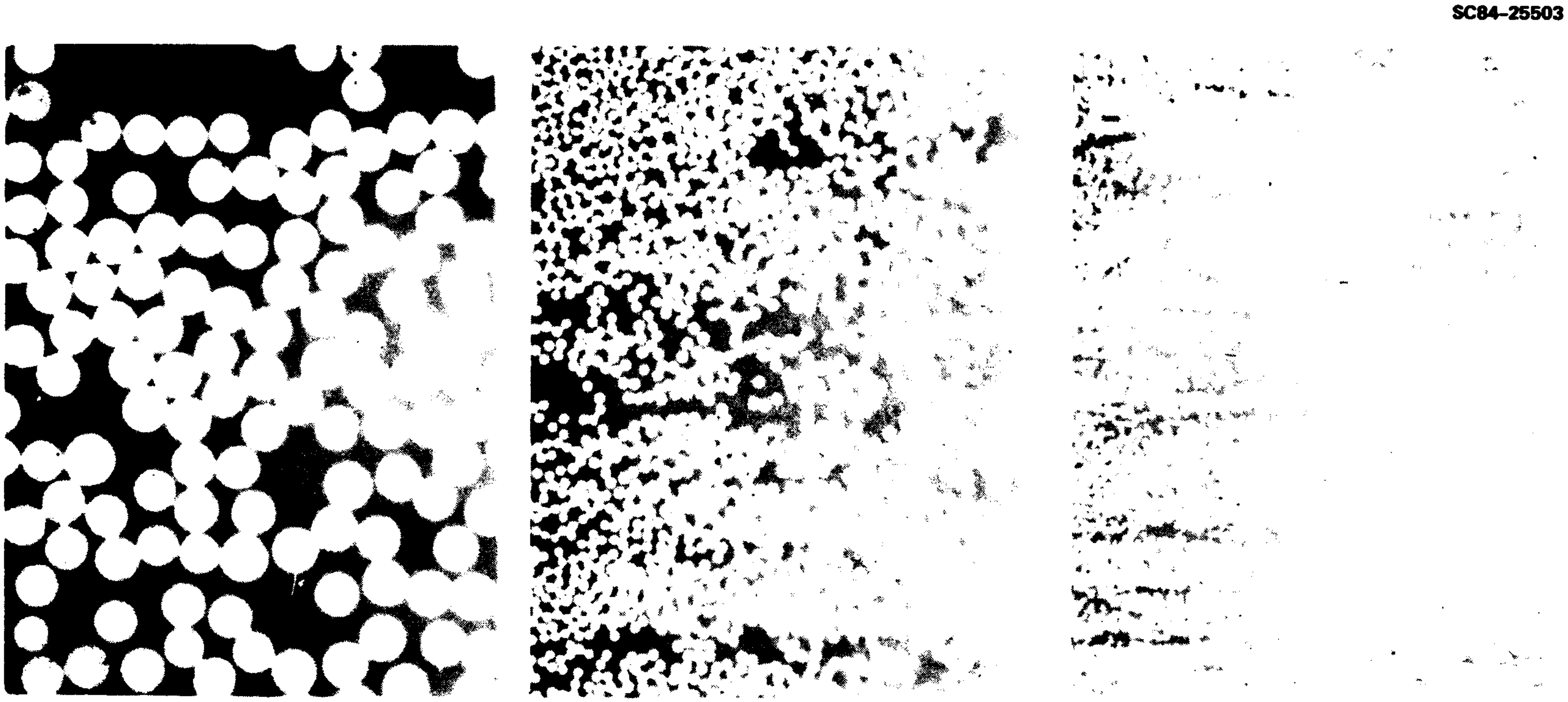

1000X 250X 100X

Fig. 73 Photomicrographs of AS4/ATB cross sections.

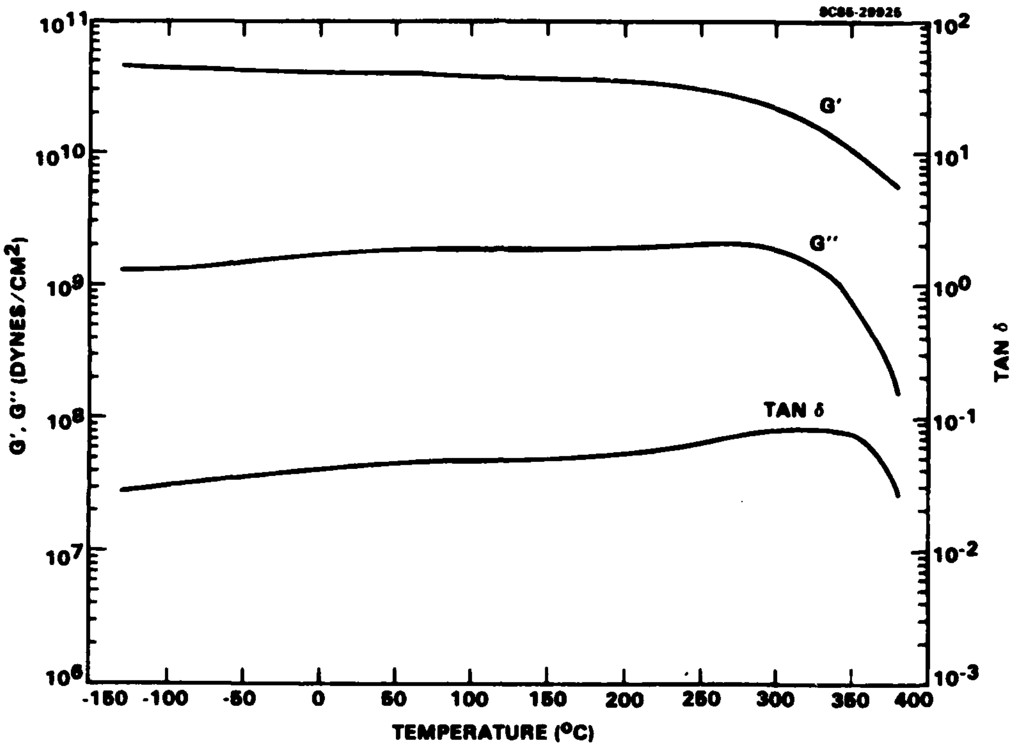

Fig. 74 Dynamic viscoelastic analysis of AS4/ATB.

3.3.4.2 Four-Point Shear Strength

The interlaminar shear strength of AS4/ATB was evaluated by four-point and short-beam shear tests. The four-point test data for material tested dry and moisture equilibrated at 71°C (160°F) and 95% RH is given in Table 36. The equilibrium moisture uptake of the four-point shear specimens was 0.13%. This is more than an order of magnitude lower than many state-of-the-art 177°C (350°F) service epoxy-based composite materials. Only about a 5% decrease in shear strength was measured for the moisture-conditioned material. Although the shear strength retention at 177°C (350°F) is over 80%, the actual values of the shear strength are only about 70% that of state-of-the-art 177°C (350°F) epoxies. The failure mode of the four-point shear specimens was interlaminar in all cases

Table 36

Four-Point Shear Strength of AS4/ATB Composite

Test Temp. °C (°F)	Shear Strength (Dry) MPa (ksi)	Shear Strength (Wet) MPa (ksi)	Failure Mode
24 (75)	56.0 (8.12) ± 0.8 (0.12)	54.1 (7.84) ± 2.2 (0.32)	Interlaminar
121 (250)	53.2 (7.71) ± 1.3 (0.19)	48.7 (7.07) ± 1.1 (0.16)	Interlaminar
177 (350)	46.5 (6.74) ± 0.3 (0.05)	44.5 (6.45) ± 1.1 (0.16)	Interlaminar
232 (450)	35.1 (5.1) ± 0.6 (0.1)	--- ---	Interlaminar

3.3.4.3 Short-Beam Shear Strength

Short-beam shear data for AS4/ATB are given in Table 37. The shear strength values are 20-25% higher than measured in the four-point test. The shear strength retention at 177°C (350°F) is ~ 80%, the same value found in the four-point test. The short-beam shear data for AS4/ATB are about 75% of the values typically reported for state-of-the-art epoxies by this test.

Table 37

Short-Beam Shear Strength of AS4/ATB Composite

Test Temp. °C (°F)	Shear Strength MPa (ksi)	Failure Mode
24 (75)	78.6 (11.4) (0.2)	Interlaminar
121 (250)	71.0 (10.3) ± 1.4 (0.2)	Interlaminar
177 (350)	62.1 (9.0) ± 0.7 (0.1)	Interlaminar
232 (450)	46.2 (6.7) ± 0.7 (0.1)	Interlaminar

The failure surfaces of four-point shear specimens were examined by SEM. The areas studied were those in which failure initiated, as described in Section 3.2.4.3. Views at several magnification levels are given in Figs. 75-77. They show a disorderly distribution of fractured resin debris which may be indicative of a brittle resin. By contrast, the interlaminar shear failure surfaces of state-of-the-art graphite/epoxy composites show resin deformation producing a somewhat orderly platelet-like arrangement.[3] Another feature of the shear failure surfaces is the large amount of unbonded fiber surface evident. This may in some part account for the low interlaminar shear strengths.

3.3.4.4 Flexural Strength and Modulus

The 0° three-point flexural properties of AS4/ATB composite are given in Table 38. The values reported were normalized to 60% fiber volume. The failure mode observed was primarily in compression. An 80% retention of strength at 121°C (250°F) and a 72% retention at 177°C (350°F) is shown. The absolute values of the flexural strength, however, are only about 75% that typically obtained for 177°C (350°F) service graphite/epoxy composites.

The flexural properties of specimens moisture-equilibrated at 71°C (160°F) and 95% RH are given in Table 39. The effects of moisture appear to be smaller than the scatter in the flexural properties from one laminate to another.

3.3.4.5 Transverse Flexural Properties

The transverse 90° room temperature four-point flexural properties of AS4/ATB are given in Table 40. The stress-strain data for one experiment are plotted in Fig. 78. The transverse flexural strength, modulus and strain-to-failure are comparable to state-of-the-art 177°C (350°F) service graphite/epoxy composites.

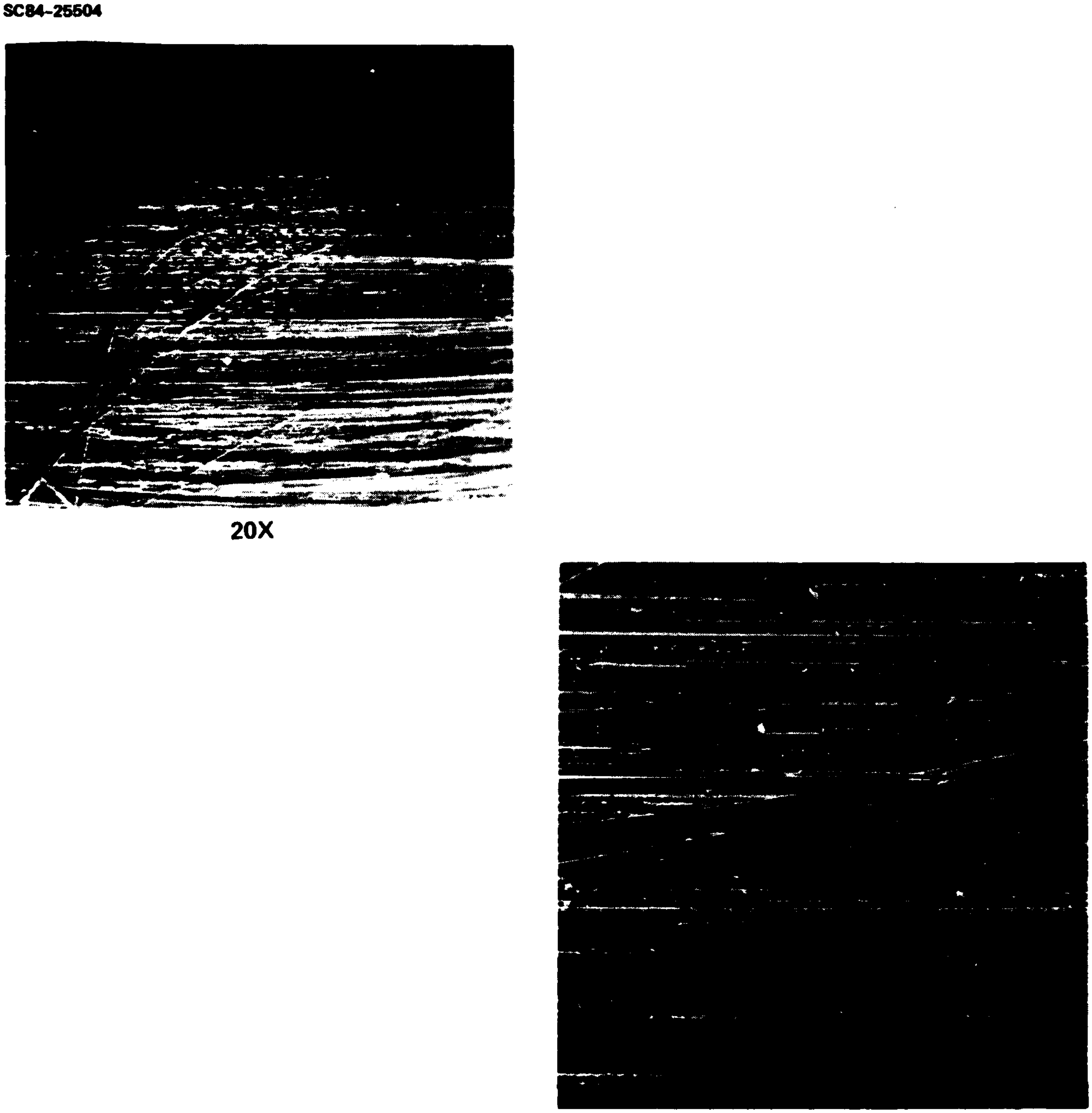

20X

100X

Fig. 75 SEM micrographs of AS4/ATB interlaminar shear fracture surface.

SC84-25505

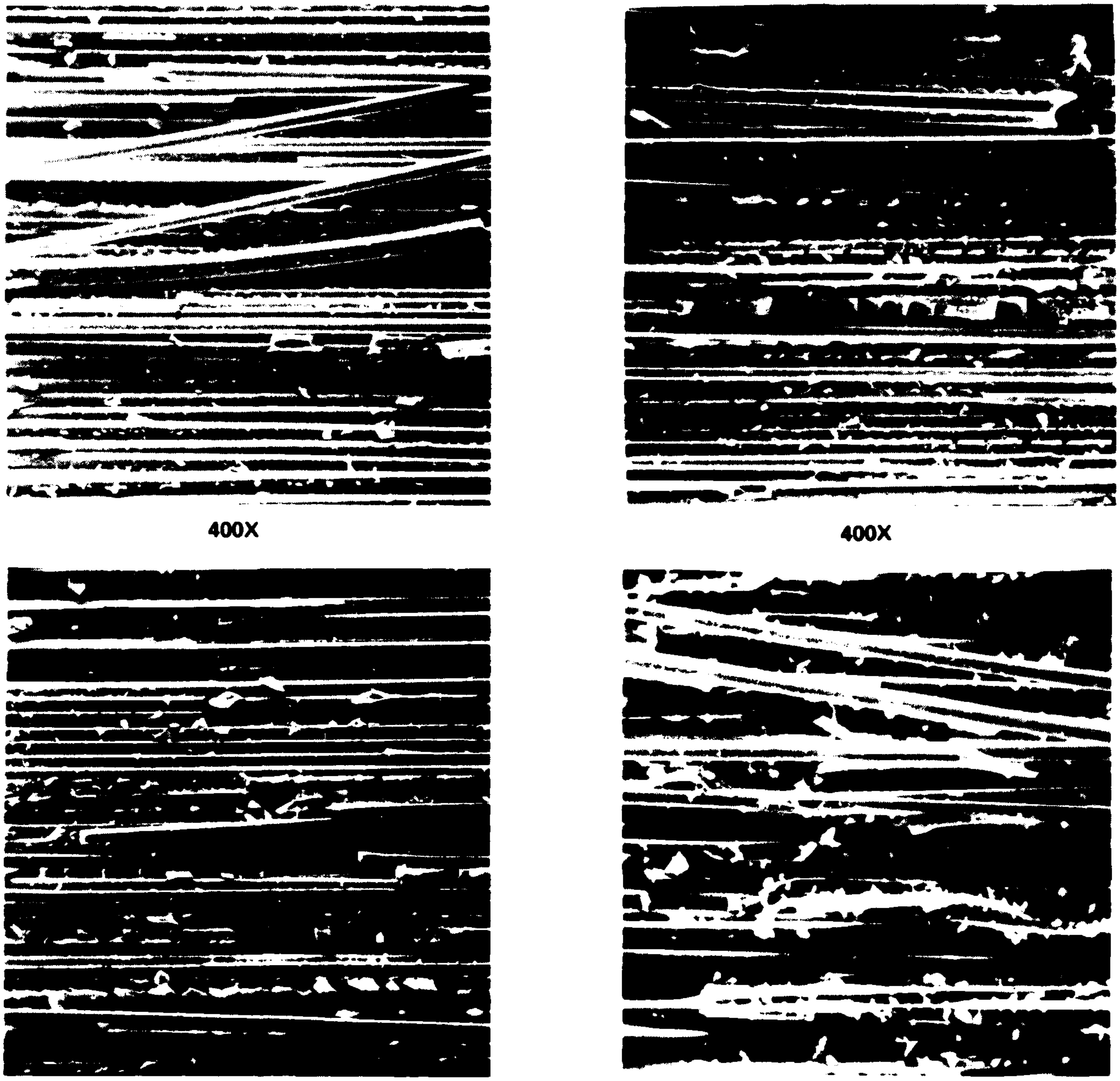

400X

400X

400X

400X

Fig. 76 SEM micrographs of AS4/ATB interlaminar shear fracture surface.

SC84-25506

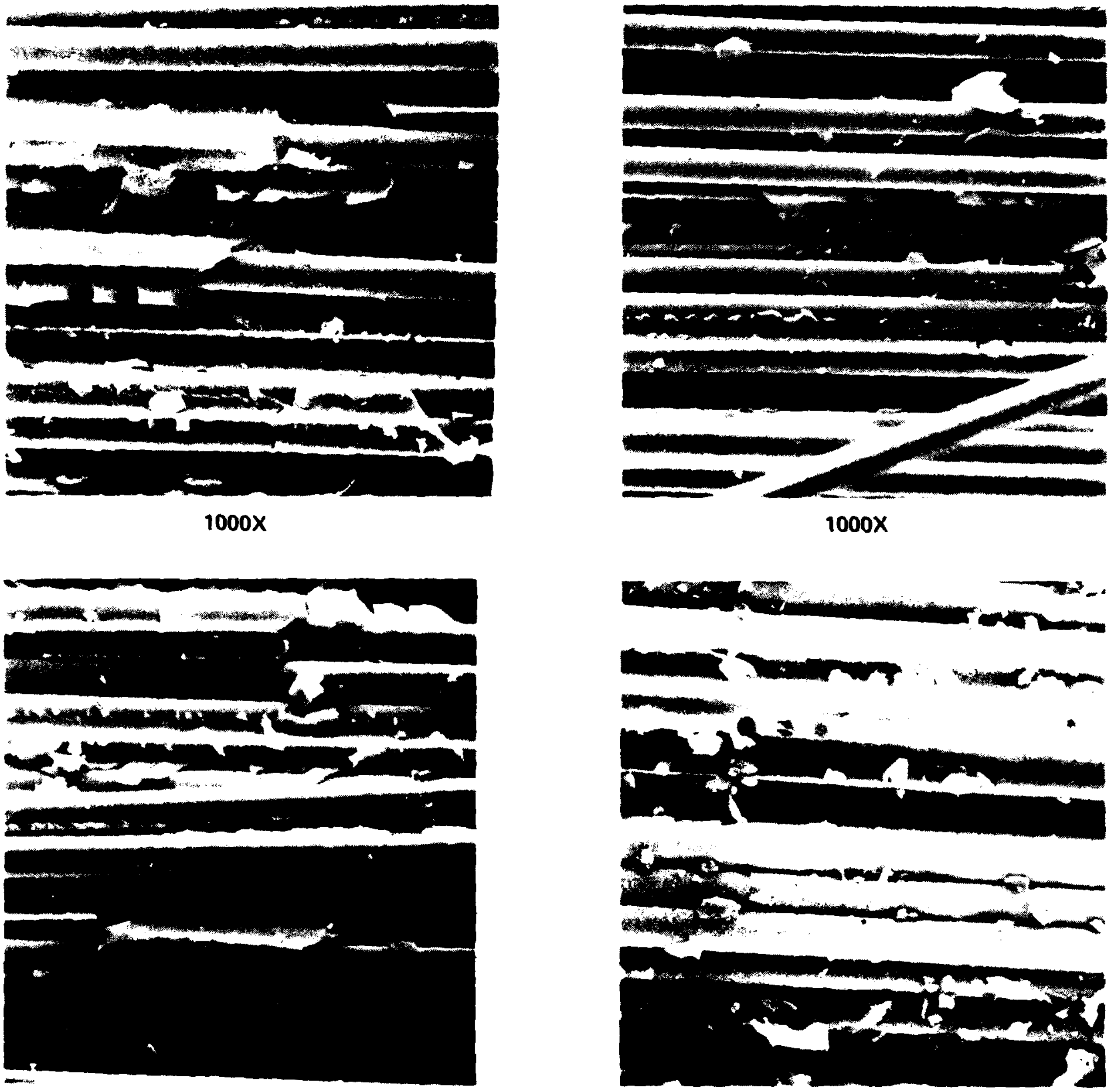
1000X

1000X

1000X

1000X

Fig. 77 SEM micrographs of AS4/ATB interlaminar shear fracture surface.

Table 38

Three-Point Flexural Properties of AS4/ATB Composite

Test Temp. °C (°F)	Flexural Strength Dry GPa (ksi)	Flexural Modulus Dry GPa (msi)	Failure Mode
24 (75)	1.45 (210) ± 0.01 (1)	140 (20.2) ± 3 (0.5)	Compression
121 (250)	1.17 (169) ± 0.03 (5)	137 (19.9) ± 2 (0.3)	Compression
177 (350)	1.05 (153) ± 0.03 (5)	137 (19.9) ± 2 (0.3)	Compression

Table 39

Three-Point Flexural Properties of AS4/ATB Composite, Moisture Conditioned at 71°C (160°F) and 95% RH

Test Temp. °C (°F)	Flexural Strength Wet GPa (ksi)	Flexural Modulus Wet GPa (msi)	Failure Mode
24 (75)	1.35 (196) ± 0.08 (11)	144 (20.9) ± 9 (1.4)	Compression
121 (250)	1.24 (180) ± 0.01 (2)	145 (21.1) ± 3 (0.4)	Compression
177 (350)	1.19 (172) ± 0.12 (17)	135 (21.3) ± 17 (2.4)	Compression

Table 40

Transverse Flexural Properties of AS4/ATB

Flexural Strength MPa (ksi)	90° Strain-To-Failure μin./in.	90° Flexural Modulus GPa (msi)
66.1 (9.60)	8167	8.76 (1.27)
68.9 (10.0)	8293	9.17 (1.33)
56.5 (8.2)	6833	9.38 (1.36)

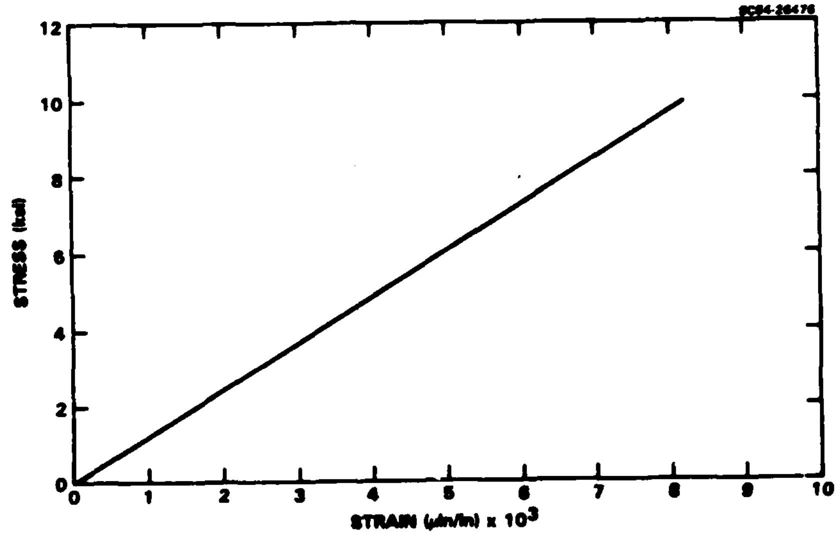

Fig. 78 Stress-strain curve for 90° flexural test of AS4/ATB.

3.3.4.6 Fracture Toughness

The Mode I delamination fracture toughness (G_{1c}) of unidirectional AS4/ATB composite was measured by the method developed by Devitt et al.[5] Data for the two tests are given in Table 41. The values given are the average of 10-15 determinations taken along the crack length of individual specimens. Data for several other composite materials are given for comparative purposes, as described in Section 3.2.4.6. The apparent fracture toughness of AS4/ATB is similar to state-of-the-art 177°C (350°F) graphite epoxies. SEM photomicrographs of the G_{1c} failure surfaces of AS4/ATB are shown in Figs. 79-81.

Table 41

G_{1c} Fracture Toughness of AS4/ATB

Composite Material	G_{1c} (N/m)
AS4/ATB	197 ± 7 216 ± 6
AS4/BATQ-H (ATP)	552 ± 40 534 ± 88
AS1/3501-5A	219 ± 25 190 ± 10
XAS/PEEK (MG-1)	1846 ± 25 1640 ± 11

SC84-27958

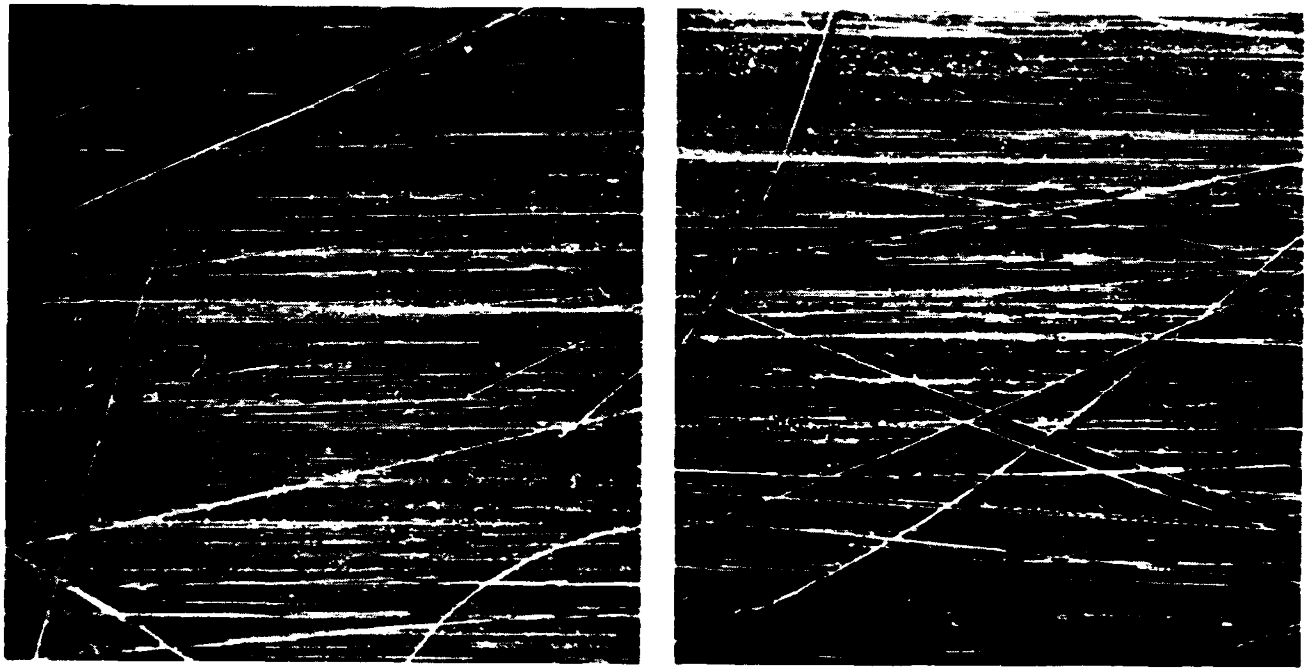

Fig. 79 SEM micrographs of AS4/ATB G_{1c} fracture surface, 40X.

SC84-27962

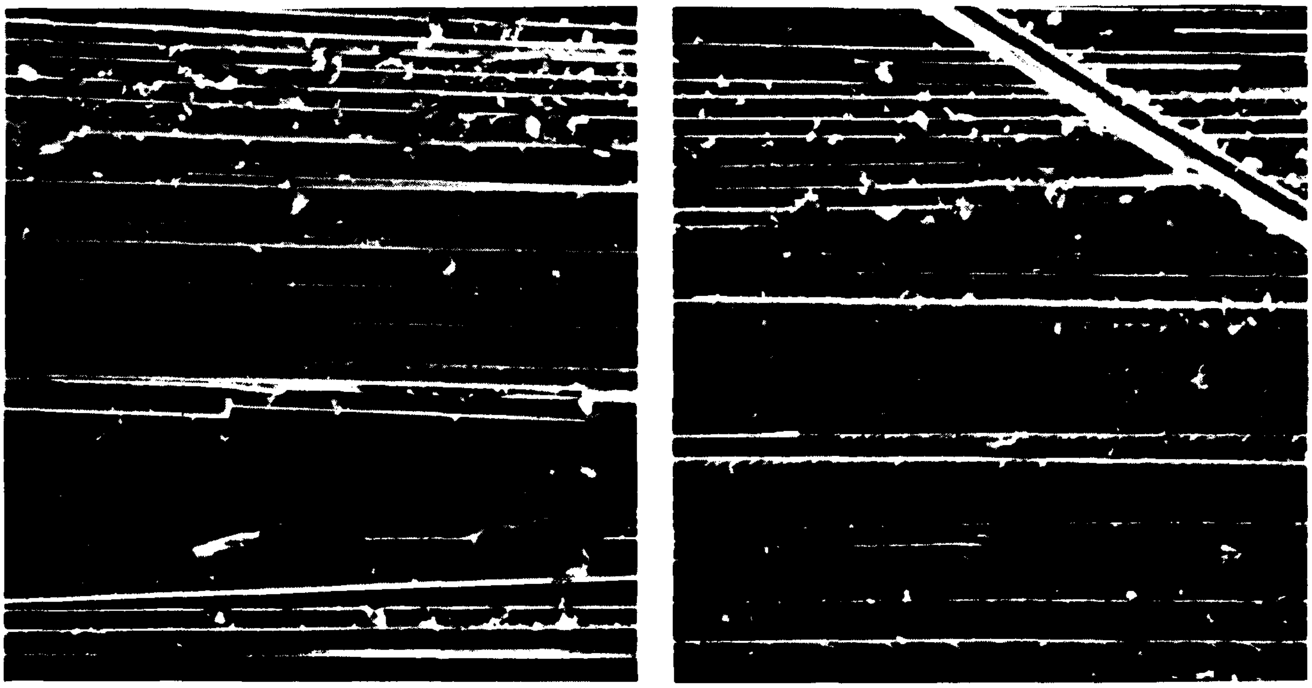

Fig. 80 SEM micrographs of AS4/ATB G_{1c} fracture surface, 400X.

SC84-27966

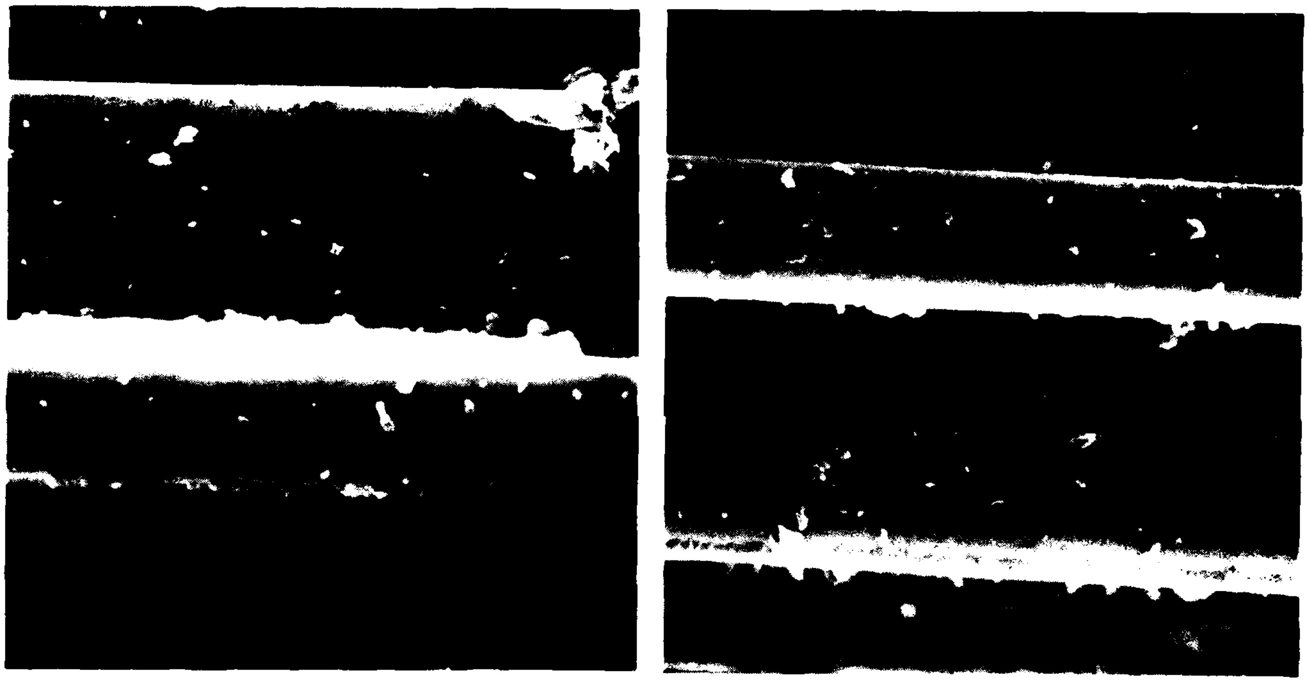

Fig. 81 SEM micrographs of AS4/ATB G_{1c} fracture surface, 2500X.

A rough surface texture is observed, indicating failure occurred in more than one ply. This effect, similar to that described for AS4/BATQ-H (ATP) in Section 3.2.4.6, leads to artificially high G_{1c} values. The photomicrographs for AS4/ATB also revealed an extensive amount of unbonded fiber present, as well as the presence of many fractured resin particles. These features are not observed in state-of-the-art graphite/epoxy or graphite/PEEK composite materials discussed in Section 3.2.4.6.

3.3.4.7 Short Cure Cycle Evaluation

A shortened cure cycle was evaluated for processing AS4/ATB composite. In this cycle, the temperature was ramped directly to 170°C (338°F) and held for 6 h, eliminating the 24 h hold at 140°C (284°F) of the long cure cycle. The laminate precompaction and autoclave cure was the same as discussed in Section 3.3.3.2. The physical properties of a 15-ply unidirectional laminate processed in this way are given in Table 42. Photomicrographs of cross sections did not show evidence of voids or other defects.

Table 42

Physical Properties of 15-Ply Unidirectional AS4/ATB Laminate (Short Cure Cycle)

Ply Thickness	7.1 mil/ply
Density	1.50 g/cm^2
Resin Content	34.8%
Fiber Volume	54.5%
T_g	267°C (513°F)
NDI Scan	100%

The four-point and short-beam shear strengths obtained with the long and short cure cycle are compared in Tables 43 and 44, respectively. No significant differences are indicated.

Table 43

Four-Point Shear Strength of AS4/ATB Composite, Long and Short Air Force Cure and Postcure Cycles

Cure Cycle	Shear Strength MPa (ksi)	Failure Mode
Short	62.7 (9.09) ± 0.7 (0.10)	Interlaminar
Long	56.0 (8.12) ± 0.8 (0.12)	Interlaminar

Table 44

Short-Beam Shear Strength of AS4/ATB Composite, Long and Short Air Force Cure and Postcure Cycles

	Shear Strength MPa (ksi)		
Test Temp. °C (°F)	Short Cure Cycle	Long Cure Cycle	Failure Mode
24 (75)	84.8 (12.3) ± 0.7 (0.1)	78.6 (11.4) ± 1.4 (0.2)	Interlaminar
121 (250)	67.8 (9.84) ± 2.1 (0.30)	71.0 (10.3) ± 1.4 (0.2)	Interlaminar
177 (350)	61.4 (8.90) ± 1.1 (0.16)	62.1 (9.0) ± 0.7 (0.1)	Interlaminar

Three-point flexural test data are given in Table 45. The flexural strengths are equivalent. The transverse flexural properties are summarized in Table 46. For this test, the long cure cycle material appears to have a higher strength and strain-to-failure than the cured by the short cure cycle.

Based on these limited mechanical property data, no significant differences are indicated between AS4/ATB composite processed by the long or short cure cycles. Both cure cycles result in rather poor mechanical properties.

Table 45

Three-Point Flexural Properties of AS4/ATB Composite Long and Short Air Force Cure and Postcure Cycles

Cure Cycle	Flexural Strength GPa (ksi)	Flexural Modulus GPa (msi)	Failure Mode
Short	1.28 (186) ± 0.03 (4)	101 (14.7) ± 1 (0.2)	Compressive
Long	1.45 (210) ± 0.01 (1)	140 (20.2) ± 3 (0.5)	Compressive

Table 46

Transverse Flexural Properties of AS4/ATB Composite Long and Short Air Force Cure and Postcure Cycles

Cure Cycle	Flexural Strength MPa (ksi)	90° Strain-To-Failure μin./in.	90° Flexural Modulus GPa (msi)
Short	57.3 (8.31)	6540	8.76 (1.27)
	52.4 (7.60)	5712	9.17 (1.33)
	53.4 (7.74)	5961	9.38 (1.36)
Long	66.1 (9.60)	8167	8.14 (1.18)
	68.9 (10.00)	8293	8.34 (1.21)
	56.5 (8.20)	6833	8.27 (1.20)

3.4 Air Force m-ATS Resin

ATS (acetylene-terminated sulfone) resin was one of the earliest materials developed by the Air Force Materials Laboratory utilizing acetylene technology. The molecular structure of this resin is shown in Fig. 82. The ATS resin studied in the program was a purified (n = 1) m-ATS material prepared by Fluorochem Inc., Irwindale, CA. Liquid chromatographic analysis revealed this resin to contain less oligomer and impurities than previously synthesized materials. It is also a liquid at room temperature which makes it easier to process than earlier solid materials.

SC85-29985

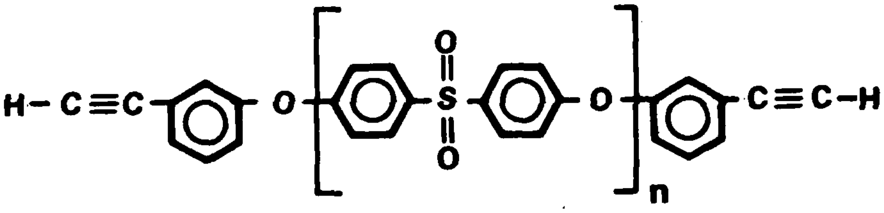

Fig. 82 Molecular structure of m-ATS resin.

3.4.1 Materials Validation

3.4.1.1 Differential Scanning Calorimetry

The DSC thermograms for the cure of m-ATS resin at various heating rates are given in Fig. 83. The dependence of the peak exotherm temperatures on heating rate are plotted in Fig. 84 where an activation energy for cure of 26.2 kcal/mole is found. A summary of the DSC data is given in Table 47.

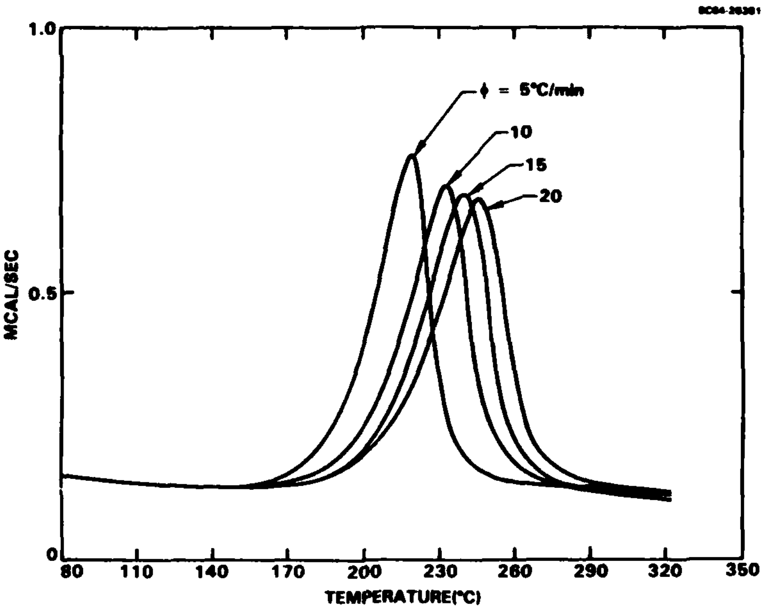

Fig. 83 DSC thermograms of m-ATS resin.

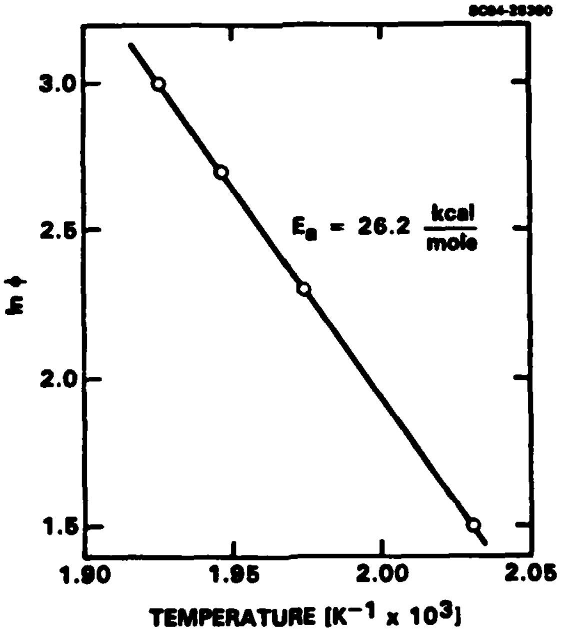

Fig. 84 Dependence of DSC exotherm peak temperature with heating rate for m-ATS resin.

Table 47

DSC Analysis of ATS Neat Resin

Uncured melt temperature		---
Exotherm onset temperature	ϕ = 10°C/min	155°C (311°F)
Exotherm peak temperature	ϕ = 10°C/min	233°C (451°F)
Exotherm completion temperature	ϕ = 10°C/min	284°C (543°F)
Heat of polymerization		125 cal/g
Activation energy for polymerization		26.2 kcal/mole

3.4.1.2 Cure Rheology

The rheological behavior of m-ATS resin during various linear heating rate experiments is shown in Fig. 85. The low dynamic viscosity of m-ATS is very similar to the behavior of ATB described in Section 3.3.1.2. Gelation occurred at a temperature of ~ 200°C (392°F) in these cure cycles. The isothermal cure behavior is plotted in Fig. 86. The viscoelastically defined gelation times are given in Table 48. These gel times are much shorter than measured for ATB resin. The temperture dependence of the gel time data is plotted in Fig. 87, where an activation energy to gelation of 22.1 kcal/mole is defined.

3.4.2 Composite Cure Cycle Development

3.4.2.1 Prepreg Preparation

AS4/m-ATS prepreg was prepared by the same hot-melt pultrusion technique described in Section 3.3.3.1. A summary of the prepreg properties is given in Table 49. The resin content of AS4/m-ATS prepreg was reduced to 33% by a controlled bleed of individual plies. By doing this, the fiber volume of cured AS4/m-ATS was increased to ~ 59%.

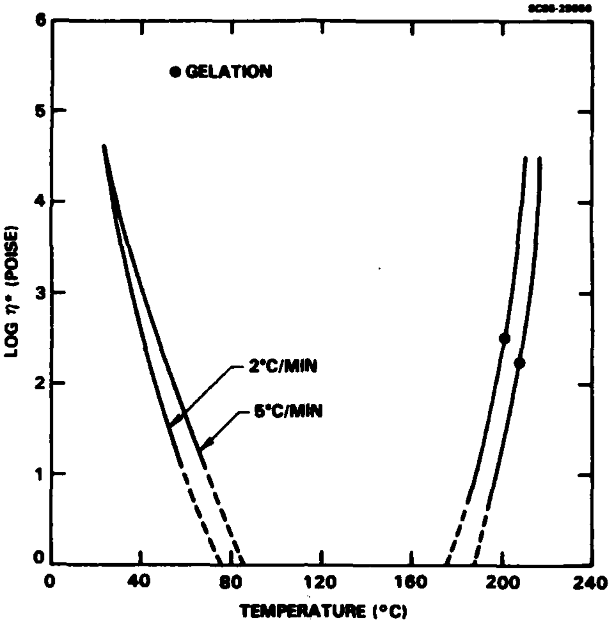

Fig. 85 Dynamic viscosity during cure of m-ATS resin at different heating rates.

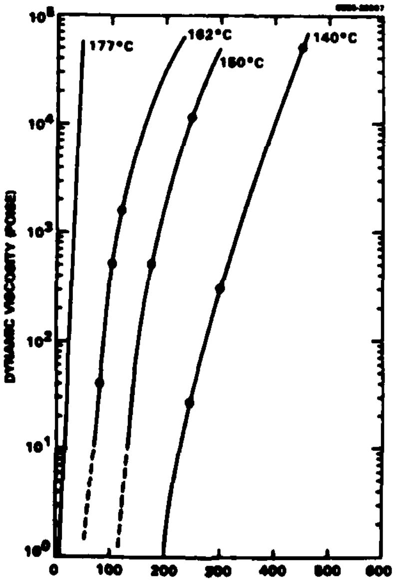

Fig. 86 Dynamic viscosity during cure of m-ATS resin at different temperatures.

Table 48

Dynamic Viscoelastic Analysis of Gelation for m-ATS Resin

T (°C)	T (°F)	$t_{G' = G''}$ (min)
140	284	250
150	302	125
162	324	70
177	350	29

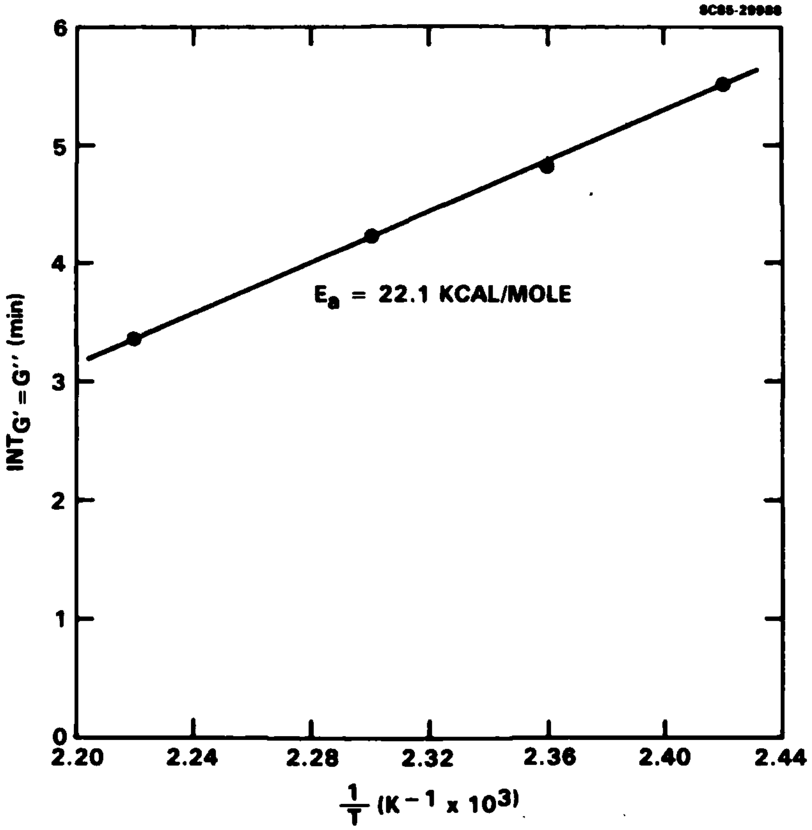

Fig. 87 Dependence of dynamic moduli crossover time with cure temperature for m-ATS resin.

Table 49

AS4/m-ATS Prepreg Properties

Resin	Neat m-ATS
Fiber	AS4 12K, unsized
Pultrusion Die	0.0147 cm x 0.559 cm
Prepregging Temperature	60°C
Pultrusion Viscosity	~ 300 Poise
Pultrusion Rate	5 cm/min
Tows Per Inch	5
Resin Content	33%
Areal Fiber Weight	174 g/m^2
Fiber Collimation	Good
Resin Uniformity	Good
Tack	Good
Drape	Good

3.4.2.2 Laminate Fabrication

AS4/m-ATS laminates were precompacted and autoclave cured using the Air Force Materials Laboratory's procedures described in Section 3.3.3.2 for processing AS4/ATB. Neat resin tensile tests were not carried out for m-ATS because an optimum cure and postcure cycle for this system had already been developed by the Air Force Materials Laboratory. The autoclave portion of the cure cycle is described in Table 50. The postcure consisted of 10 h at 300°C (577°F) in air. The physical properties of 16-ply unidirectional laminates prepared by this procedure are given in Table 51. Photomicrographs of composite cross sections are shown in Fig. 88. The material showed no evidence of voids.

Table 50

AS4/m-ATS Autoclave Cure Cycle

1. Place laminate on caul plate and apply 100 psi air.
2. Ramp to 140°C (284°C) at ~ 2°C/min (~ 3.6°F/min).
3. Hold 24 h at 140°C (284°F).
4. Ramp to 177°C (350°F).
5. Hold 5 h at 177°C (350°F).
6. Cool to RT at ~ 2°C/min (~ 3.6°F/min).

Table 51

Physical Properties of 16-Ply Unidirectional AS4/m-ATS

Ply Thickness	6.5 mils/ply
Density	1.60
Resin Content	33.9%
Fiber Volume	58.9%
T_g (Rheometrics)	281°C (536°F)
NDI Scan	100%

3.4.3 Composite Testing and Evaluation

3.4.3.1 Dynamic Viscoelastic Analysis

The temperature dependence of the dynamic viscoelastic properties of AS4/m-ATS is shown in Fig. 89. From the peak maximum of the dynamic shear loss modulus, G", a T_g of 281°C (536°F) is defined. At about 250°C (482°F), however, the dynamic shear storage modulus, G', begins to drop sharply.

3.4.3.2 Four-Point Shear Strength

The results of four-point shear testing of 16-ply unidirectional AS4/m-ATS composite are given in Table 52. Three specimens were tested at each condition. Wet testing was conducted on specimens conditioned to equilibrium at 71°C (160°F) and 95% RH. The room temperature and 177°C (350°F) strengths are very close to those determined for AS4/ATB and described in Section 3.3.4.2. The shear strengths are only about 70% of those found for state-of-the-art 177°C (350°F) graphite/epoxy materials. A strength retention at 177°C (350°F) of 75% and 60% at 232°C (450°F) is observed. The failure mode of the specimens was interlaminar.

A significant decrease in shear strength was found for the hot-wet tests. About a 15% decrease at 177°C (350°F) and 35% at 232°C (450°F) was found. Only about a 5% lowering of four-point shear strength was measured for AS4/ATB composite in hot-wet testing.

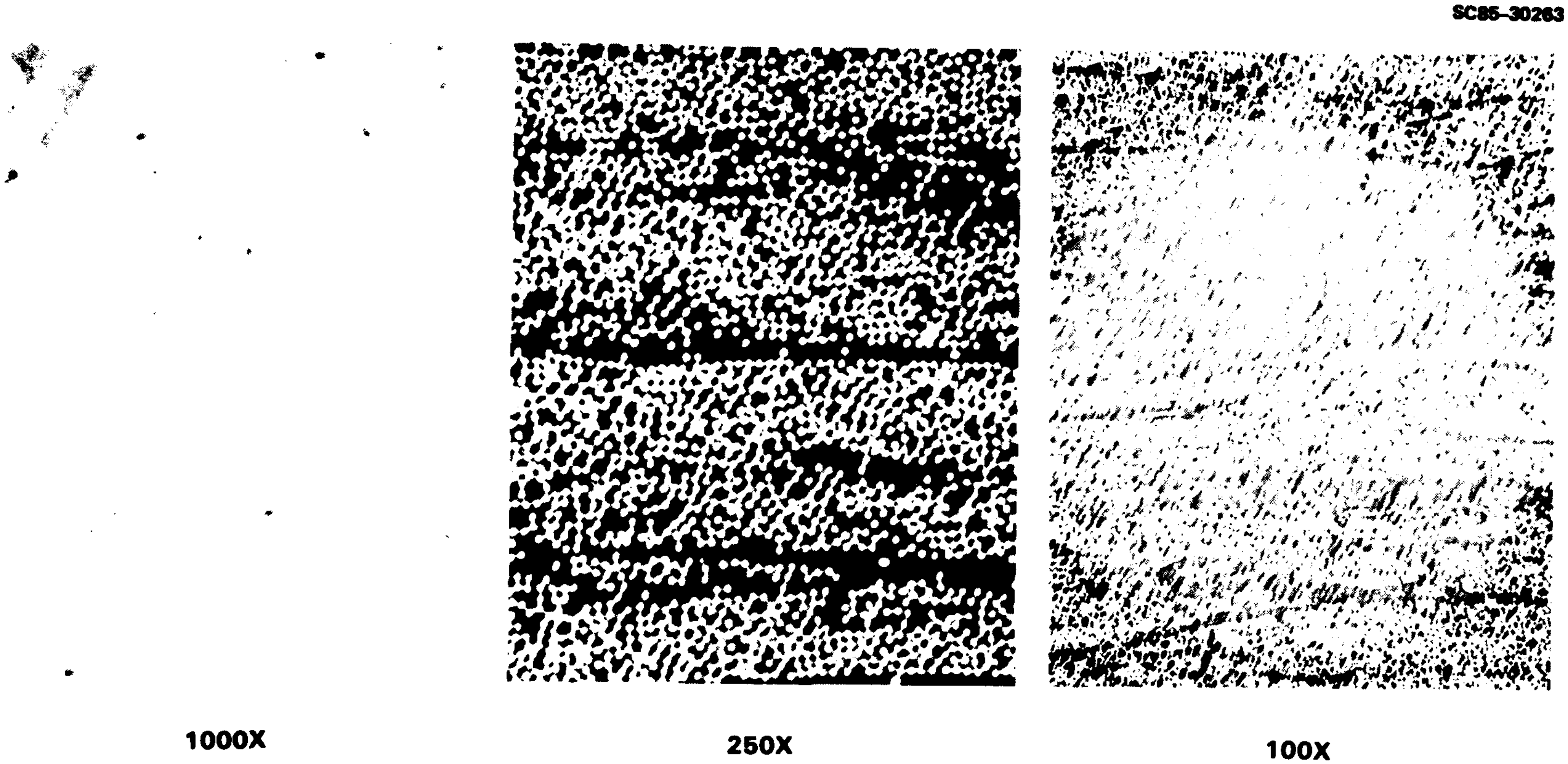

Fig. 88 Photomicrographs of AS4/m-ATS cross sections.

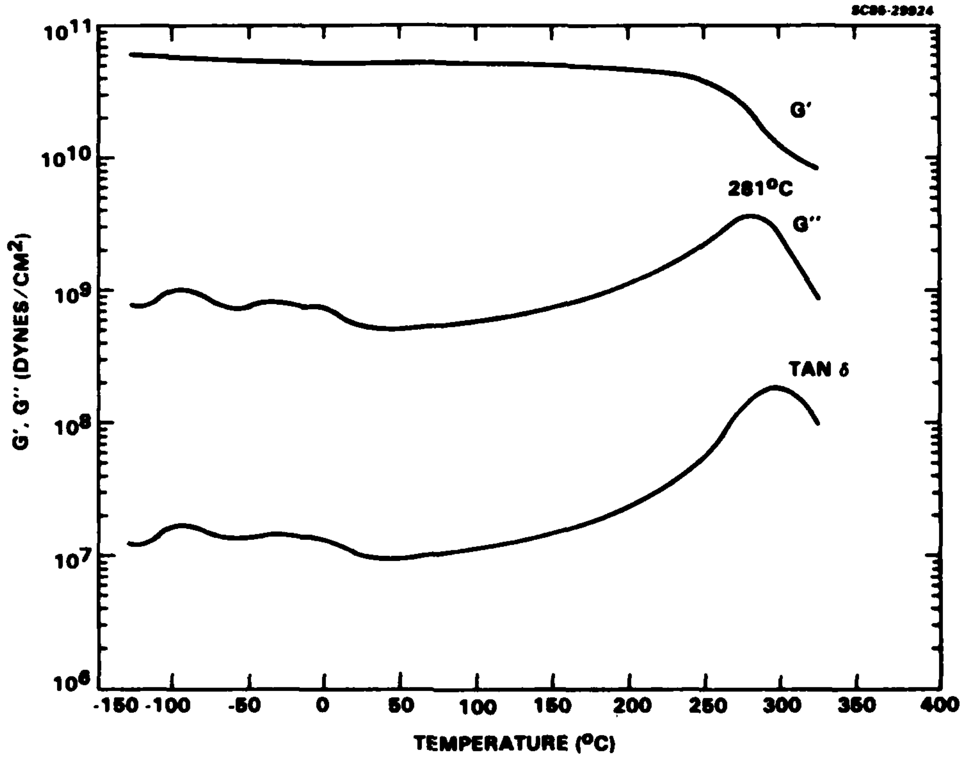

Fig. 89 Dynamic viscoelastic analysis of AS4/m-ATS.

Table 52

Four-Point Shear Strength of AS4/m-ATS Composite

Test Temperature °C (°F)	Shear Strength Dry MPa (ksi)	Shear Strength Wet MPa (ksi)	Failure Mode
24 (75)	62.7 (9.1) ± 0.7 (0.1)	61.4 (8.9) ± 5.5 (0.8)	Interlaminar
177 (350)	44.1 (6.4) ± 0.7 (0.1)	38.6 (5.6) ± 2.1 (0.3)	Interlaminar
232 (450)	35.2 (5.1) ± 0.7 (0.1)	22.8 (3.3) ± 0.7 (0.1)	Interlaminar

3.4.3.3 Short-Beam Shear Strength

The short-beam shear strength of AS4/m-ATS composite is given in Table 53. Again, the room temperature and 177°C (350°F) values are close to those described for AS4/ATB in Section 3.3.3.3. A strength retention of 72% at 177°C (350°F) and 51% at 232°C (450°F) are found. The failure mode of the short-beam shear specimens was not evident. Only a deformation of the specimens was observed. The moisture conditioning specimens showed about a 10% lower strength at 177°C (350°F) and 20% at 232°C (450°F).

Table 53

Short-Beam Shear Strength of AS4/m-ATS Composite

Test Temperature °C (°F)	Shear Strength Dry MPa (ksi)	Shear Strength Wet MPa (ksi)	Failure Mode
24 (75)	92.3 (13.4) ± 2.1 (0.3)	88.3 (12.8) ± 4.8 (0.7)	Not apparent
177 (350)	66.9 (9.7) ± 0.7 (0.1)	61.4 (8.9) ± 0.6 (0.1)	Not apparent
232 (450)	47.6 (6.9) ± 0.7 (0.1)	38.6 (5.6) ± 5.5 (0.8)	Not apparent

SEM micrographs of four-point shear failure surfaces are shown in Figs. 90-92. A large amount of fragmented resin was observed as was for AS4/ATB composite. Not as much exposed fiber surface was evident as compared to AS4/ATB. Like ATB, the failure mode appears to produce a less orderly resin deformation than state-of-the-art 177°C (350°F) service graphite epoxies.

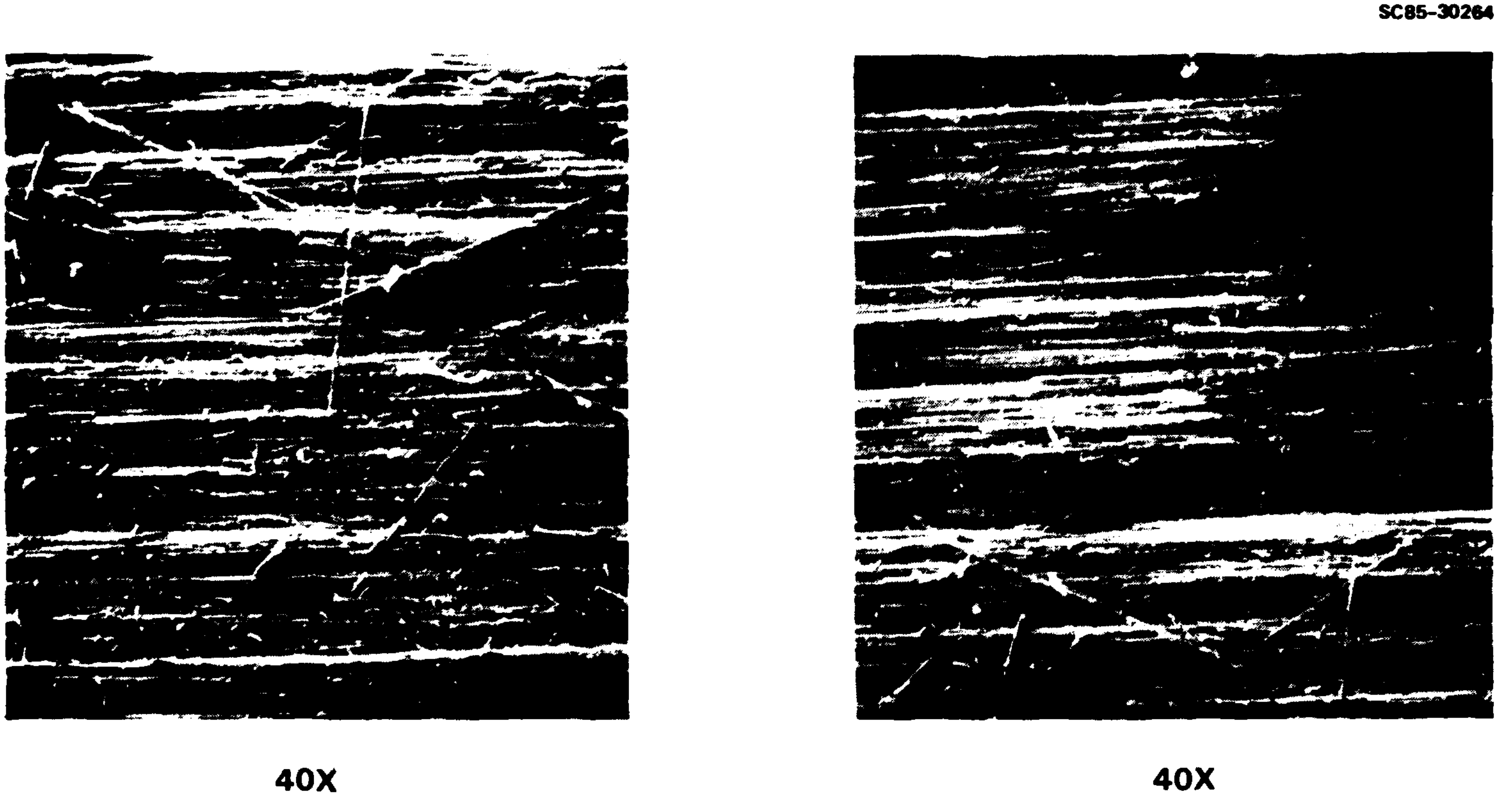

Fig. 90 SEM micrographs of AS4/m-ATS interlaminar shear fracture surface.

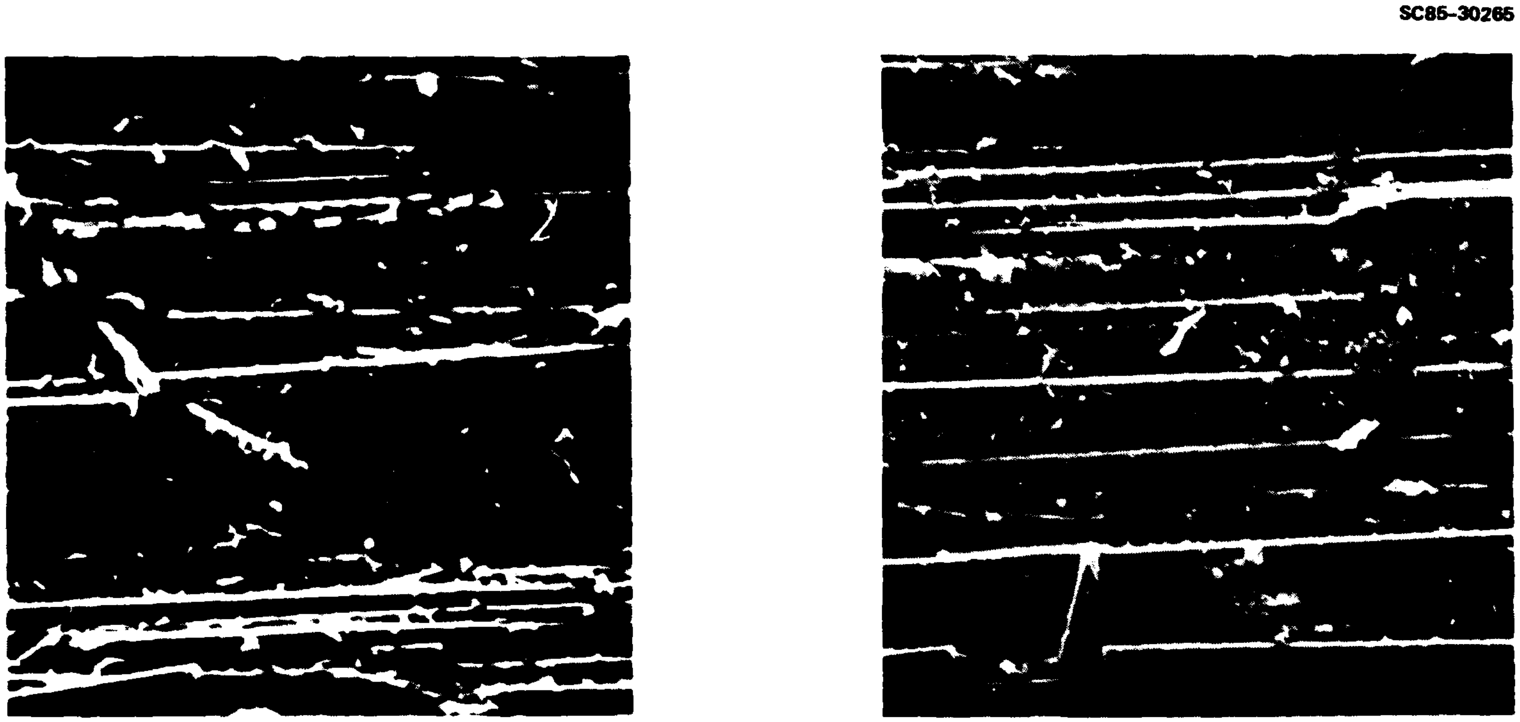

400X

400X

Fig. 91 SEM micrographs of AS4/m-ATS interlaminar shear fracture surface.

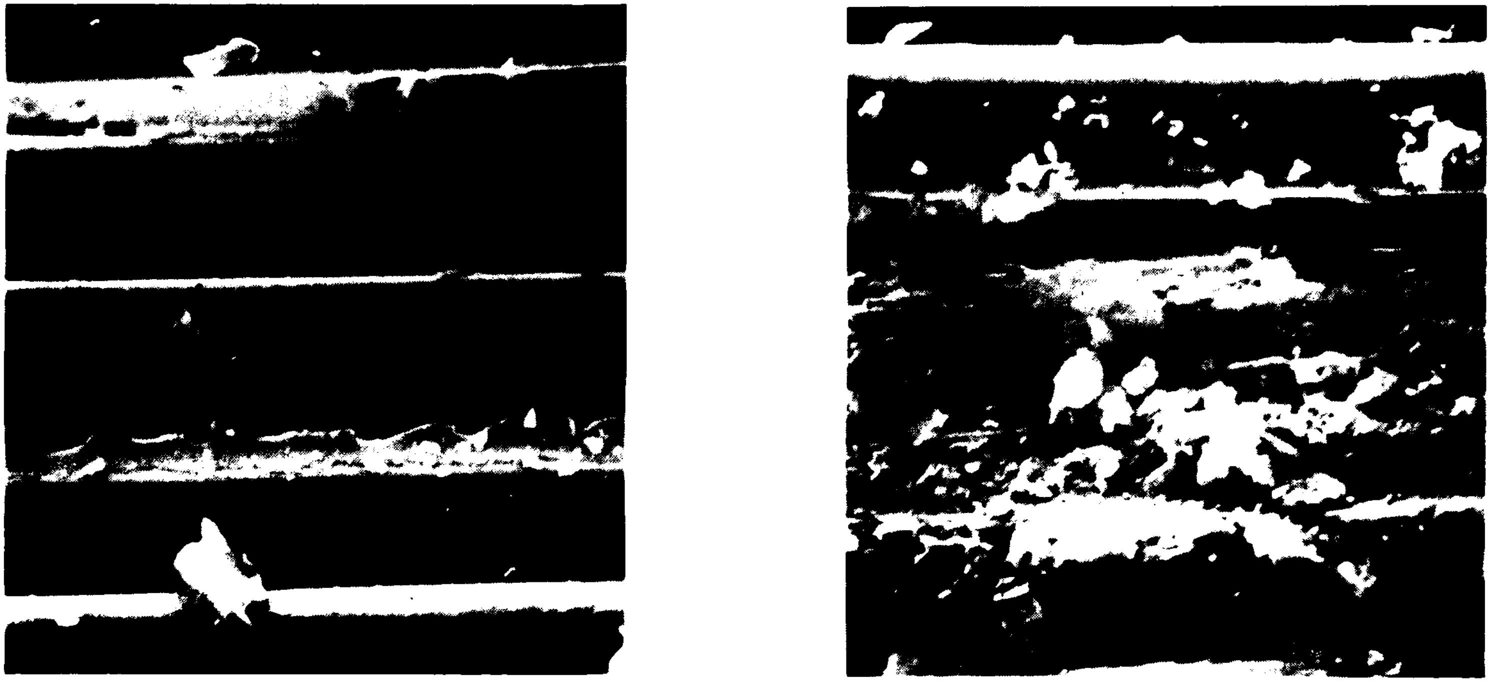

2000X 2000X

Fig. 92 SEM micrographs of AS4/m-ATS interlaminar shear fracture surface.

3.4.3.4 Flexural Strength and Modulus

The three-point flexural properties of AS4/m-ATS are given in Table 54. The values reported were normalized to 60% fiber volume. The room temperature and 177°C (350°F) data are near the values found for AS4/ATB as described in Section 3.3.4.4. All the specimens failed in compression. The flexural properties of material equilibrated at 71°C (160°F) and 95% RH are given in Table 55. The room temperature flexural strength of the moisture-conditioned composite is significantly higher than the dry tested material. At temperatures of 177°C (350°F) and 232°C (450°F), the detrimental effects of moisture are shown.

Table 54

Three-Point Flexural Properties of AS4/m-ATS Composite

Test Temp. °C (°F)	Flexural Strength GPa (ksi)	Flexural Modulus GPa (msi)	Failure Mode
24 (75)	1.37 (198) ± 0.06 (9)	132 (19.2) ± 7 (1.0)	Compressive
177 (350)	1.09 (158) ± 0.1 (1)	133 (19.3) ± 12 (0.2)	Compressive
232 (450)	0.81 (118) ± 0.03 (5)	123 (17.9) ± 5 (0.7)	Compressive

Table 55

Three-Point Flexural Properties of AS4/m-ATS Composites, Moisture Conditioned at 71°C (160°F) and 95% RH

Test Temp. °C (°F)	Flexural Strength GPa (ksi)	Flexural Modulus GPa (msi)	Failure Mode
24 (75)	1.65 (239) ± 0.03 (4)	126 (18.4) ± 3 (0.4)	Compressive
177 (350)	1.10 (160) ± 0.1 (2)	111 (16.1) ± 4 (0.6)	Compressive
232 (450)	0.54 (78) ± 0.02 (3)	79 (11.5) ± 7 (1.0)	Compressive

3.4.3.5 Transverse Flexural Strength

The transverse 90° flexural properties of AS4/m-ATS are given in Table 56. Three specimens were tested at room temperature and 177°C (350°F). The room temperature strength and strain-to-failure are 25 and 32% lower, respectively, than determined for AS4/ATB and discussed in Section 3.3.4.5.

Table 56

Transverse Flexural Properties of AS4/m-ATS

Temperature °C (°F)	90° Flexural Strength MPa (ksi)	90° Strain-to-Failure μin./in.	90° Flexural Modulus GPa (msi)
23 (75)	49.6 (7.2) ± 1.4 (0.2)	5245 ± 233	9.0 (1.3) ± (0.1)
177 (350)	46.9 (6.8) ± 5.5 (0.8)	5574 ± 550	9.0 (1.3) ± (0.1)

3.4.3.6 Fracture Toughness

The Mode I delamination fracture toughness (G_{1c}) of unidirectional AS4/m-ATS composite was determined by the method developed by Devitt et al.[8] Data for the test conducted is given in Table 57. The value is the average of 10-15 determinations taken along the crack length of the specimen. Data for other materials tested are also given in Table 57. The fracture toughness for AS4/m-ATS is significantly lower than reported for AS4/ATB. SEM micrographs of the delamination failure surface (Figs. 93-95) show a smoother delamination surface than observed for AS4/ATB or AS4/BATQ-H (ATP). It appears that failure did not occur as extensively in multiple crack fronts as found for AS4/BATQ-H (ATP) and AS4/ATB. For this reason, the G_{1c} value may not be as high as observed in AS4/BATQ-H (ATP) and AS4/ATB.

Table 57

G_{1c} Fracture Toughness of AS4/m-ATS

Composite Material	G_{1c} (N/m)
AS4/m-ATS	137 ± 12
AS4/ATB	197 ± 7 216 ± 6
AS4/BATQ-H (ATP)	552 ± 40 534 ± 88
AS1/3501-5A	219 ± 25 190 ± 10
XAS/PEEK (MG-1)	1846 ± 25 1640 ± 11

SC85-30267

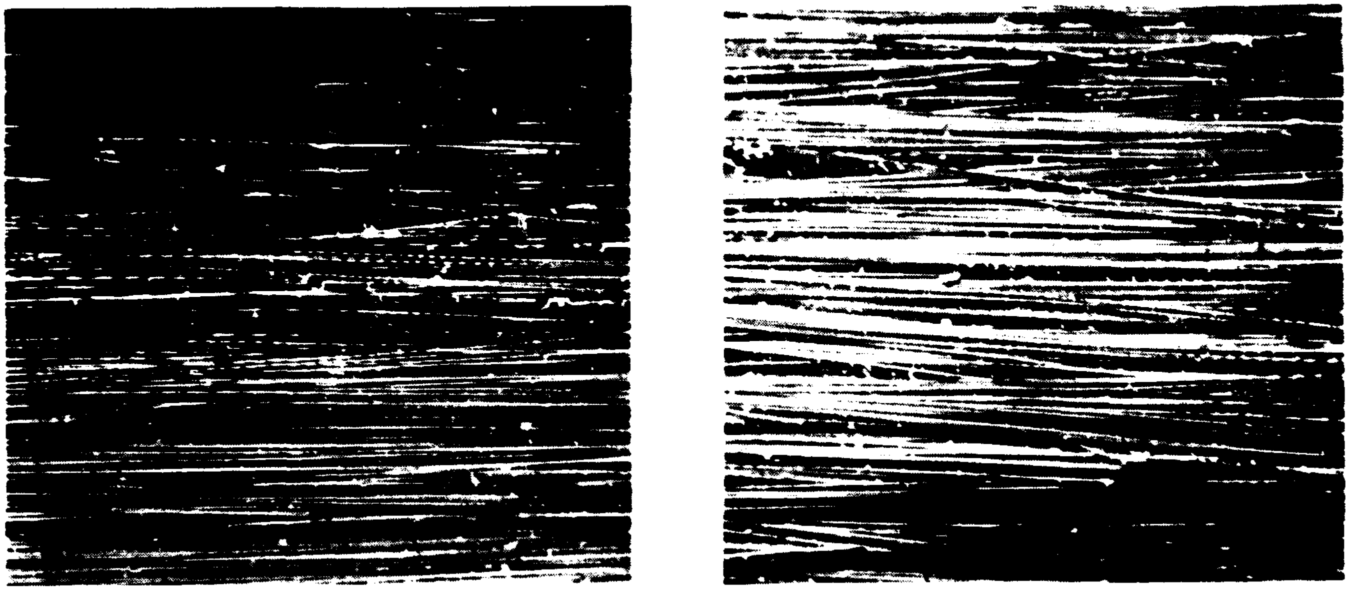

Fig. 93 SEM micrographs at AS4/m-ATS G_{1c} fracture surface, 40X.

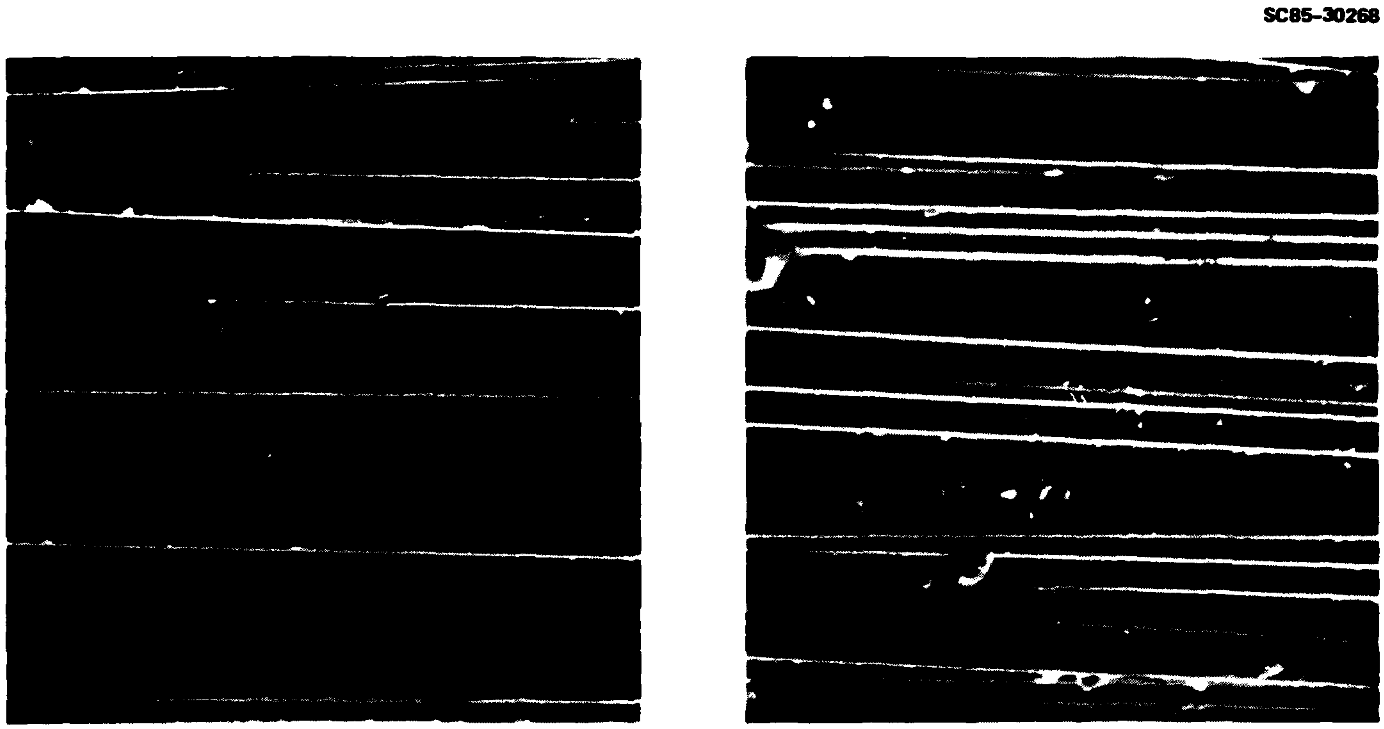

Fig. 94 SEM micrographs of AS4/m-ATS G_{1c} fracture surface, 400X.

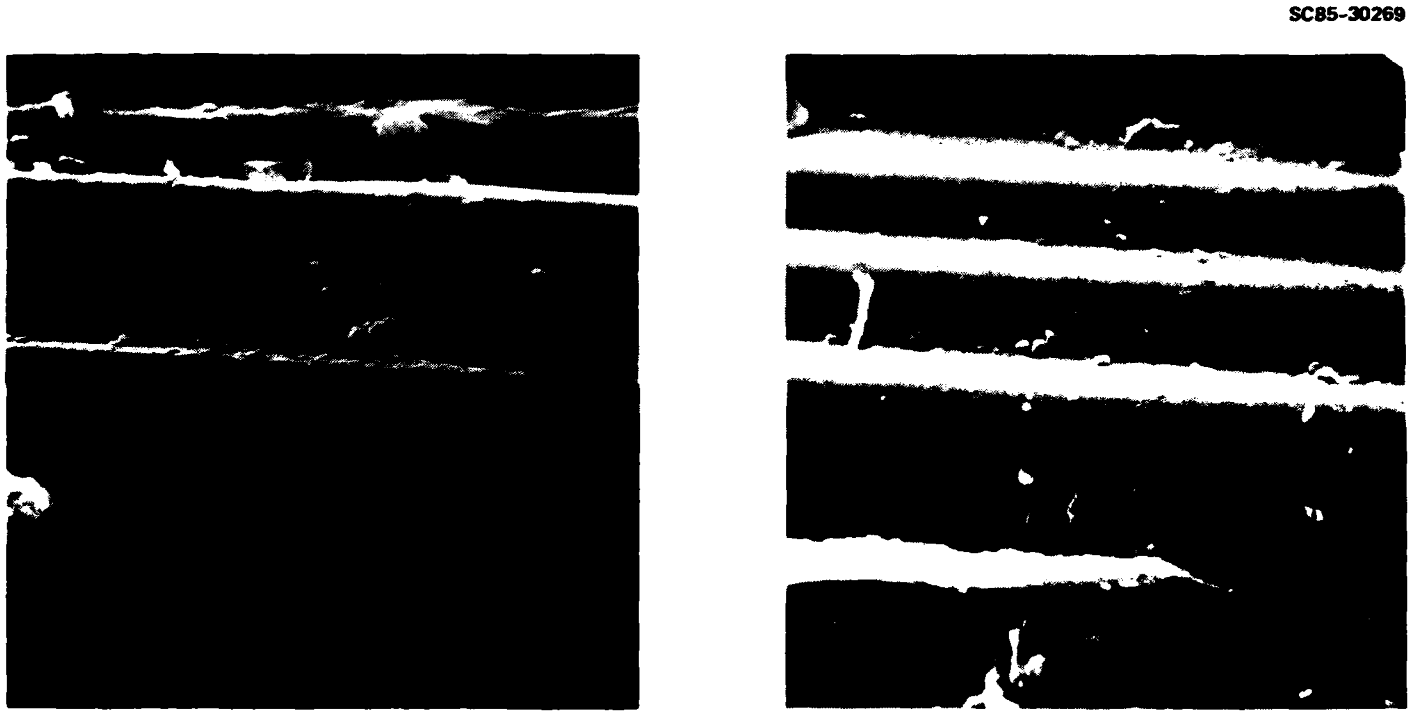

Fig. 95 SEM micrographs of AS4/m-ATS G_{1c} fracture surface, 2500X.

3.4.3.7 Edge Microscopic Examination

Tensile testing and edge microscopic examination of a 16-ply $[\pm 45]_s$ laminate of AS4/m-ATS was made. Both 0° and 90° directions were examined for microcracks. Micrographs of these cross sections are shown in Figs. 96 and 97, respectively. The presence of microcracks was observed in the center two plies, as shown in Fig. 96, for examination in the 0° direction. No cracks were found in the 90° view seen in Fig. 97. Tensile testing was carried out for 4 in. x 0.5 in. specimens cut from the laminate with the edges polished. The average in-plane shear strength of three specimens was 126.7 MPa (18372 psi).

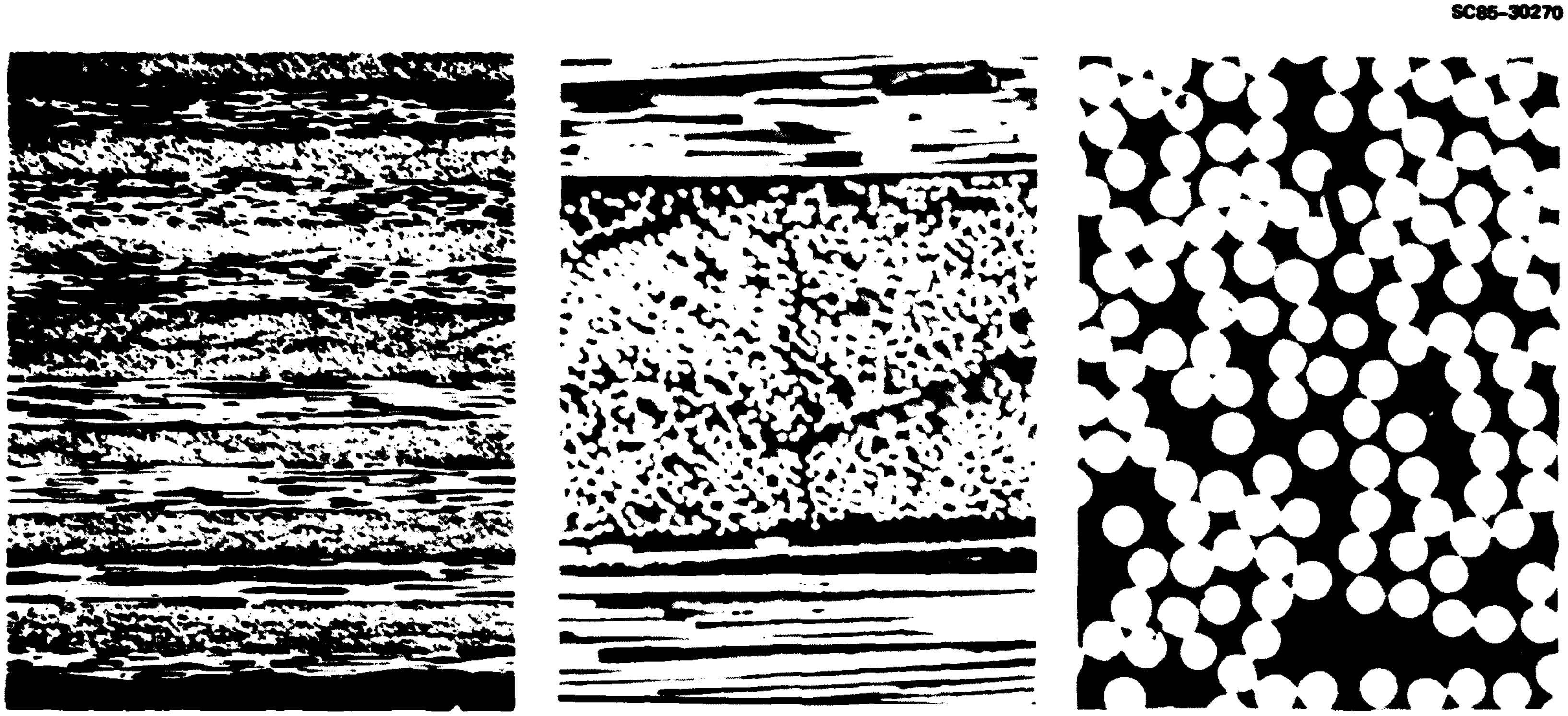

100X

250X

1000X

Fig. 96 Photomicrographs of AS4/m-ATS crossply laminate, 0^o view.

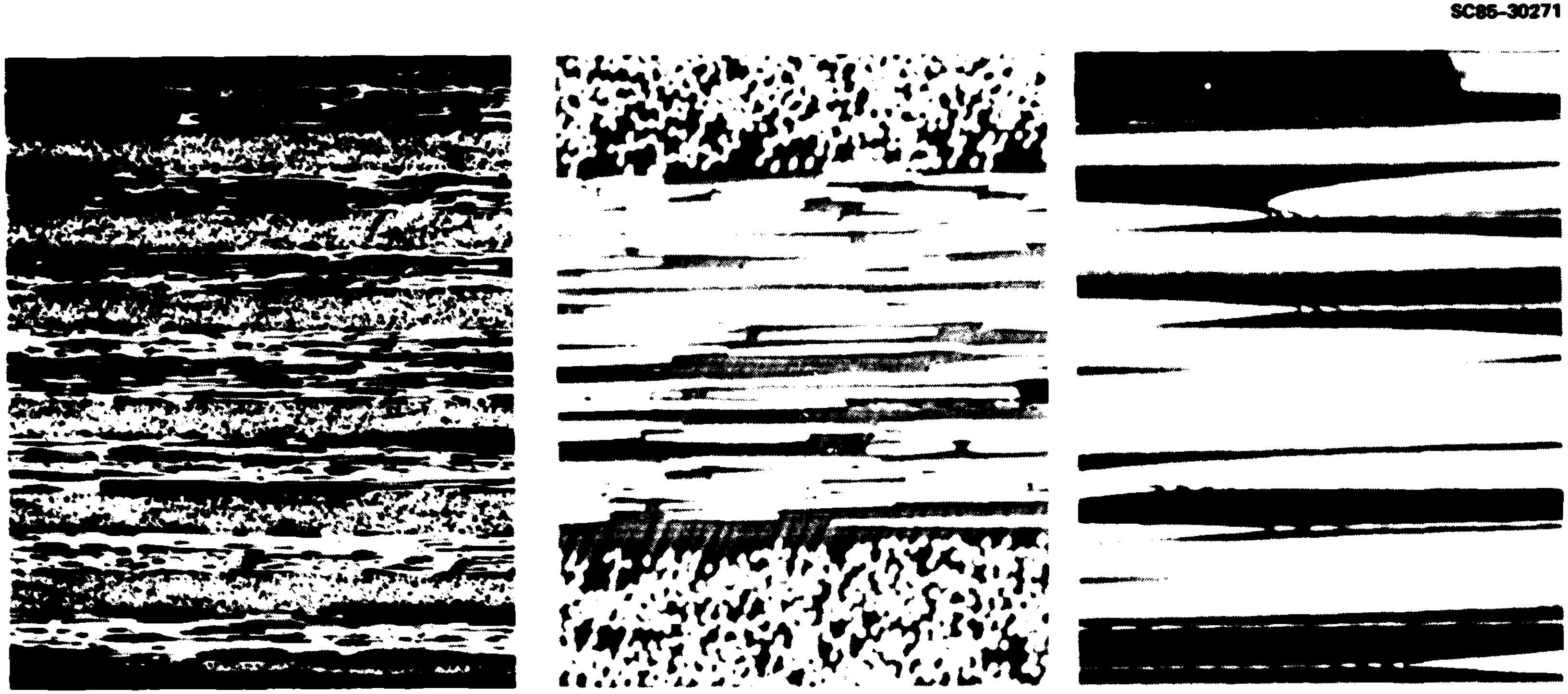

100X 250X 1000X

Fig. 97 Photomicrographs of AS4/m-ATS crossply laminate, 90^{0} view.

4.0 CONCLUSIONS

4.1 Hughes HR600P Resin

A unique advantage of the HR600P resin system was its potential to be autoclave processed at 204°C (400°F) or less and subsequently oven postcured to yield a 316°C (600°F) service composite. However, a number of problems were encountered during its evaluation. The neat resin tensile properties indicated that the material would not meet the hoped for service temperature of 316°C (600°F). Some evidence indicated that the sluggishness of the isoimide to imide conversion might be responsible.

Solvent impregnation was made using a metahylethylhetone/toluene mixture. The prepreg out-time was short, resulting in a fragile material with poor tack and drop. A number of autoclave processing variations were used in an attempt to produce high quality laminates. Extensive porosity, as indicated by ultrasonic C-scan and photomicrographs of cross sections, was always observed. Laminates which exhibited only moderate porosity after autoclaving became blistered after postcure. Press molding of laminates also resulted in significant porosity and poor mechanical properties.

The cause for much of the porosity problem was later identified by Hughes Aircraft and National Starch Corporation as due to the the presence of amic acid forms of the prepolymer. The amic acid was thought to result from moisture contamination during resin synthesis.

4.2 ATB Resin

The evaluation of ATB resin demonstrated several of its advantages as a composite matrix. The material exhibits favorable flow and processing characteristics similar to state-of-the-art 177°C (350°F) service epoxies. The "no bag" processing technique produced flaw-free laminates in all cases. The resin is ideal for hot-melt impregnation and the prepreg has excellent tack and drape, as well as long shelf life and out-time. A unique property of the resin is its low (~ 0.2%) moisture uptake. This results in an insensitivity of the prepreg to humid conditions and a negligible effect on composite mechanical properties in hot-wet tests. The cured resin has a T_g of over 250°C (482°F) and the strength retention at 177°C (350°F) is 70-80% for interlaminar shear and flexural properties.

Several deficiencies in the system were also observed. Transverse flexural and delamination fracture toughness tests indicated the system to be poorer than state-of-the-art 177°C (350°F) service epoxies. Examination of neat resin tensile and composite interlaminar shear failure surfaces also revealed characteristics typical of a very brittle material. The interlaminar shear and flexural properties were only about 70% of those generally obtained for 177°C (350°F) service graphite/epoxy composite. These low strengths and poor fracture toughness may, in part, be due to what appeared to be poor fiber/matrix bonding, as indicated by the presence of extensive bare fiber in SEM micrographs of interlaminar shear failure surfaces.

4.3 BATQ-H (ATP)

Neat resin tensile testing of BATQ-H (ATP) confirmed its high tensile strength of almost 110 MPa (16 ksi) and strain-to-failure of over 6%. The work showed that solvent-based prepreg could be prepared by a modification of the hot-melt pultrusion method. Void-free laminates were fabricated by press molding. The translation of the tough neat resin properties to composite was somewhat ambiguous. Apparent G_{1c} fracture toughness values of approximately twice that of state-of-the-art epoxies were found; however, the failure mode occurred in several crack fronts simultaneously, resulting in artificially high values. The transverse flexural strength and strain-to-failure were approximately twice that of state-of-the-art epoxies.

The interlaminar four-point shear strength of the composite was only about 70 MPa (10 ksi) at room temperature. Tests at 232°C (450°F) resulted in thermoplastic creep which eventually led to a compressive failure. This behavior points to a serious limitation of the system.

The flexural strength and modulus of the composite were similar to state-of-the-art epoxies. Strength retention at 177°C (350°F) was about 72%, the same as for ATB-based composite. As with ATB, the fiber/matrix bond appeared poor from SEM micrographs of interlaminar shear failure surfaces.

4.4 m-ATS Resin

The conclusions reached after evaluating this new purer version of ATS resin are similar to those described in earlier studies of ATS_G, a product of Gulf Research and Development Corporation. The prepregging and processing of m-ATS, which is a liquid at room temperture, is much easier than earlier solid forms of the resin.

The composite properties of AS4/m-ATS were similar to those found for AS4/ATB. The interlaminar shear strength was only about 70% that of state-of-the-art 177°C (350°F) service graphite/epoxies. The shear strength retention at 177°C (350°F) was 75% and at 232°C (450°F), about 56%.

The 0° three-point flexural properties were also lower than for state-of-the-art epoxy-based composites and similar to AS4/ATB. The hot-wet strength retention of AS4/m-ATS, however, was much poorer than for AS4/ATB. The 90° four-point flexural properties of AS4/m-ATS were also lower than for AS4/ATB.

The delamination fracture toughness of AS4/m-ATS was only 137 N/m, which is about 35% lower than for AS4/ATB on state-of-the-art 177°C (350°F) service graphite/epoxy composites. This poor fracture toughness was also revealed by microcracking observed in edge microscopic examination of quasi-isotropic laminates. It appears that the extended cure cycle utilized in preparing AS4/m-ATS did not enhance the fracture toughness as hoped.

APPENDIX. HOT-MELT PREPREGGER

A single-tow pultrusion hot-melt prepregger was used to prepare prepreg of BATQ-H (ATP), ATB and m-ATS resins with unsized Hercules AS4, 12K graphite fiber. Three views of the prepregger are shown in Fig. A-1. The system consists of a resin reservoir and metering device mounted on the moving arm of a standard lathe. The resin reservoir is 4 in. long and 2.5 in. wide, and has a conical hole 2.5 in. in diameter at the top and 0.75 in. in diameter at the bottom. Two smooth metal rollers are staggered along the length of the reservoir. A two-part die 0.75 in. in diameter is fitted at the bottom of the reservoir. This die has an elliptically shaped hole which is 0.44 in. long by 0.10 wide at the top and tapers to approximately 0.220 in. by 0.0065 in. at the bottom.

The single graphite tow enters the resin reservoir at the top, where it is immersed in resin. The tow passes over and between the two staggered metal rollers, which tend to spread the tow and assure complete wetting by the resin. The fiber tow moves through the die which controls the amount of resin retained. The impregnated tow then passes over a smooth moving roller and onto the drum of the lathe. The lathe is set at five threads per inch which results in five tows per inch giving an areal fiber weight of 174 g/m^2. The temperature of the resin reservoir was controlled by heating elements embedded at the four corners. The temperature was adjusted to give a resin viscosity of ~ 300 Poise.

The resin content of the prepreg was controlled mainly by the dimensions of the pultrusion die in the resin reservoir. The effect of changes in the width of this die on prepreg resin content is shown in Fig. A-2. The narrowest width tested was approximately 0.058 in. which gave a resin content of about 35.5%. At this width, the fiber tow was under considerable tension moving through the die, and any further reduction in width would result in fiber breakage. This was a serious disadvantage of the technique, as about a 32% resin content was desired for the net resin processing used. For solvent-based prepregging, such as BATQ-H (ATP), this was not a problem, because the resin content could be controlled by resin solution concentration.

SC83-24499

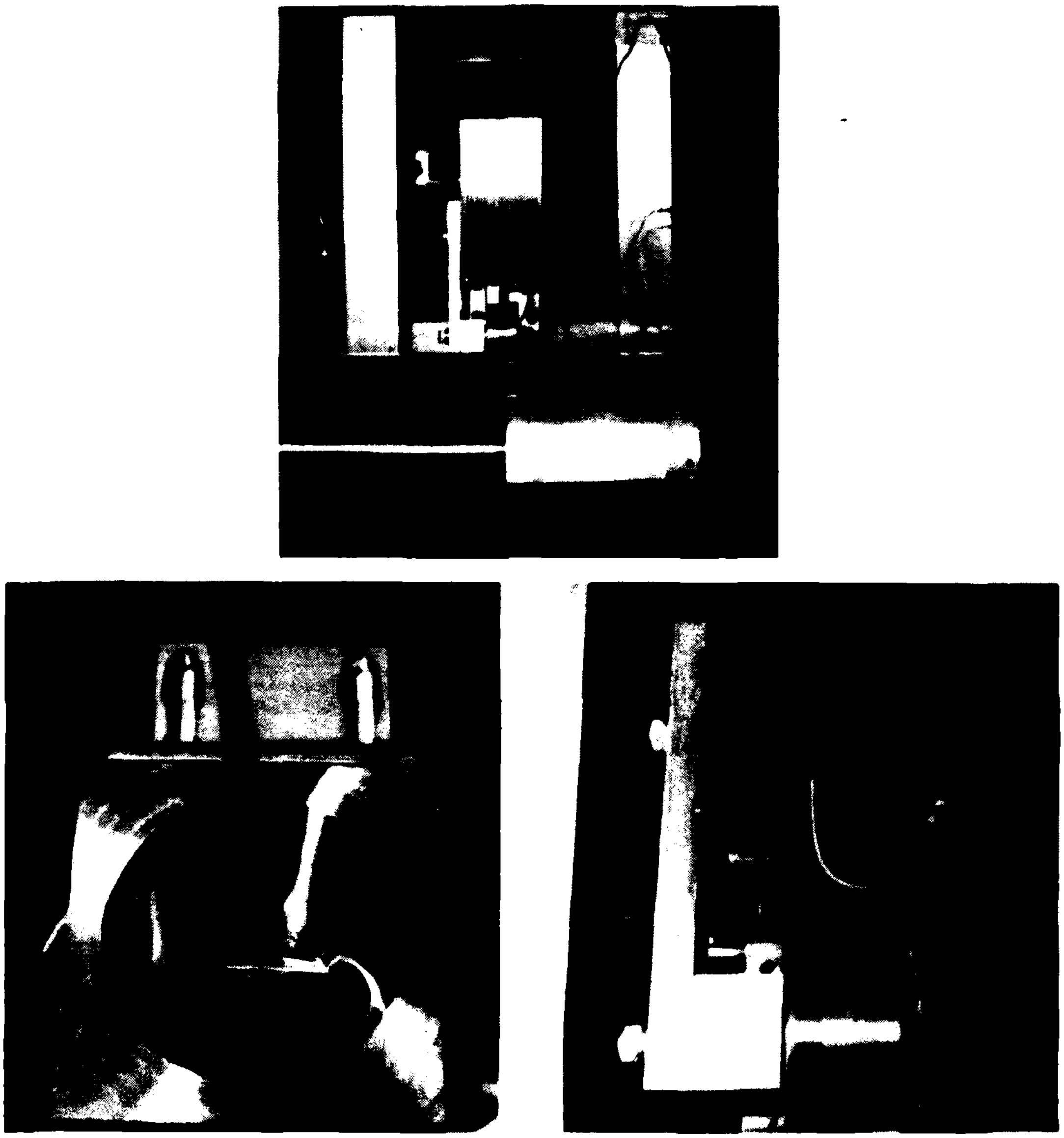

Fig. A-1 Single tow hot-melt pultrusion prepregger.

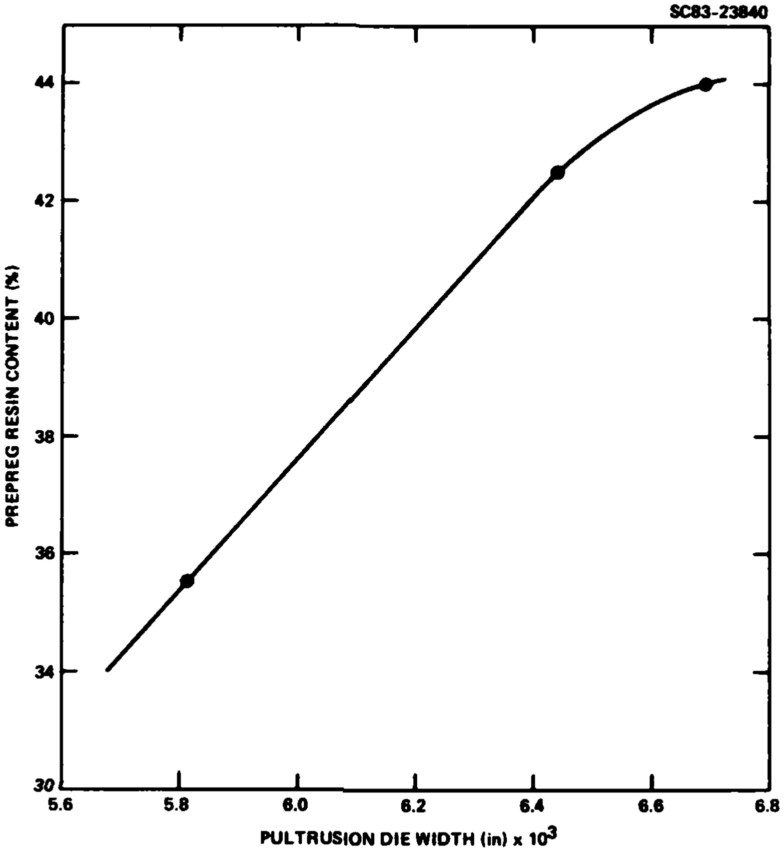

Fig. A-2 The effect of hot-melt prepregger pultrusion die width on AS4/ATB prepreg resin content.

REFERENCES

1. Duswalt, A.A., Thermochem. Acta. 18, 56 (1974).

2. Tung, C.M., and Dynes, P.J., J. Appl. Polym. Sci. 27, 569 (1982).

3. Browning, C.E., Abrams, F.L., and Whitney, J.M., "Composite Material Quality Assurance and Processing," ASTM STP 797, p. 54.

4. Lee, C.Y., Air Force Materials Laboratory 50 g Evaluation of BATQ-H(ATP) Resin.

5. Dewitt, D.F., Schapery, R.A., and Bradley, W.L., J. Composite Materials 14, 270 (1980).

6. Hartness, J.T., SAMPE Quarterly, Jan., 1980, p. 33.

U S GOVERNMENT PRINTING OFFICE 1986 - 559-065/20898